massDOT
Massachusetts Department of Transportation

April 2023
Report No. 23-040

Multisource Data Fusion for Real-Time and Accurate Traffic Incident Detection via Predictive Analytics

Principal Investigator (s)
Dr. Polichronis Stamatiadis
Dr. Nathan H. Gartner
Dr. Yuanchang Xie

University of Massachusetts Lowell

Research and Technology Transfer Section
MassDOT Office of Transportation Planning

U.S. Department of Transportation
Federal Highway Administration

Technical Report Document Page

1. Report No.	2. Government Accession No.	3. Recipient's Catalog No.
23-040	n/a	n/a

4. Title and Subtitle	5. Report Date
Multisource Data Fusion for Real-Time and Accurate Traffic Incident Detection via Predictive Analytics	April 2023
	6. Performing Organization Code

7. Author(s)	8. Performing Organization Report No.
Polichronis Stamatiadis, Nathan H. Gartner, Yuanchang Xie, and Ruifeng Liu	23-040

9. Performing Organization Name and Address	10. Work Unit No. (TRAIS)
University of Massachusetts Lowell One University Avenue, Lowell, MA 01840	n/a
	11. Contract or Grant No.

12. Sponsoring Agency Name and Address	13. Type of Report and Period Covered
Massachusetts Department of Transportation Office of Transportation Planning Ten Park Plaza, Suite 4150, Boston, MA 02116	Final Report - April 2023 (May 2021 – April 2023)
	14. Sponsoring Agency Code n/a

15. Supplementary Notes
Project Champion - Chester Osborne, MassDOT

The objectives of this study are to (1) identify data sets available to MassDOT that can be used for real-time incident detection; (2) investigate how data from different sources can be integrated to improve incident detection; and (3) develop guidance for establishing trigger points to alert Highway Operations Center (HOC) operators about incidents on the road. Speed data available through the Regional Integrated Transportation Information (RITIS) platform are used for developing two alternative strategies:

(a) an Artificial Intelligence (AI) model using supervised learning based on Long Short-Term Memory (LSTM) and Variational Autoencoders (VAE) layers for classifying records as normal events or incidents, and

(b) an empirical rule-based method using historical speeds to establish threshold values, below which an alarm is issued requiring the HOC operator's attention.

Results on the AI model and a verified incident data set indicate a False Alarm Rate (FAR) of 0.0069% and a detection rate of 91.70%. For the empirical rule-based model, a 30-day off-line "field-test" was conducted for June 2021. Most of the events recorded by the MassDOT HOC were detected, and for most of these events the detection time was well before the "SENT-ON" time recorded in the HOC incident database.

17. Key Word	18. Distribution Statement
real-time incident detection, speed data, artificial intelligence, long short-term memory, multisource data	n/a

19. Security Classified (of this report)	20. Security Classified (of this page)	21. No. of Pages	22. Price
unclassified	unclassified	138	n/a

Form DOT F 1700.7 (8-72) Reproduction of completed page authorized

This page left blank intentionally.

Multisource Data Fusion for Real-Time and Accurate Traffic Incident Detection via Predictive Analytics

Final Report

Prepared By:

Polichronis Stamatiadis[1]
Nathan H. Gartner[1]
Yuanchang Xie[1]
Ruifeng Liu[2]

[1] Dept. of Civil and Environmental Engineering
[2] Dept. of Computer Science
University of Massachusetts Lowell
Lowell, MA 01854

Prepared For:

Massachusetts Department of Transportation
10 Park Plaza, Boston, MA 02212

April 2023

This page left blank intentionally.

Acknowledgments

Prepared in cooperation with the Massachusetts Department of Transportation, Office of Transportation Planning, and the United States Department of Transportation, Federal Highway Administration.

The project team would like to acknowledge the support and guidance of Chester Osborne, Director of TSMO, MassDOT, as the project champion/technical representative for this study; Michael Flanary, MassDOT Office of Transportation Planning, as the monitor for this study; and Michael Fitzpatrick and Brian Jacques, MassDOT Highway Operations Center, for additional project support.

The project team would also like to acknowledge the efforts of Rick Ayers, University of Maryland, Center for Advanced Transportation Technology (CATT) Laboratory, for providing support with data available in the Regional Integrated Transportation Information (RITIS) platform.

Disclaimer

This page left blank intentionally.

Executive Summary

This study of Multisource Data Fusion for Real-Time and Accurate Traffic Incident Detection via Predictive Analytics, was undertaken as part of the Massachusetts Department of Transportation Research Program. This program is funded with Federal Highway Administration (FHWA) State Planning and Research (SPR) funds. Through this program, applied research is conducted on topics of importance to the Commonwealth of Massachusetts transportation agencies.

This report presents the results of a research project conducted by the University of Massachusetts Lowell for MassDOT under an Intergovernmental Service Agreement titled "Multisource Data Fusion for Real-Time and Accurate Traffic Incident Detection via Predictive Analytics." The project aims to fuse data from multiple sources to enable rapid detection of traffic incidents in real time. Accurate and fast incident detection is essential for triggering Highway Operations Center (HOC) response plans that aim to reduce incident-related congestion.

The objectives of this research were to

- Identify data sets in MassDOT current environs as well as data sets from other sources and providers that can be harvested to support real-time incident detection, understanding of data latency, and value to program.
- Investigate how data from these and other sources can be merged for accurate and real-time traffic incident detection and improved travel time reliability.
- Develop guidance for setting trigger points to alert HOC operators to incidents that affect travel on the roadway. These trigger points must be sensitive enough to detect disruptive events, and yet refined sufficiently to not create false positives. Different roadways may have different trigger points based on temporal and spatial conditions such as direction, weather, time of day, and season.

The results of the study, including the data sources, corridor selection, model development, and field testing, are described in the following sections.

Section 2: Literature Review

Traffic incident management (TIM) performance can be assessed in terms of the various time-based components of the incident timeline, which starts when an incident occurs, identifies key interim activities, and finishes with traffic returning to normal. The goal of TIM and related HOC activities is to shorten the gap between these two times.

An automatic incident detection (AID) system consists of two parts: (a) data collected from various sources and (b) data processed by a suitable AID algorithm. The section reviews the different data sources and collection methods and lists the principal incident detection performance indicators:

- Detection Rate (DR)
- False Alarm Rate (FAR)
- Mean Time to Detect (MTTD)

For effective Traffic Management Center operations, an AID system should have a short MTTD while maximizing DR and minimizing FAR. However, these measures are not independent since there is a trade-off between detection rate, detection time, and false alarm rate. For most algorithms, the detection rate tends to increase the longer the algorithm takes in evaluating the detector data. Conversely, the false alarm rate tends to decrease as the detection time increases. Therefore, to maximize the detection rate while minimizing the false alarm rate, the detection time needs to increase. If the algorithm thresholds are adjusted to detect less severe incidents more quickly, minor fluctuations in traffic demands can cause the false alarm rate to rise. To minimize detection times, AID systems must detect only those incidents that have a major impact on traffic by reducing the sensitivity of the AID algorithms.

Section 3: Available Data Sources

Information on roadway traffic conditions that can be used for the purpose of incident detection has to be reliable and must be available with very short latency. Several information sources are available to MassDOT.

Regional Integrated Transportation Information Data: RITIS fuses data from INRIX and local transportation agencies. INRIX data are based on GPS readings from several different sources including fleet vehicles such as delivery vans, long haul trucks, and taxis. The information available through the RITIS platform is aggregated over one-minute time intervals and over distinct roadway segments (called XD segments) and includes the following:

- one-minute average values of the space mean speed,
- travel times,
- reference speed,
- the confidence value (C-value), and
- the confidence score.

Data can be averaged for different time periods ranging from five minutes to one hour. Speed information is also available in a graphic form, called a “congestion scan.” RITIS has included Waze reports in these congestion scans, shown as tags at the location and time the report was generated.

MassDOT GoTime Data: The MassDOT GoTime program uses Bluetooth sensors installed along several state highways to collect information on the time and Mac-Address of devices on vehicles as they pass in front of the sensor. Using data from sequentially placed sensors, the system can determine travel times on segments of the roadway using the locations of the sensors.

The GoTime data are averaged over one-minute time intervals and are incorporated in the RITIS platform. The information that is available through the platform for each segment is similar to the INRIX data:

- one-minute average values of the space mean speed,
- travel times, and
- reference speed.

Waze Reports: Waze collects traffic information through crowdsourcing on traffic events such as traffic incidents, crashes, stopped vehicles, road construction, debris on the road, and so forth,

in the form of reports created by its users. Such information can be used, primarily for verifying the presence of an incident detected by an AID algorithm but also for detecting incidents, especially under light traffic conditions, when the occurrence of a traffic incident will cause minor reductions to the average speed.

In conclusion, data available to MassDOT can be used in an AID system. Such data include one-minute space mean speeds on roadway segments, for the entire network, with very short latency. These data sets can be used for the development/training and testing of candidate methodologies for automatic incident detection.

Section 4: Corridor Selection

The first step in selecting the corridor was to count the number of incidents that occurred on different state roadways. Interstates I-93, I-95, and I-495 appear to have the most incidents; they also have very high average daily volumes. Selecting a corridor simply based on route incident frequency can lead to biased results, since longer routes often have more incidents. Therefore, the team took into consideration both route length and route incident frequency. The incident records provided by MassDOT covered 136 state roadways for the period of January 2017 to April 2021. Based on this information it was calculated that Interstate 93 has more than double the number of incidents of any other state route; therefore, it appeared to be a good candidate as a test bed for developing and testing the incident detection strategy. To focus on a specific section of the roadway, the average number of incidents per mile per direction of I-93, split in two parts (Quincy–Boston, Boston–NH border) was calculated. During the period considered (i.e., 1/2017 to 4/2021), the segment of I-93 in District 6 (I-93-D6) had about three times the number of incidents per mile per direction than any other state route and, therefore, was selected as the test bed. The high incident frequency for I-93-D6 is most likely due to the high traffic volumes carried by this freeway segment.

A variety of distributions of incidents on I-93-D6 were prepared using data for the calendar years from 2018 to 2020. The following distributions were considered:

- incidents in each month of the year,
- incidents in each day of the week,
- incidents in each hour of the day, and
- spatial distribution of incidents along the selected roadway.

This analysis was performed to ensure there was a sufficient number of incidents that could be used for the development and testing of the incident detection strategy, comprising a variety of traffic, weather, and light conditions, to name a few.

One-minute space-mean-speed data for the period 1/2018 to 12/2021 were downloaded from the RITIS platform for each eXtreme Definition (XD) segment of the roadway. There are a total of 57 XD segments in the section of I-93 in District 6: there are 24 XD segments in the northbound direction and 23 XD segments in the southbound direction. INRIX XD segments are an INRIX-proprietary road segmentation system. The incidents included in the database provided by MassDOT HOC were stratified based on the time of occurrence (month of the year, workday/weekend, time of day), and within each strata a fraction of the incidents was used for

the development of the incident detection strategy. The remainder of the incidents were used for testing the strategy.

Section 5: Model Development and Implementation

Two models for detection of traffic incidents were developed and tested in this study. The first model is based on Artificial Intelligence (AI) and the second is an empirical rule-based model. The two models were applied for detection of traffic incidents on the selected segment of Interstate 93.

AI Model: AI has been widely used for solving regression and classification problems. Traffic incident detection essentially is a classification problem. The traffic state at a specific moment is characterized by a feature vector representing speed, occupancy, and so forth. This feature vector is then fed into a pretrained AI classifier and classified as either incident or non-incident. Two key elements for a successful AI-based classification application are choice of classifier and feature selection.

There are two main types of classifiers: supervised and unsupervised. Supervised classifiers require each input feature to be clearly labeled (e.g., as incident or non-incident). Labeling input features can be very time-consuming process. Some recent methods such as deep learning typically require a large set of labeled input features to avoid model overfitting. On the other hand, unsupervised classifiers only need the input features and do not need labels. These methods can calculate the similarity/dissimilarity among the input features based on some distance metrics and automatically classify them into different categories. A supervised learning method integrating long short-term memory (LSTM) and variational autoencoders (VAE) is adopted in this study.

Two performance metrics are used in this study, which are FAR and DR. Smaller FAR and larger DR values are more desirable. Various VAE model configurations have been evaluated. The best performing VAE model are FAR = 0.0069% and DR = 91.70%.

Empirical Rule-Based Methods: This method uses threshold values on the observed traffic parameters, i.e., space mean speeds along with their corresponding confidence parameters, available through the RITIS platform. When the currently observed speed on a road segment drops below the selected threshold value, an alarm will be issued requiring the HOC operator's attention. For this purpose, first the distributions of speeds at different time periods and different locations must be developed, and then various percentile values of speed, to be set as thresholds, can be tested for their effectiveness in detecting incidents. Once the distributions for all XD segments in the test corridor and for all time periods were developed, the threshold values of speeds observed in these segments for non-incident conditions must be established. If the speed observed in a segment falls below the threshold value, an alarm will be issued requiring the operator's attention to verify that there is an incident or cancel the alarm.

Comparison of AI and Rule-Based Methods: The AI model appears to be able to detect more incidents than the rule-based methods in some cases. However, it is difficult to understand how the AI model works. On the other hand, the various rule-based methods also perform well. An important benefit of the rule-based methods is that users can adjust the parameters based on experience. The effects of these parameters are easy to understand.

Section 6: Field Testing

To test further the incident detection methodologies described above, under a variety of situations, selected strategies were applied to both the northbound and southbound directions of the test corridor over a continuous 30-day period. During June 2021, there were 24 Level 2 events recorded by the MassDOT HOC, with eight of them involving disabled motor vehicles (DMV) and the rest being traffic crashes. All the events recorded by the HOC were detected by the strategy described above. For most of these events, the detection time was well before the SENT-ON time recorded in the HOC database. Overall, the strategy that was developed using the empirical rules described above can detect incidents that result in perturbations in the one-minute average speeds observed for at least three consecutive minutes. Minor events that do not cause such perturbations cannot be detected.

This page left blank intentionally.

Table of Contents

Technical Report Document Page i
Acknowledgments v
Disclaimer v
Executive Summary vii
Table of Contents xiii
Table of Tables xv
Table of Figures xvii
List of Acronyms xxi
1 Introduction 1
1.1 Task 1: Review of Literature, Current Practices, and Available Data 1
1.2 Task 2: Corridor Selection and Data Collection 2
1.3 Task 3: Model Evaluation 2
1.4 Task 4: Testing of Algorithm 2
2 Literature Review 3
2.1 Traffic Incident Detection: Current Practices 3
2.2 Data Sources and Collection Methods 4
2.3 Incident Detection Performance Indicators 8
2.4 Incident Detection Algorithms 10
3 Available Data Sources 17
3.1 RITIS Data 17
3.2 MassDOT GoTime Data 22
3.3 Waze Reports 23
3.4 Conclusions 24
4 Corridor Selection 25
4.1 Incident Frequencies 25
4.2 Distributions of Incidents on I-93-D6 31
5 Model Development and Implementation 37
5.1 AI Model 37
5.1.1 Description of AI Model and Model Inputs 37

5.1.2 Data Preparation 40
5.1.3 Results of AI Method 42
5.2 Empirical Rule-Based Methods 49
5.2.1 Overview of the Rule-Based Methods 49
5.2.2 Data 49
5.2.3 Speed Distributions 50
5.2.4 Establishment of Threshold Values 56
5.2.5 Threshold by persisting speed differences on current and adjacent XD segments 60
5.2.6 Beta Distribution 66
5.3 Comparison of AI and Rule-Based Methods 71
5.4 Other Modeling Efforts 74
6 Field Testing 77
7 Conclusions 81
8 Appendixes 83
8.1 Events Reported by MassDOT HOC on South I-93, June 1 to June 30, 2021 83
8.2 Results of Incident Detection Strategy Test, June 1 to June 30, 2021 84
9 References 113

Table of Tables

Table 2.1: Recommended target values of performance indicators 10
Table 2.2: AID performance review in Australia in 2010 11
Table 2.3: AI and statistical procedures for AID 14
Table 4.1: Incidents on Massachusetts state routes from 1/2017 to 4/2021 26
Table 4.2: Year-to-Year Change of Incidents on Massachusetts State Routes 27
Table 4.3: Incidents per mile per direction for the top six routes 28
Table 4.4: XD segments on I-93-D6 35
Table 6.1: Mean and standard deviation of speed distributions on XD 1263148464 78
Table 6.2: One-minute speed observations on XD 1263148464 78
Table 6.3: Percentiles of observed speeds on XD 1263148464 79
Table 8.1: Events reported by MassDOT HOC on SB and NB of South I-93 (test corridor) during June 2021 83

This page left blank intentionally.

Table of Figures

Figure 2.1: Incident timeline 3
Figure 2.2: DR and FAR as a function of MTTD 9
Figure 2.3: AID using loop detector data 12
Figure 3.1: RITIS-generated 24-hour congestion scan 18
Figure 3.2: Color thresholds used in RITIS congestion scans 18
Figure 3.3: Icons for Waze reports used in RITIS congestion scans 18
Figure 3.4: TMC consecutive segments 120P05791, 120+05791, and 120P05790 along I-90 W19
Figure 3.5: XD consecutive segments 1263123361, 1263123409, and 429079803 along I-90 WB 19
Figure 3.6: Comparison between XD segments (1263123361, 1263123409, and 429079803) in cyan and a long TMC segment (120+05791) in black 20
Figure 3.7: Data on XD segment 1263123361 (upstream from segment with the incident) 20
Figure 3.8: Data on XD segment 1263123409 (segment with the incident) 21
Figure 3.9: Data on XD segment 429079803 (downstream from segment with the incident) 21
Figure 3.10: GoTime consecutive segments along I-90 WB 22
Figure 3.11: Comparison of GoTime and TMC segments along I-90 WB 23
Figure 4.1: Incidents on the top six state routes 28
Figure 4.2: Incidents/mile/direction on the top six state routes 29
Figure 4.3: Incidents/mile/direction on the top six state routes 30
Figure 4.4: Incidents per month on I-93-D6 31
Figure 4.5: Incidents per day on I-93-D6 32
Figure 4.6: Incidents per hour of the day on I-93-D6 33
Figure 4.7: Incident locations on I-93-D6 33
Figure 5.1: Structure of the proposed VAE model 38
Figure 5.2: Structure of the proposed VAE model 39
Figure 5.3: Structure of a typical LSTM model [*34*] 40
Figure 5.4: Segment of I-93 selected for this study 41
Figure 5.5: AI model incident detection results using a threshold value of 0.9990 44
Figure 5.6: AI model incident detection results using a threshold value of 0.9985 44
Figure 5.7: AI model incident detection results using a threshold value of 0.9980 45
Figure 5.8: AI model incident detection results using a threshold value of 0.9975 45

Figure 5.9: AI model incident detection results using a threshold value of 0.9970 46
Figure 5.10: Congestion scan results for southbound traffic 46
Figure 5.11: AI model incident detection results using a threshold value of 0.9980 47
Figure 5.12: AI model incident detection results using a threshold value of 0.9975 47
Figure 5.13: AI model incident detection results using a threshold value of 0.9970 48
Figure 5.14: Congestion scan results for southbound traffic 48
Figure 5.15: Speed changes on consecutive XD segments due to an incident 50
Figure 5.16: Congestion scan results for an incident in XD segment 1263231759..... 50
Figure 5.17: One-minute distributions of observed speeds 52
Figure 5.18: One-minute distributions of observed speeds, 5:00–6:00 a.m. 53
Figure 5.19: Five-min. distributions of observed speeds, 5:00–6:00 a.m. 54
Figure 5.20: Smoothed 5-minute speed distributions, 5:00–6:00 a.m. 55
Figure 5.21: Smoothed 5-minute speed distributions: (a) weekdays; (b)weekends 55
Figure 5.22: Incident detection results on 01/15/2021 using a $\boldsymbol{\beta}$=1.5 for SB I-93 57
Figure 5.23: Incident detection results on 01/15/2021 with $\boldsymbol{\beta}$=1.75 for SB I-93 57
Figure 5.24: Incident detection results on 01/15/2021 with $\boldsymbol{\beta}$=2 for SB I-93 58
Figure 5.25: Incident detection results on 01/15/2021 with $\boldsymbol{\beta}$=2.25 for SB I-93 58
Figure 5.26: Congestion map for SB I-93, Friday, January 08, 2021 59
Figure 5.27: Congestion scan for SB I-93, Friday, January 22, 2021 59
Figure 5.28: Incident detection results with Eq. (5-3) and $\boldsymbol{\beta}$=1.5 for SB I-93 61
Figure 5.29: Incident detection results with Eq. (5-3) and $\boldsymbol{\beta}$=1.75 for SB I-93 61
Figure 5.30: Incident detection results with Eq. (5-3) and $\boldsymbol{\beta}$=2.0 for SB I-93 62
Figure 5.31: Incident detection results with Eq. (5-3) and $\boldsymbol{\beta}$=2.25 for SB I-93. 62
Figure 5.32: Incident detection results with Eq. (5-4) and $\boldsymbol{\beta}$=1.5 for SB I-93 64
Figure 5.33: Incident detection results with Eq. (5-4) and $\boldsymbol{\beta}$=1.75 for SB I-93 64
Figure 5.34: Incident detection results with Eq. (5-4) and $\boldsymbol{\beta}$=2.0 for SB I-93 65
Figure 5.35: Incident detection results with Eq. (5-4) and $\boldsymbol{\beta}$=2.25 for SB I-93 65
Figure 5.36: Beta probability density functions 11:00 a.m. to 12:00 noon weekdays..... 67
Figure 5.37: Beta probability density functions 3:00 p.m. to 4:00 p.m. weekdays 67
Figure 5.38: Incident detection results using Beta distribution, 1st percentile..... 68
Figure 5.39: Incident detection results using Beta distribution, 1.25th percentile 68
Figure 5.40: Incident detection results using Beta distribution, 1.5th percentile 69

Figure 5.41: Incident detection results using Beta distribution, 1.75th percentile 69
Figure 5.42: Incident detection results using Beta distribution, 2nd percentile..... 70
Figure 5.43: Incident detection results using Beta distribution, 2.25th percentile 70
Figure 5.44: Congestion scan results for NB traffic on 01/15/2021 71
Figure 5.45: Incident detection results using a beta threshold value of 2.0 for NB traffic..... 72
Figure 5.46: AI model incident detection results using a threshold value of 0.9980 for NB traffic 72
Figure 5.47: Congestion scan results for SB traffic on 05/15/2021..... 73
Figure 5.48: Incident detection results using a beta threshold value of 2.0 for SB traffic 73
Figure 5.49: AI model incident detection results using a threshold value of 0.9980 for SB traffic 74
Figure 5.50: PyCaret evaluation results 75
Figure 8.1: June 1, 2021..... 84
Figure 8.2: June 2, 2021..... 85
Figure 8.3: June 3, 2021..... 86
Figure 8.4: June 4, 2021..... 87
Figure 8.5: June 6, 2021..... 88
Figure 8.6: June 7, 2021..... 89
Figure 8.7: June 8, 2021..... 90
Figure 8.8: June 9, 2021..... 91
Figure 8.9: June 10, 2021..... 92
Figure 8.10: June 11, 2021..... 93
Figure 8.11: June 12, 2021..... 94
Figure 8.12: June 13, 2021..... 95
Figure 8.13: June 14, 2021..... 96
Figure 8.14: June 15, 2021..... 97
Figure 8.15: June 17, 2021..... 98
Figure 8.16: June 18, 2021..... 99
Figure 8.17: June 19, 2021..... 100
Figure 8.18: June 20, 2021..... 101
Figure 8.19: June 21, 2021..... 102
Figure 8.20: June 22, 2021..... 103
Figure 8.21: June 23, 2021..... 104

Figure 8.22: June 24, 2021 105
Figure 8.23: June 25, 2021 106
Figure 8.24: June 26, 2021 107
Figure 8.25: June 27, 2021 108
Figure 8.26: June 28, 2021 109
Figure 8.27: June 29, 2021 110
Figure 8.28: June 30, 2021 111

List of Acronyms

Acronym	Expansion
AADT	Average Annual Daily Traffic
ADASYN	Adaptive Synthetic Sampling
AI	Artificial Intelligence
AID	Automatic Incident Detection
ANN	Artificial Neural Network
ARRB	Australian Road Research Board
ATMS	Advanced Traffic Management System
BCE	Binary Cross-Entropy
CCTV	Closed-Circuit Television
CV	Connected Vehicle
DMV	Disabled Motor Vehicle
DR	Detection Rate
DSRC	Dedicated Short-Range Communications
FAR	False Alarm Rate
FHWA	Federal Highway Administration
GAN	Generative Adversarial Network
GPS	Global Positioning System
HOC	Highway Operations Center
HOV	High Occupancy Vehicle
HPMS	Highway Performance Monitoring System
IDC	International Data Corporation
LSTM	Long Short-Term Memory
MAC	Media Access Control
MassDOT	Massachusetts Dept. of Transportation
MLP	Multilayer Perceptron
MTTD	Mean Time To Detect
NB	North Bound
NLP	Natural Language Processing
OEM	Original Equipment Manufacturer
PA	Pennsylvania
PDO	Property Damage Only
PeMS	Performance Measurement system
PNN	Probabilistic Neural Network
RBM	Restricted Boltzmann Machine
RCID	RoadCast Incident Detection
RITIS	Regional Integrated Transportation Information System
SB	South Bound
SNB	Semi-Naïve-Bayes algorithm
SND	Speed Threshold Determination
STD	Speed Threshold Determination
STPN	Spatiotemporal Pattern Network
STVV	Spatiotemporal Video Volumes
SVM	Support Vector Machine
TI	Traffic Incident
TIM	Traffic Incident Management

Acronym	Expansion
TMC	Traffic Message Channel
TRB	Transportation Research Board
TSMO	Transportation Systems Management and Operations
TTD	Time To Detect
UDA	Unsupervised Deep Augmentation
VAE	Variational Autoencoders
XD	eXtreme Definition Segment

1 Introduction

Traffic incidents are a leading contributor to non-recurring congestion and secondary crashes. Each year congestion and crashes together cost the nation more than $1 trillion. Once traffic queues are formed, it is very difficult to dissipate them and return traffic to normal operations. This is especially true for highway segments where traffic demands are near capacity and where any disturbance may lead to long queues and stop-and-go conditions. Therefore, real-time and accurate incident detection plays a critical role in TIM and congestion mitigation. The sooner incidents are detected, the sooner safety personnel can respond to the incidents and clear them from the roads, thereby allowing traffic lanes to reopen, allowing the system to recover, and helping to prevent secondary incidents.

The ability to detect, respond, and clear such non-recurring events will lead to improved travel conditions by reducing congestion and traffic emissions, safer roads, more robust highway operations, and enhanced travel time reliability, resulting in better traveler experience, which are critical to strengthening the economy of Massachusetts and improving the environment and quality of life. These are all directly linked to the mission of MassDOT.

MassDOT, through its Highway Operations Center and other departments, has access to traffic information from multiple sources that can be used for the accurate and timely detection of such events.

Hence, the following research objectives were identified:

- Identify data sets in MassDOT current environments as well as data sets from other sources and providers that can be harvested to support real-time incident detection and understand data latency and their impacts on traffic incident detection.
- Investigate how data from different sources can be merged for accurate and real-time traffic incident detection and improved travel time reliability.
- Develop guidance for the setting of trigger points to alert HOC operators to incidents that affect travel on the roadway. These trigger points must be sensitive enough to detect disruptive events, and yet refined sufficiently to not create false positives. Different roadways may have different trigger points based on temporal and spatial conditions such as direction, weather, time of day, and season.

To achieve those objectives the research consisted of the four tasks described next.

1.1 Task 1: Review of Literature, Current Practices, and Available Data

Task 1 starts with a review of the current state of the art in traffic incident detection strategies and identifying relevant data sets that MassDOT has access to or may acquire. The reliability of these data sources will be considered. The traffic incident detection practices of other state DOTs and regional organizations will be reviewed. This will include how they collect, integrate,

analyze, and archive data and use them for incident detection. It will include review of the algorithms they use for incident detection. We will also review scientific publications to ensure that the latest developments in incident detection using advanced data analytics are considered.

1.2 Task 2: Corridor Selection and Data Collection

Task 2 is to identify a corridor to be used as a test bed for evaluating and enhancing the candidate incident detection models. The corridor must have a sufficient number of incidents and be covered by the data sources identified in Task 1, such that deployment of the model will have the most impact. Historical data should be available to confirm the types, times, locations, and durations of those traffic incidents in this corridor. Ideally, the selected corridor is covered by traffic cameras so that video data can be collected to verify incidents. Also, data should be available for the corridor during both normal operations and incident conditions over an extended period of time covering different weather conditions (e.g., sunny, rainy, foggy, snowy). As part of the corridor selection, the team will also collect related incident, traffic, and weather data, which will be used in Task 3.

1.3 Task 3: Model Evaluation

Using historical data, the team will evaluate advanced algorithms off-line to detect the onset and location of congestion that can be used as a trigger to alert HOC operators so they can identify the incident in real time and initiate a response. The historical incident data will be separated into training and validation sets for testing and enhancing the algorithms. The trigger can be defined based on measures such as speed (from loop detectors and crowdsourcing) and occupancy. For example, a trigger will be generated if certain speed and occupancy criteria on a roadway segment surpass, or drop below, prespecified threshold values. These trigger points must be sensitive enough to detect incidents and yet sufficiently refined to not create false positives. The team will also explore AI methods (e.g., long short-term memory networks) that may be more flexible and reliable in handling data from multiple sources.

1.4 Task 4: Testing of Algorithm

In Task 4, field testing of the model will be performed. Measures of effectiveness and reliability that will be used include the detection rate, false alarm rates, and mean time to detect. The trigger points will be based on the model developed in Task 3. Field implementation results will be used to further fine-tune the candidate models. In addition, the outcome will be used to develop guidance for the setting of trigger points or threshold values to alert HOC operators about incidents on the roadway. Different roadways have different characteristics and therefore may require a different set of trigger points. Guidance on how such trigger points can be adjusted will also be provided. The results of the study, including the data sources, corridor selection, model development, and field testing, are described in the next sections.

2 Literature Review

2.1 Traffic Incident Detection: Current Practices

Non-recurring traffic incidents, caused by accidents, breakdowns, or sudden lane drops resulting from debris can lead to congestion and interruption of traffic flow. Not all vehicle accidents result in traffic interruptions, therefore from the perspective of traffic management, it is more effective to detect interruptions to traffic rather than detect vehicle accidents exclusively. Traffic managers are tasked with the detection, response, and clearing incidents in a timely manner. The faster incidents are cleared, the lower the chance for secondary incidents to occur.

TIM performance can be assessed in terms of the various time-based components of the incident timeline, as indicated in Figure 2.1 [*1*].

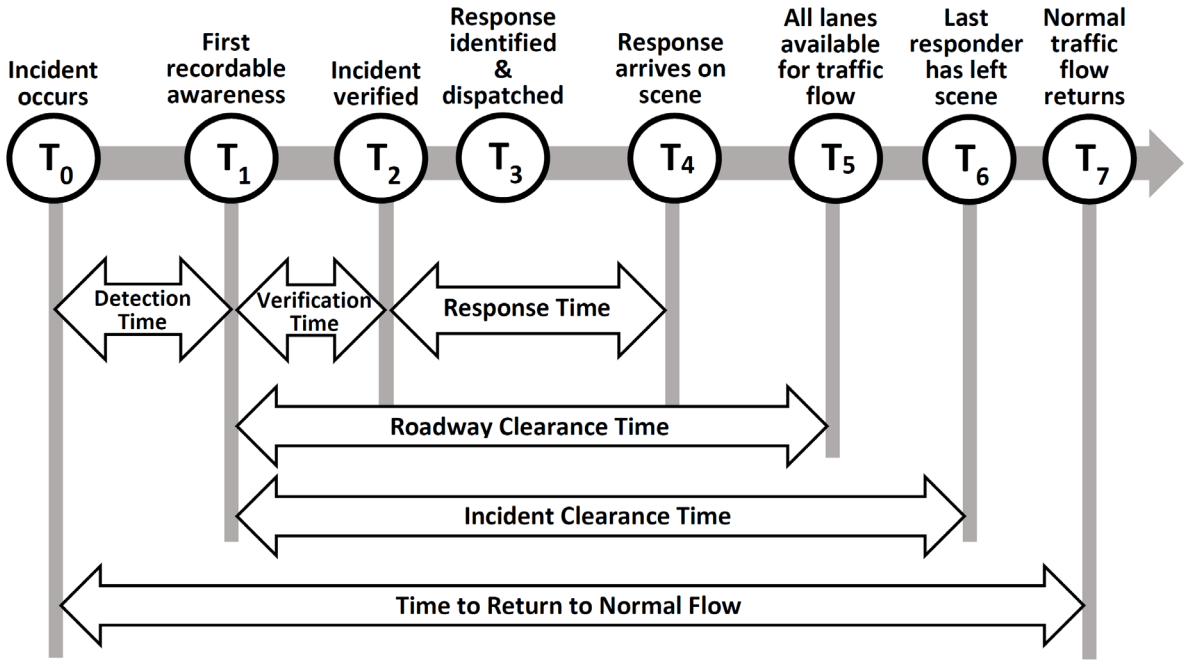

Figure 2.1: Incident timeline

The incident timeline starts when an incident occurs, identifies key interim activities, and finishes with traffic returning to normal.

The **detection time** ($T_1 - T_0$) is the time between the incident occurring and the incident being reported. It is the role of incident detection algorithms to make this time as short, but also as reliable, as possible.

The **verification time** ($T_2 - T_1$) is the time between the incident being reported and the incident being verified. Traffic management centers can typically assist with verification through use of their closed-circuit television (CCTV) cameras.

The **response time** ($T_4 - T_2$) is the time between the incident being verified and the responder arriving on scene. Response time is dependent on the incident location and each responding party's proximity to the incident.

The goal of TIM and related Traffic Management Center activities is to shorten the gap between T_0 and T_7. Traffic monitoring for incident management, traveler information, and traffic management is predominantly done using CCTV systems, driver reports, and highway crew patrols. Traffic management centers have been researching and implementing various automatic incident detection (AID) algorithms/procedures in their advance transportation management systems (ATMS). The reliability and efficacy of these systems depend on the sources of traffic data they use.

An AID system consists of two parts: (a) data collected from various sources and (b) data processed by a suitable AID algorithm. The following sections review methods being implemented by traffic management centers or traffic operations centers (TOC), and methods being researched or proposed by researchers.

2.2 Data Sources and Collection Methods

- **Inductive loop detector**: This is one of the most common data sources for AID systems. Inductive loop detectors have been widely used by state Departments of Transportation (DOTs) to collect traffic count, speed, occupancy, and so forth, on highways. They have also been extensively used at intersections to provide input data to traffic signal controllers. These detectors are less sensitive to the environment (e.g., temperature, lighting, snow, strong wind, vibration) and provide robust traffic measurements. However, since they are installed underneath the pavement, it is difficult to repair them if broken. Another major issue is that such detectors often are used to generate annual average daily traffic (AADT) data to meet the Highway Performance Monitoring System (HPMS) reporting requirements. The generated traffic measurements are not streamed in real time to HOC, making them unsuitable for incident detection. Additionally, these detectors are installed at limited locations on major highways and intersections [*2*]. Therefore, they can only provide situational awareness for highway segments near those locations. For incidents that happen far away from those locations, they will not be detected in a timely manner, which is critical to emergency response. Even if an incident is detected, it is difficult to accurately estimate its location with a sparse inductive loop detector network. Again, knowing the location of an incident is very important for efficient emergency response operations. These problems can be addressed by adding more detectors and investing in communication and Intelligent Transportation infrastructure. For example, Caltrans maintains PeMS (performance measurement system), which consists of about 40,000 detectors covering freeways across all major metropolitan areas of California, providing both real-time and historical traffic data. However, the cost can be prohibitive, especially for states with a significant portion of their highways in rural areas.
- **Microwave sensor**: Similar to inductive loop detectors, microwave sensors are installed at limited locations. Also, the collected data often are not streamed in real time to HOC for AID purposes. In this sense, microwave sensors share the aforementioned limitations of inductive loop detectors. However, compared to inductive loop detectors, microwave

sensors are easier and less expensive to install and maintain. Some new microwave sensors can cover multilane road segments of several hundred feet long and track individual vehicles in these segments, while inductive loop detectors can only measure traffic at a single point or a very short segment (e.g., 20 ft).

- **CCTV camera**: All state DOTs operate and maintain a CCTV camera network. These cameras provide important video feeds for identifying and confirming traffic incidents. However, in most state DOTs, such CCTV traffic videos are reviewed manually to confirm traffic incidents (detected/reported using other methods) and/or provide traffic situational awareness. They are not utilized to automatically detect traffic incidents, although technically it is possible to utilize video image processing (VIP) algorithms to process live feeds from CCTV cameras and generate data such as vehicle count, speed, and density for detecting incidents [*2*]. Like inductive loop and microwave detectors, CCTV cameras are deployed at limited locations, although they are getting increasingly popular. One concern with CCTV is privacy, especially for high-definition cameras. Such a problem can be addressed in many ways. One solution is to utilize edge computing devices to process videos in the field and discard them after processing (i.e., only keep and stream the extracted traffic measurements). With the wide deployment of CCTV cameras and adoption of AI based video processing algorithms, CCTV cameras may potentially become a major data source in the future for traffic incident detection. Some toll road authorities are using high-definition CCTV cameras for toll-by-plate purposes. This application can generate segment travel time data beyond count, speed, and density, similar to what Bluetooth readers (see discussion below) can do. Such travel time data allows HOC operators to identify congested segments. However, it cannot provide much useful information related to location (e.g., where the congestion starting and ending points are), unless the distance between upstream and downstream cameras is really short.
- **Bluetooth data**: Bluetooth technology has been widely used in collecting travel time data. It detects the media access control (MAC) addresses of Bluetooth devices on vehicles passing by and matches upstream and downstream MAC addresses to derive travel time. This is similar to matching upstream and downstream license plate numbers as some toll road authorities are doing (see discussion above) to determine the toll rate and charge users. The difference is that Bluetooth readers are less expensive and do not require sophisticated data processing algorithms (e.g., AI algorithms for detecting and recognizing license plates). Portable Bluetooth readers have been developed and can be easily deployed as needed. Given that most new cars are equipped with Bluetooth, this data source is becoming increasingly important and reliable. However, there are two major limitations for Bluetooth data. First, the data sample is often biased. It is not uncommon to have multiple people (i.e., multiple Bluetooth devices) in one vehicle. This often leads to biased travel time measurements. Second, like all previously discussed data sources, the coverage of Bluetooth readers is still limited for incident detection purposes. A dense network of Bluetooth readers is needed to quickly detect incidents and accurately estimate their locations.
- **E-ZPass data**: E-ZPass (or other similar systems such as SunPass) data is similar to Bluetooth data. The main difference is that E-ZPass uses the dedicated short-range communications (DSRC) technology to read transponders in individual vehicles instead of MAC addresses. Since each vehicle has a unique transponder ID, the travel time data

generated by E-ZPass data is more reliable than Bluetooth data. A clear limitation with the E-ZPass data is that it is only available for toll roads.

- **Probe vehicle and GPS data**: Data generated by mobile devices (e.g., smartphones) and commercial fleets (i.e., on-board GPS) are playing an increasingly important role in traveler information systems and incident detection. These GPS devices generate detailed vehicle trajectories (e.g., vehicle locations every 1 second). A significant advantage of probe vehicle and GPS data is that state DOTs do not need to invest in any data collection infrastructure and do not need to worry about the maintenance of data collection systems either. Although purchasing data from the private sector can be expensive, DOTs can save the trouble and cost associated with maintaining their own data collection infrastructure. Probe vehicle and GPS data usually have a much larger coverage than traditional data sources such as inductive loop detectors, microwave detectors, and CCTV cameras. The actual coverage depends on how many users are contributing their data. Many data sources/vendors can be considered under this probe vehicle and GPS data category, including Google, Wejo, INRIX, and HERE. Most of these data vendors provide aggregated information, such as segment speed and travel time. State DOTs take what these vendors provide and are not given the details of how the data are aggregated. The length of each segment is also decided by the vendors. Different vendors often have different standards/ways to divide roads into segments. When DOTs obtain data from multiple vendors, they face the challenge of reconciling data aggregated using different segment definitions, which is not a trivial task. In addition, state DOTs lose the opportunity to extract more granular and useful information from the aggregated probe vehicle and GPS data. Using AID as one example, DOTs may want to have short segments in areas prone to incidents (ideally in all areas if computational power is not a constraint). With short segments, changes in individual vehicles' speeds and travel times can be quickly reflected in the corresponding segment measures. On the other hand, providing aggregated data and hiding the details to some extent is beneficial to DOTs, as they often do not have the resources to handle the large volume of raw trajectory data and extract critical information from them.
- **Driver incident reports**: Almost every driver now has a smartphone. When a crash occurs, it typically does not take much time for the driver(s) involved or for passing by drivers to call 911 and report it. Some state DOTs rely a lot on such information for AID. A limitation of driver incident reporting is that non-collision (e.g., road debris) and property-damage-only (PDO) incidents may be underreported.
- **Social media**: Some researchers proposed to use data from social media such as Twitter for AID. They use the natural language processing (NLP) method to extract useful information from social media feeds for AID. For instance, after identifying an incident-related tweet, words related to "when," "where," and "how bad the incident is" will be extracted and analyzed if they exist. A major issue with this data source is that incidents are not guaranteed to be posted in a timely manner and with sufficient details to determine their nature and location information.
- **Crowdsourced reports (i.e., Waze)**: This data source is related to both driver incident reports and social media. Waze can be considered a social media, although it is used specifically for travel. In the meantime, many Waze users/drivers do report incidents they see on the road, but not directly to 911. Therefore, it is listed as a separate data source. Crowdsourced reports here specifically refer to the information (e.g., speed trap, object on

road, crash) reported by drivers, not the location information anonymously collected by Waze from users (which is considered as probe vehicle and GPS data in this report). Many state DOTs are using Waze incident reports for AID. Issues with Waze incident reports are these: (1) submitting a Waze incident report while driving is dangerous; (2) usually there are delays between when an incident is spotted and when it is reported by different drivers, and such delays make it difficult to identify the exact incident location; and (3) sometimes there are incorrect reports. For example, an incident has already been cleared, but it still shows up in Waze. In a quantitative comparison by Iowa DOT (IDOT) of various sources of incident detection, Waze was ranked the 4th (out of 8) largest contributing sources. While essentially free, Waze incident reports still must be validated by other means, and it captured only 43.2% of ATMS recorded incidents during the analysis period (although this most likely has increased as the number of users increases) [*3*].

- **Connected Vehicles (CV) as Data Sources:** Recent studies have demonstrated that connected vehicle (CV) data provide an abundant source of information for enhancing the comprehension of traffic flows and developing advanced traffic management strategies [*4*,*5*]. The availability of such rich data sources makes it practical for transportation agencies to incorporate them into traffic management systems. Two companies, Wejo and Waycare, have announced that they will jointly deliver CV data for 20 locations across the United States [*6*]. In collaboration with Waycare, Wejo offers raw probe vehicle trajectory data for traffic management, providing traffic managers with the ability to detect and predict incidents, and to respond more efficiently based on real-world, near real-time data in a single platform. Wejo's data is collected from OEM devices in some new vehicles and offers a 1–3 second data capture rate with a latency of 30 seconds. As the number of connected vehicles sold globally is expected to rise, the sampling rate and reliability of such probe vehicle data will improve significantly. With appropriately developed algorithms, such raw data can be very useful for AID purposes.
- **Unmanned Aerial Vehicles in Traffic Management:** The utilization of small unmanned aerial vehicles (UAVs), commonly referred to as drones, is on the rise across all industries. Drone-based traffic monitoring can overcome the limitations of traditional monitoring methods due to its simplicity, mobility, and ability to cover large areas. Real-time high-resolution videos captured by drones can be transmitted to TMCs to assist on-ground personnel in road monitoring, traffic guidance, traffic activity analysis, individual vehicle identification and tracking, license plate reading, and other related activities. A recent paper provides a comprehensive review of research studies that employ UAV technology for online and off-line extraction of traffic parameters from video data using vision processing techniques, thereby enhancing traffic surveillance and monitoring mechanisms [*7*].

2.3 Incident Detection Performance Indicators

Incident detection algorithms are used to process traffic data from a variety of sources and need to be tailored to the individual characteristics of each road segment. Algorithms can be automatic or non-automatic. Automatic incident detection (AID) algorithms will automatically trigger an alarm when traffic conditions deviate from previously defined limits, whereas non-automatic algorithms are based on witness reports.

Several indicators are used to evaluate and compare the performance of automatic incident detection (AID) systems and algorithms [*8*]. The three principal incident detection performance indicators employed in incident detection are as follows:

- Detection Rate: DR is defined as the ratio of the number of incidents detected by an algorithm and the number of incidents known to have occurred within a specified time period and network area. The total number of incidents in a measurement period is usually compiled from incident reports from police and the public, and from observations at a Traffic Management Center. DR is usually expressed as a percentage.

$$DR(\%) = 100 \times \frac{\text{No. of detected incidents}}{\text{No. of total incidents}} \tag{2-1}$$

- False Alarm Rate: The FAR is a measure of the accuracy of an AID algorithm. An algorithm must decide whether an incident exists in every time period for every location where the algorithm is applied. A false alarm arises when an algorithm incorrectly reports an incident where no incident actually exists. Therefore, the FAR is typically defined as the ratio of the number of incidents falsely reported by an algorithm to the number of incident decisions the algorithm has to make.

$$FAR(\%) = 100 \times \frac{\text{No. of false alarms}}{\text{No. of decision intervals}} \tag{2-2}$$

  For a FAR of 1% and a 1-min decision interval, the number of potential false alarms in an hour is 60 × 1% = 0.6 per hour. With a 20-s decision interval, the number of potential false alarms becomes three times as much or 1.8 per hour. FAR is also defined as the ratio of the number of false detections versus the number of verified incidents known to have occurred. The FAR is usually greater when defined in terms of total incidents rather than incident decision intervals. The interval-based FAR definition is more commonly reported in the literature. Minimization of the FAR is critical to gain credibility for any AID system.

- Time to detect or mean time to detect: The TTD measures how efficiently an incident detection algorithm performs. The TTD is the difference between the time the incident is detected by the algorithm and the time the incident occurred. The MTTD is widely used in the literature and is defined as the average TTD of a number of incidents (n) detected. TTD and MTTD values are expressed in seconds or minutes.

$$TTD_i = \text{Time } i^{th} \text{ incident detected} - \text{Time } i^{th} \text{ incident occurred} \tag{2-3.a}$$

$$MTTD(\text{s}) = \frac{1}{n}\sum_{i=1}^{n} TTD_i \qquad (2\text{-}3.b)$$

where n is the number of incidents detected.

For effective Traffic Management Center operations, an AID system should have a short MTTD while maximizing DR and minimizing FAR. However, these measures are not independent since there is a trade-off between detection rate, detection time, and false alarm rate. Figure 2.2 shows the general relationship that typically exists between these measures [*9*]. For most algorithms, especially the comparative incident detection algorithms, the detection rate tends to increase the longer the algorithm takes in evaluating the detector data. Conversely, the false alarm rate tends to decrease as the detection time increases. Therefore, if we want to maximize the detection rate while minimizing the false alarm rate, the detection time needs to increase.

As indicated above, the goal of most incident detection algorithms is to minimize the detection time to shorten the overall response time. If the algorithm thresholds are adjusted to detect less severe incidents more quickly, minor fluctuations in traffic demands can cause the false alarm rate to rise. Therefore, to minimize detection times, agencies must be willing to live with detecting only those incidents that have a major impact on traffic demands by reducing the sensitivity of the AID algorithms.

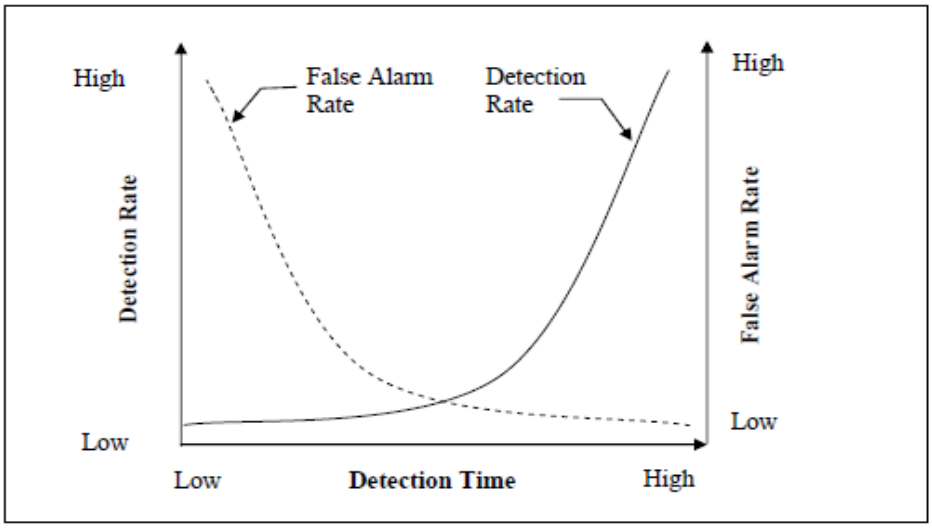

Figure 2.2: DR and FAR as a function of MTTD

Given these relationships, a given deployment must consider the relative importance of DR, FAR, and MTTD. One approach is to compute a performance index (PI) as suggested by Chung and Rosalion [*10*]:

$$PI = \left(\frac{100-DR}{100}\right)^m \times FAR^n \times MTTD^p \qquad (2\text{-}1)$$

where m, n, p are coefficients that indicate the relative importance of MTTD, FAR, and DR (m, n, $p > 0$). A larger coefficient value denotes a greater importance for the specific measure. For equal importance, all coefficients can be set to one. A lower PI value indicates a better algorithm performance. Determining a set of coefficients that minimizes the PI involves an optimization process across a large incident data set, as indicated in Chung and Rosalion [*10*]. Given the different operating needs among agencies, the target values of the performance indicators can vary among different systems. Table 2.1 provides a set of possible target values based on calibration tests and a review of practices [*11*].

Table 2.1: Recommended target values of performance indicators

Performance Indicators	Target Values
Detection Rate	$\geq 80\%$
False Alarm Rate	$\leq 1\%$
Mean Time to Detect	≤ 5 min

2.4 Incident Detection Algorithms

Incident detection algorithms are based on observation of the traffic state of roadway segments. Significant fluctuation of parameters describing the traffic state of a segment can be used for detecting traffic incidents. Flow rate, spot speed, and occupancy at certain locations have been used extensively in a wide variety of incident detection methodologies over the years (e.g., California and University of California Berkeley algorithms). The performance of such algorithms, using fixed point observations, depends greatly on the location and density of detectors.

Incident detection methodologies using probe vehicles (from commercial vehicles with data collection equipment) have been developed over the last few decades: an incident can be detected by observing the acceleration-deceleration rates of probe vehicles [*12*], by statistical differences in the average travel times on a segment and travel times of adjacent segments [*13*,*14*], or by trying to detect abnormal car movements that occur during incidents [*15*]. Using real-time GPS data, trajectories of vehicles can be traced to detect incidents [*16*]. The data must be preprocessed to match each trace to a map position. Using a phone-based app push traffic alerts and route alternatives were offered to motorists in exchange for their position data.

To achieve better results in determining the traffic state, fusing information from different sources, for example fixed detector data with probe vehicle data, has been considered. Fusion of data from multiple sources can enhance the reliability of the input data to an AID algorithm and thus enhance its performance. Data fusion methods can be based on statistical (multivariate analysis and data mining), probabilistic (Bayesian) or AI (ANN, PNN, evolutionary algorithms) approaches [*17*,*18*]. Data fusion in complex systems, such as traffic networks, requires a layered approach. In El Faouzi et al. [*18*], five levels of data fusion are recommended:

- Level 0: preprocessing data from each source to common formats and representations,
- Level 1: gathering data from all sources into a common framework for analysis,
- Level 2: state estimation using Level 1 data sets and other institutional knowledge,
- Level 3: incident/event identification and processing in the context of state estimation, and
- Level 4: continual refinement and integration of new information.

A comparison of AID algorithms that have been deployed and in use in Australia is shown in Table 2.2. AI approaches using ANN and PNN exhibit high performance implying high value for TMCs in deployment [*11*].

Table 2.2: AID performance review in Australia in 2010

Algorithm	DR (%)	FAR (%)	MTTD (min)
McMaster [*19*]	68–88	<0.01	2.1–3.2
DELOS [*20*]	78	0.176	1.1
ANN [*21*]	89	0	2.4
ANN [*21*]	89	0	2.4
ANN [*22*]	83	0.065	3.4
PNN [*23*]	98–100	0–0.5	0.3–2.5
California 8 Algorithm [*10*]	71	0.005	8.9
DELOS [*10*]	73	0.03	5.5
ANN [*10*]	97	0.176	5.2
PNN [*24*]	93	0.057	2.7
ANN [24]	83	0.065	3.4
California 8 (2010) [*11*]	84	0.075	8.3
ARRB VicRoads [*11*]	84	0	6.7

Incident detection methodologies based on AI algorithms and combining information from different sources have the potential to detect incidents successfully and efficiently. There are several different procedures based on AI that take advantage of the specific data available and with various levels of performance. The most notable such methodologies are listed next.

- Some studies treat AID as a classification problem. Within a data set, records are classified into two categories: (i) normal traffic records and (ii) incident records. The AI model identifies and classifies upcoming records into one of the categories, and the one that falls into the incident-class would be the incident detected. To resolve the problem of imbalanced and small training samples (due to the rarity of incidents compared to normal conditions), a generative adversarial network (GAN) is used to generate data with the same statistics as the training set. Information from several detectors in sequence is considered to ultimately classify a record. To generate such a model, a support vector machine (SVM) algorithm was used that reached a 90.68% detection rate and a 7.11% the false alarm rate [*25*].
- Some studies tried to monitor changes in the value of certain traffic parameters. It is assumed that if such changes exceed or drop below a certain threshold value, this indicates that an incident occurred. Historical data is used to determine the threshold values (Figure 2.3). Some denoizing methods could also be applied on the threshold, by using external data sets, such as weather, spatiotemporal information, or more, to increase the accuracy [*26*].

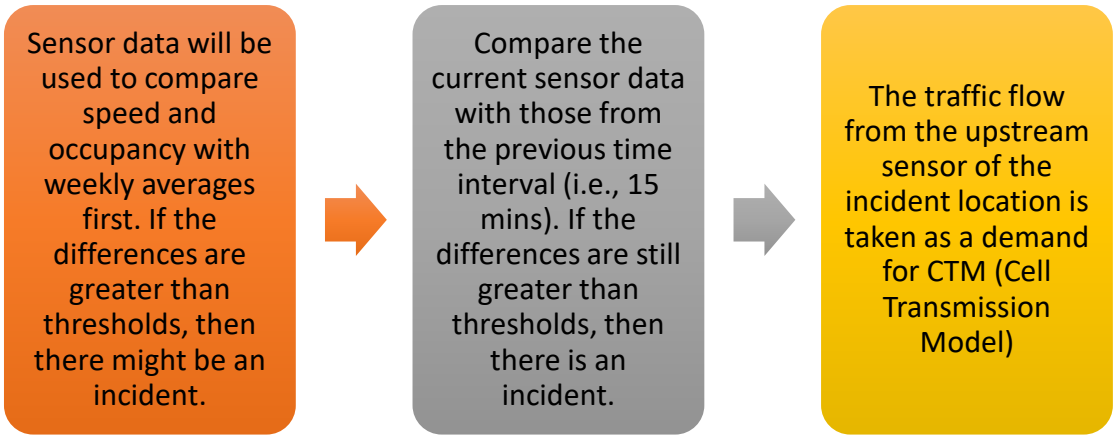

Figure 2.3: AID using loop detector data

- In a more elaborate model, the correlation between certain traffic parameters is recognized. Consequently, the autocorrelation between those parameters should stay relatively similar if the traffic state remains unchanged and vice versa. Hence, incidents can be detected by tracking the evolution of the autocorrelation between these parameters. Such algorithms reached a 92.8% detection rate and 7.1% for the false alarm [*27*].
- Another study practices a more brute force approach: after partitioning the traffic network into multiple segments, the average speed of each segment would be computed. If the average speed difference between downstream and upstream is more than a threshold, then there is an incident [*28*].
- Researchers also generate different methods to handle non-numerical data sets, such as video sets or photosets. Some studies use surveillance videos as one of the input data to find deep representations of spatiotemporal video volumes (STVV). From these deep features, they use the one-class SVM to generate incident scores for this STVV. The incident would be detected by comparing the incident scores [*29*].

- Mining texts from social media platforms, such as Twitter, has also been used for incident detection, as an efficient and cost-effective alternative. The process of adaptive data acquisition (Twitter data) establishes a dictionary of important keywords and their combinations that can imply traffic incidents (TI). A tweet is then mapped into a high dimensional binary vector in a feature space formed by the dictionary and classified into either TI related or not. All the TI tweets are then geocoded to determine their locations, and further classified into one of the five incident categories. The "bag of words" model is applied, meaning that only the count of the occurrences of words in Twitter Text Dictionary is used, regardless of the order [*30*].
- Besides these newer methods, some classical data mining algorithms and prevalent deep neural network methods have been used for AID as well. A probabilistic neural network (Naïve Bayes neural network), for instance, is mostly applied on classification and pattern recognition problems. It detects an incident based on the probability distribution functions of each class between accident and non-accident conditions [*31*,*32*,*3323,32,36*].

To improve the detection rate and reduce the false alarm rate of an algorithm, more data features can be used, and more complex models can be built. However, the inevitable direct result of this will be to raise the computational time. Real-time incident detection models require us to discover the incident as soon as possible. One of the evaluation measurements is MTTD. Therefore, it is essential to utilize the minimum number of variables that are sufficient to reflect and estimate the current traffic state. Table 2.3 lists the AI and statistical applications for incident detection that have been reviewed for this study.

Table 2.3: AI and statistical procedures for AID

Strategy	Method Name	Publication/Article	Summary
Machine learning algorithms	RoadCast incident detection (RCID)	A random forest incident detection algorithm that incorporates contexts [*34*].	RoadCast uses one random forest algorithm for each detector and each target variable being forecasted. RCID had a 25% lower false alert rate when incorporating contextual data (external factors). But there is a trade-off to be made between detection and false alert rates.
	Speed threshold determination (SND) algorithm	Data-driven parallelizable traffic incident detection using spatio-temporally denoized robust thresholds [*35*].	Univariate speed threshold determination algorithm: Determination of robust summary statistics (thresholds) of each univariate time series of speeds from each road segment. Multivariate spatiotemporal threshold denoizing (bilateral filter and total variation). The thresholds determined in the previous step are denoized using the spatiotemporal correlations of the adjacent thresholds.
	Semi-naïve-Bayes algorithm (SNB) and supervised latent Dirichlet allocation (sLDA)	Real-time incident detection using social media data [*30*].	This research project mines tweet texts to extract incident information on both highways and arterials as an efficient and cost-effective alternative to existing data sources.
	Isolation tree	Automatic incident detection on freeways based on Bluetooth traffic monitoring. [*33*].	Incident detection based on comparison of the degree of anomaly of a data instance with the average path length (from the leaf nodes to the root nodes in the isolation tree).

Data augmentation	Generative adversarial networks (GAN)	Automated traffic incident detection with a smaller data set based on generative adversarial networks [*25*].	Using GAN to generate new fake balanced data set based on the known sample. The balance of the data set can improve the detection rate from 87.48% to 90.68% and reduce the false alarm rate from 12.76% to 7.11%.
	Synthetic Minority Oversampling TEchnique (SMOTE)	Real-time accident detection: Coping with imbalanced data [*31*].	Using SMOTE to increase the incident data sample. For regular SMOTE, PNN (Probabilistic Neural Network) achieves best at a TTD (Time-To-Detection) of 5 min with an ACC, DR, and FAR of 99%, 80%, and 0.5% respectively, compared to 99%, 48%, and 0.1% for SVM.
Statistical approach	N/A	Incident detection in freeways based on autocorrelation factor of GPS probe data [*27*].	Use a statistical approach for AID. 92.8% detection rate and 7.1% for the false alarm.
	N/A	Buffalo-Niagara transportation data-warehouse prototype and real-time incident detection [*36*].	Simple speed thresholds method using volume-related factors, in a binary outcome model.
	N/A	A methodology to assess the quality of travel time estimation and incident detection based on connected vehicle data [*28*].	Network is divided into several segments and the average speed of each segment is computed. If the average speed difference between downstream and upstream is more than a threshold, then there is incident.
	Technical University of Munich Algorithm	Bluetooth-based travel times for automatic incident detection – A systematic description of the characteristics for traffic management purposes [*32*].	This algorithm belongs to the category of spatial measurement-based algorithms and detects changes in travel times that could lead to an incident occurrence.
	N/A	Real-time incident detection and capacity estimation using loop detector data [*26*].	Data-driven framework using inductance loop detectors for real-time incident detection, road capacity and incident location estimation. The algorithm is based on the variation in traffic flow parameters acquired from inductance loop detectors. Threshold values of speed and occupancy are determined for incident detection based on the PeMS database.

Video based	N/A	Development of automated incident detection system using existing ATMS CCTV [*37*].	Determines the traffic incidents based on the traffic flow data reported by CCTV streams.
	SVM (support vector machine)	Deep spatiotemporal representation for detection of road accidents using stacked autoencoder [*29*].	Use one-class SVM to generate the outlier score of intermediate representation for a given STVV and the reconstruction error value. After combining these scores, final accident score would be generated. At the end, compare the final score with the empirical threshold to determine whether there is an accident.
Neural network	Spatiotemporal pattern network (STPN)	Traffic dynamics exploration and incident detection using spatiotemporal graphical modeling [*38*].	STPN + RBM (Restricted Boltzmann machine): From STPN, learn APs (Atomic pattern), RPs (Relational pattern) and importance metric. Assign binary state for each AP and RP. Using RBM to model system-wide behavior on AP and RP. Then detection is implemented by computing the probability of occurrence of a test STPN pattern vector via trained RBM.
Severity study	Naïve Bayes, *k*-nearest neighbor, support vector machines, decision tree	Automatic classification of traffic incident's severity using machine learning approaches. [*39*].	The classification model achieved nearly 90% accuracy in fivefold cross-validation.

3 Available Data Sources

Information from roadways on traffic conditions that can be used for the purpose of incident detection has to be reliable and must be available with very short latency. The following section presents the types of information that are available to MassDOT.

3.1 RITIS Data

RITIS fuses data from INRIX and local transportation agencies and has the potential for effective incident detection and incident response. INRIX data is based on GPS readings from several different sources including fleet vehicles such as delivery vans, long haul trucks and taxis, users of the INRIX traffic app, and connected vehicles. Processed INRIX data is incorporated in the RITIS/CATT-LAB platform through which it can be visualized in map form.

The information available through the RITIS platform is aggregated over one-minute time intervals and over distinct roadway segments. Roadway segments identification can be done based on two different schemes: The Traffic Message Channel (TMC) code or the eXtreme Definition (XD) code.

The information that is available through the RITIS platform for each segment of the network is

- one-minute average values of the space mean speed (over the TMC or the XD segment),
- travel times (speed/length of segment),
- reference speed,
- the confidence value (C-value), indicating that current readings represent the actual roadway conditions based on recent and historical trends, and
- the confidence score, a discrete variable indicating whether the values reported are real-time data. The variable takes the values of
    - 30: values are based on real-time data, segment has adequate GPS readings,
    - 20: historic averages, segment does not have sufficient real-time readings (15-minute granularity), or
    - 10: reference speed, no real-time readings.

Exported data can be averaged for different time periods ranging from five minutes to one hour. Besides the information listed above, speed information is also available in a graphic form, a "congestion scan." Figure 3.1 is a 24-h congestion scan generated by RITIS on June 1, 2021, along South I-93. The colors (Figure 3.2) are based on the current one-minute average speed value, without taking into consideration historical speed patterns at that location and for that period of time (time of the day, day of the week, season, etc.). Recently, RITIS has included Waze reports in these congestion scans, shown as tags at the location and time the report was generated. The length of the line attached to each of these icons indicates the time that the report stays active. The different types of Waze reports included in these scans are explained in Figure 3.3.

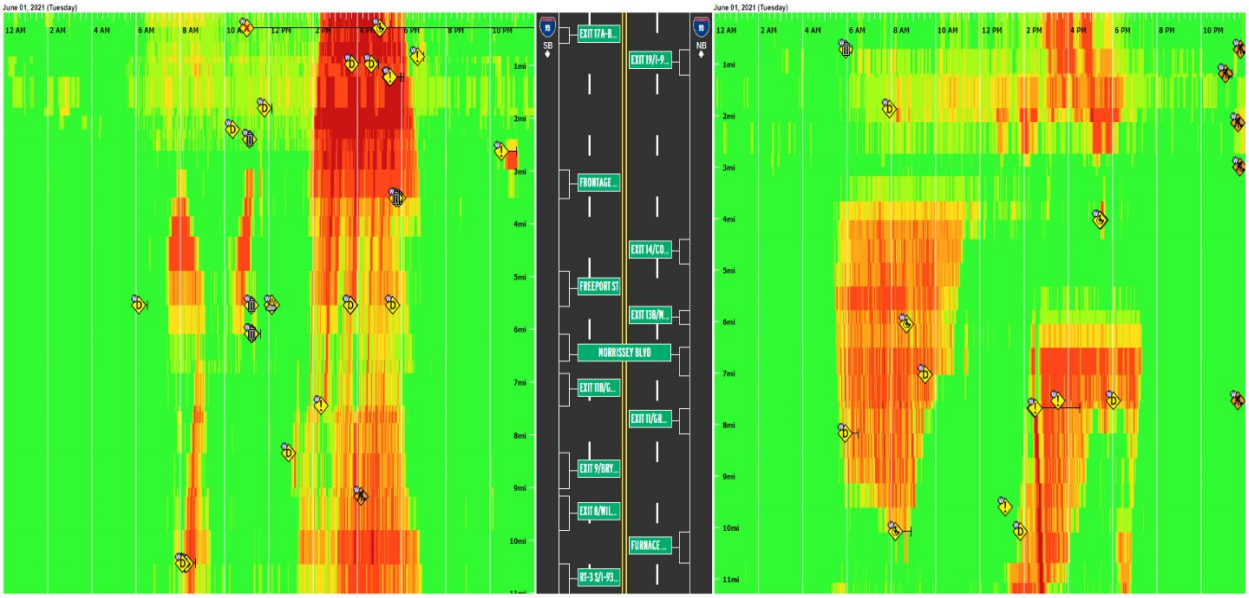

Figure 3.1: RITIS-generated 24-hour congestion scan

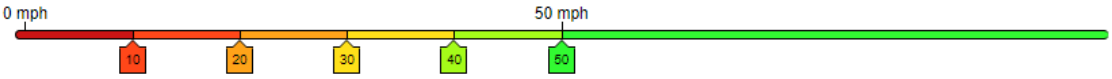

Figure 3.2: Color thresholds used in RITIS congestion scans

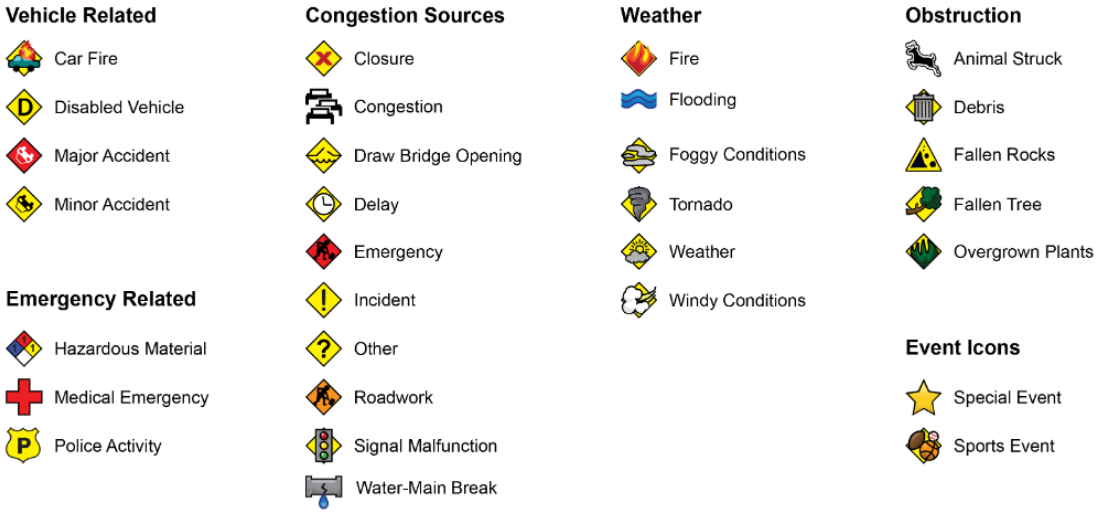

Figure 3.3: Icons for Waze reports used in RITIS congestion scans

Roadway segments can be identified based on XD or TMC codes. The difference between the two schemes is the length of the roadway segments that corresponds to a code, as follows:

- TMC segments range in length from very long, i.e., 30 miles (or even longer in some instances) to very short, i.e., 0.2 miles (Figure 3.4: the long segment 120+05791 surrounded by two very short segments 120P05791 and 120P05790); and

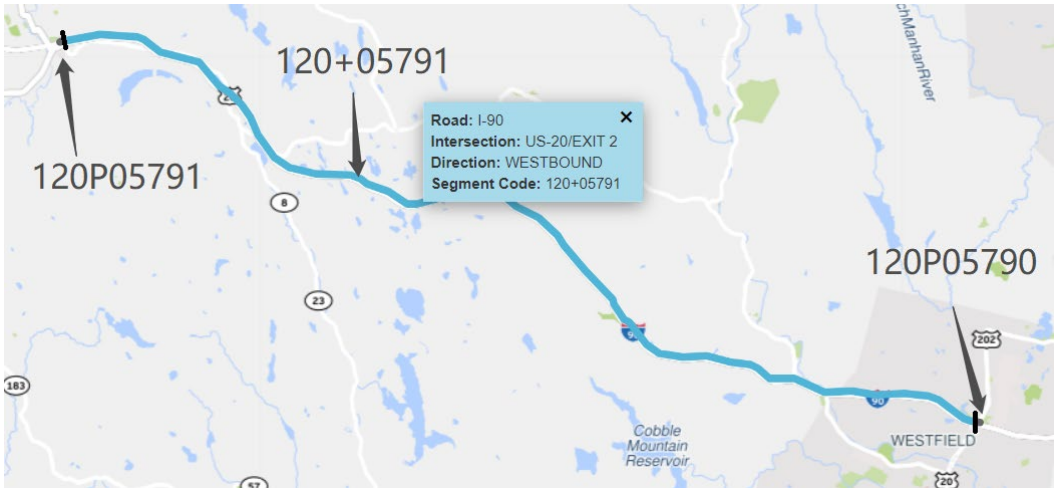

Figure 3.4: TMC consecutive segments 120P05791, 120+05791, and 120P05790 along I-90 W

- XD segments are more uniform in length and always shorter than one mile (Figure 3.5). Figure 3.6 shows the three XD segments nested inside the long TMC segment 120+05791 shown in Figure 3.4. It is expected that the spatial data granularity obtained through the XD geometry enables faster and more accurate detection of incidents.

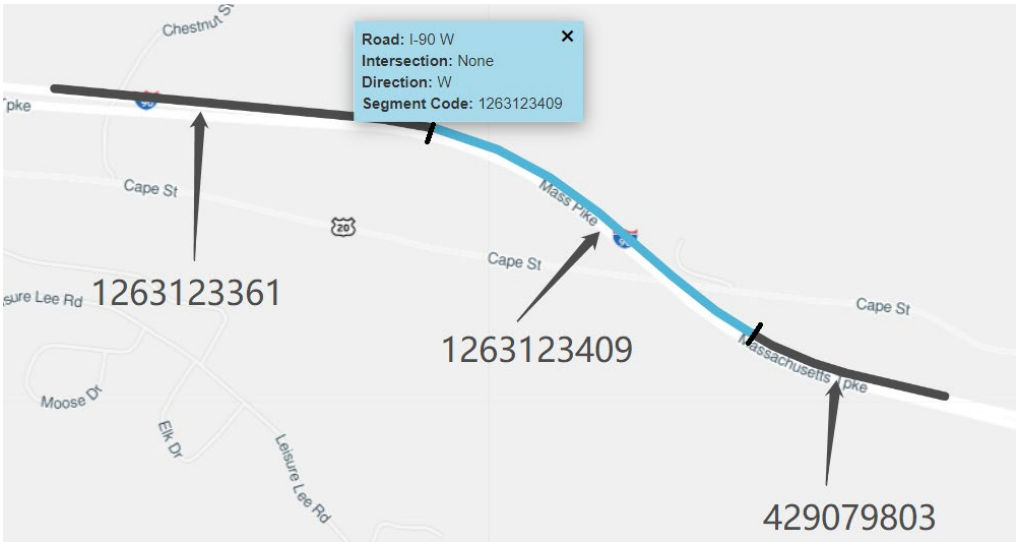

Figure 3.5: XD consecutive segments 1263123361, 1263123409, and 429079803 along I-90 WB

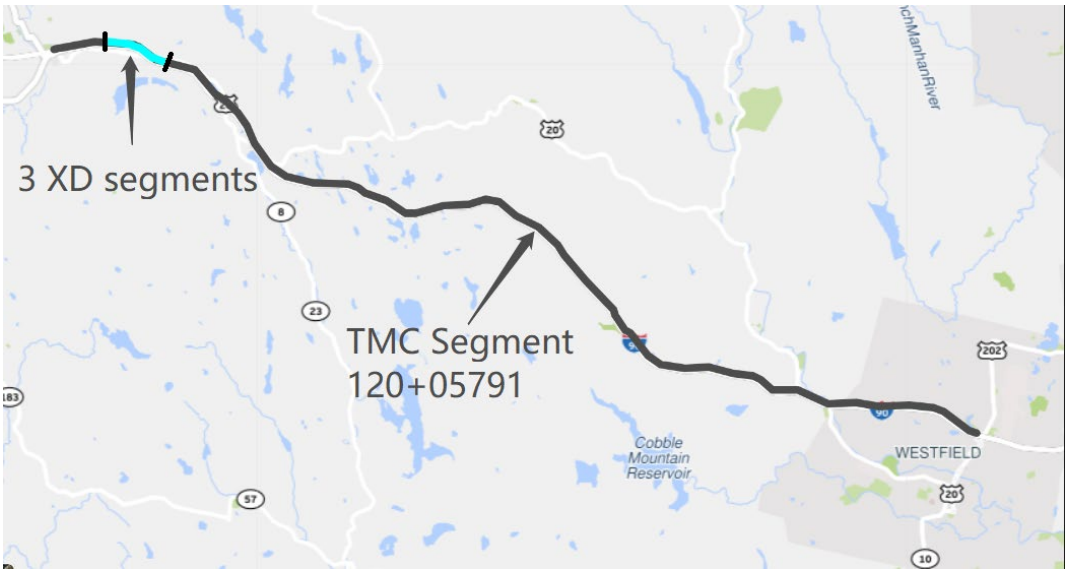

Figure 3.6: Comparison between XD segments (1263123361, 1263123409, and 429079803) in cyan and a long TMC segment (120+05791) in black

Information from sequential segments along a roadway has to be considered for the correct detection of an incident and the issuing of an alert. Figure 3.7 to Figure 3.9 show the values of the four parameters included in each record (speed, travel time, confidence score, and C-value), versus time (in minutes), during an incident on I-90 WB for XD segments 1263123361, 1263123409, and 429079803 in Figure 3.6. The incident occurred on XD segment 1263123409 (the middle segment among the 3 XD segments in Figure 3.5). The dashed lines indicate the start and end times of the incident, reported by MassDOT HOC.

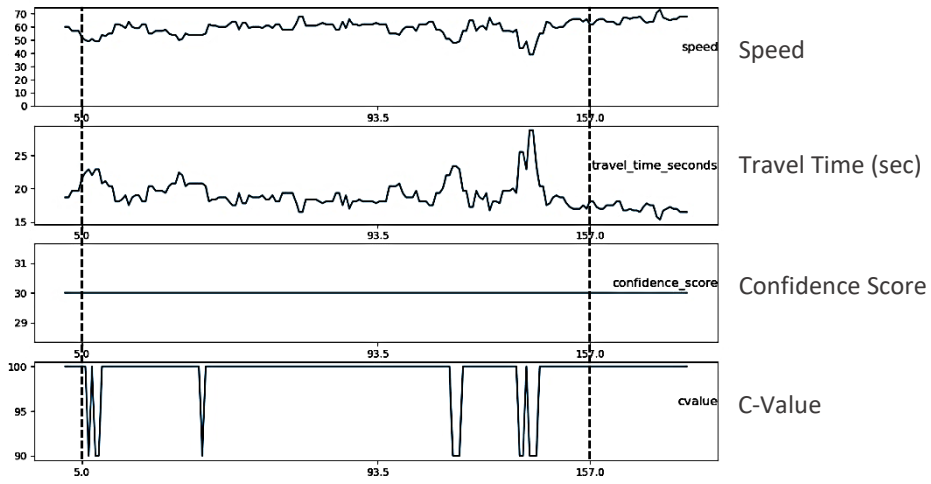

Figure 3.7: Data on XD segment 1263123361 (upstream from segment with the incident)

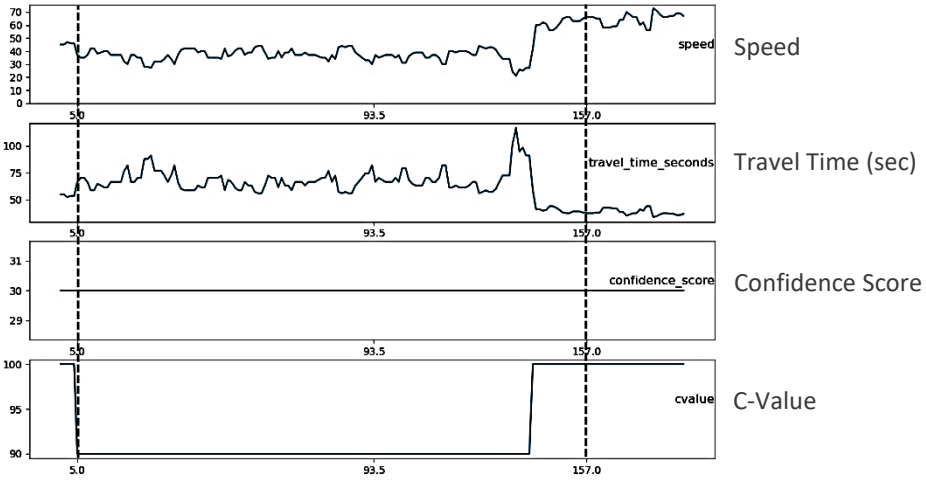

Figure 3.8: Data on XD segment 1263123409 (segment with the incident)

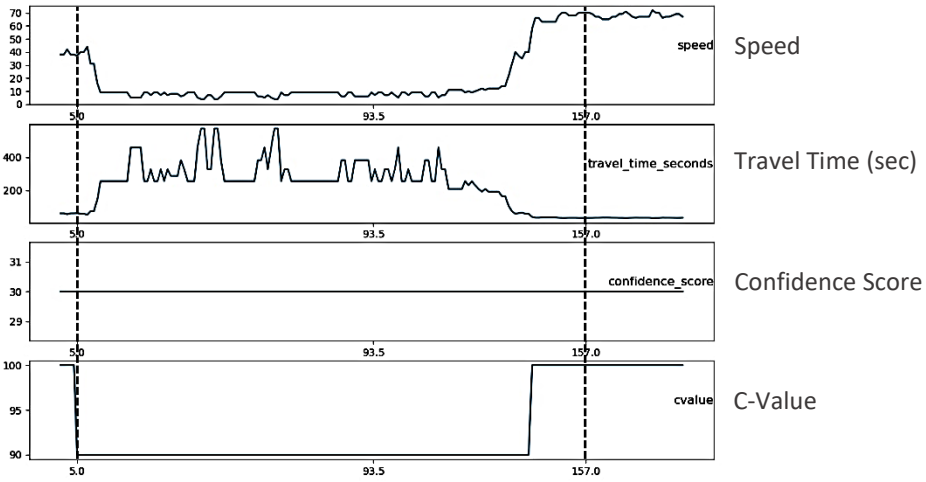

Figure 3.9: Data on XD segment 429079803 (downstream from segment with the incident)

3.2 MassDOT GoTime Data

The MassDOT GoTime program uses Bluetooth sensors installed along several state highways to collect information on the time and Mac-Address of devices on vehicles as they pass in front of the sensor. Using data from sequentially placed sensors the system can determine travel times on segments of the roadway based on the locations of the sensors.

The GoTime data are averaged over one-minute time intervals and are incorporated into the RITIS platform. The information that is available through the platform for each segment is similar to the INRIX data:

- one-minute average values of the space mean speed (over the GoTime segment),
- travel times (speed/length of segment), and
- reference speed.

The length of the segments for which data are available can be too long (longer than 30 miles), especially in rural areas. Figure 3.10 shows the GoTime segments that correspond to the incident shown in Figure 3.4.

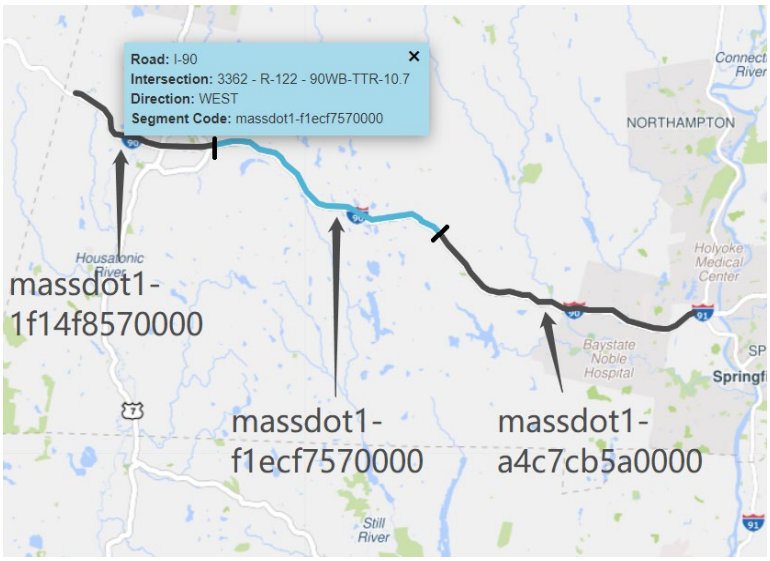

Figure 3.10: GoTime consecutive segments along I-90 WB

For comparison purposes the three TMC segments shown in Figure 3.4 are superimposed along the three GoTime segments in Figure 3.11.

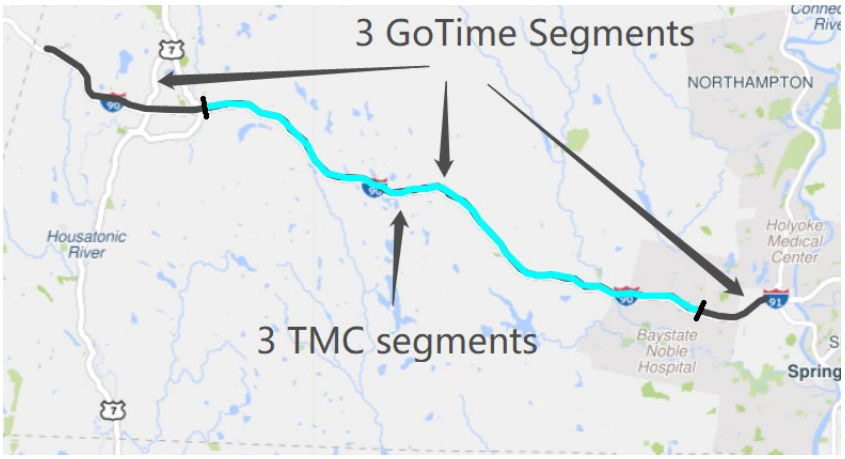

Figure 3.11: Comparison of GoTime and TMC segments along I-90 WB

Because of the long length of the segments in the GoTime program, data from this system were not used in this study. If an incident occurs at the beginning of the segment, depending on the amount of traffic, it will take too long for the average speed on the entire segment to drop enough, so the incident can be detected; if the incident occurs at the end of the segment, the average speed may not be affected at all.

3.3 Waze Reports

Waze collects traffic information through crowdsourcing on traffic events such as traffic incidents, crashes, stopped vehicles, road construction, debris on the road, etc. in the form of reports created by its users. Such information can be used, primarily for verifying the presence of an incident detected by an AID algorithm, but also for detecting incidents, especially under light traffic conditions, when the occurrence of a traffic incident causes minor reductions to the average speed.

Until February 2022, Waze reports were available through a platform supported by Waze (the Kibana platform). A user could specify the roadway segment and the time period for which reports were recovered. For the purposes of this study, for developing and testing the incident detection strategy, Waze reports would be recovered during a traffic event and for the roadway segment where the event took place. However, Waze stopped supporting the Kibana platform. MassDOT is developing a platform through which such information will be available, but until June 2022, only current events were recoverable.

Recently, RITIS incorporated Waze reports into its congestion scans, however this is not part of the information that can be downloaded from RITIS and used for the development and testing of incident detection strategies.

3.4 Conclusions

- Sources of traffic information that can be used for incident detection, ranging from conventional detectors to probe vehicles, GPS, crowdsourced data, and connected vehicles, are becoming increasingly abundant and have the potential to provide reliable and fast information on traffic incidents.
- Emerging methodologies for incident detection have the potential to correctly and quickly detect traffic incidents. They include field evaluations, ranging from traditional approaches using measurements of traffic stream characteristics, to automated incident detection based on various Artificial Intelligence strategies. AI methods can take advantage of the plethora of data available and recognize anomalies indicating the presence of a traffic incident by considering spatial and temporal relationships of data streams.
- Data available to MassDOT can be used in an AID system. Such data include one-minute space mean speeds on roadway segments and for the entire network, with very short latency. These data sets can be used for the development/training and testing of candidate methodologies for automatic incident detection.

4 Corridor Selection

The data sources that were used for developing and evaluating the incident detection strategy in this study included the one- and five-minute space mean speeds of the XD segments of the selected corridor as well as Waze incident records for the corridor. Waze reports were used for verifying the incidents detected by the proposed strategy. Both data sources cover all state roadways in Massachusetts. The corresponding data were available for 2022 and several past years. Therefore, the main criterion for selecting the corridor was the frequency of incidents. Traffic incidents are rare events as shown by the statistics in Section 2.2. For the purpose of demonstrating the effectiveness of the proposed algorithms, this research focused on a corridor with the highest incident frequencies.

The incidents used for selecting the corridor were provided by the MassDOT HOC for the period of January 2017 to April 2021. Only Roadway/Traffic events with a severity of Level 2 or above were considered. Such events include crashes, breakdowns, debris on the roadway, and so forth, and have a significant impact on traffic operations.

Based on the analysis outlined in this section, I-93-D6 was selected as the test bed for the development and the testing of the incident detection strategy. This corridor has all the properties required: it is covered by the available data to MassDOT; and it has a sufficient number of incidents during different weather, traffic and light conditions and on sections with different geometric characteristics.

4.1 Incident Frequencies

The first step in selecting the corridor was to count the number of incidents that occurred on different state roadways. During the period of January 2017 to April 2021, the incident records provided by MassDOT covered 136 state roadways. Table 4.1 summarizes the numbers of such incidents during this period on different state routes, which are ranked by their total number of incidents. The last row of Table 4.1 is for all remaining state routes with fewer than 450 incidents each.

Table 4.1: Incidents on Massachusetts state routes from 1/2017 to 4/2021

State Route	2017	2018	2019	2020	2021	Total
I-495	1,130	818	1,347	612	214	4,121
I-93	1,026	842	1,347	622	233	4,070
I-95	805	678	1,088	620	234	3,425
US-1	413	436	734	360	130	2,073
I-90	446	438	813	149	99	1945
RT-28	341	471	812	205	85	1914
RT-24	227	303	455	244	190	1,419
US-6	243	266	364	156	120	1,149
RT-3	242	227	381	147	79	1,076
I-195	215	186	321	204	80	1,006
RT-2	236	165	309	160	74	944
I-91	173	237	351	62	39	862
RT-128	217	144	230	107	101	799
I-290	185	190	318	34	22	749
RT-38	99	136	258	120	9	622
RT-1A	114	146	250	63	13	586
RT-3A	144	138	197	60	21	560
RT-9	124	122	174	51	19	490
US-3	124	93	196	38	25	476
Other State Routes	1,371	1,597	2,590	874	391	6,823

The number of incidents for 2021, in Table 4.1, is only for the first four months of the year. The year-to-year percent change in reported incidents, for the calendar years 2017 to 2020, is shown in Table 4.2. During 2019 there was a sharp increase in reported incidents throughout the state, while during 2020 there was a sharp decrease, evidently due to the reduced traffic because of the COVID-19 pandemic.

Table 4.2: Year-to-Year Change of Incidents on Massachusetts State Routes

State Route	2017–2018	2018–2019	2019–2020
I-495	−28%	65%	−55%
I-93	−18%	60%	−54%
I-95	−16%	60%	−43%
US-1	6%	68%	−51%
I-90	−2%	86%	−82%
RT-28	38%	72%	−75%
RT-24	33%	50%	−46%
US-6	9%	37%	−57%
RT-3	−6%	68%	−61%
I-195	−13%	73%	−36%
RT-2	−30%	87%	−48%
I-91	37%	48%	−82%
RT-128	−34%	60%	−53%
I-290	3%	67%	−89%
RT-38	37%	90%	−53%
RT-1A	28%	71%	−75%
RT-3A	−4%	43%	−70%
RT-9	−2%	43%	−71%
US-3	−25%	111%	−81%
Other	16%	62%	−66%

After discussions with the project monitor and other MassDOT HOC personnel it was decided to exclude Interstate I-90. For the remaining top six routes, the total number of incidents from 2017 to 2021 is shown in Figure 4.1. Interstates I-93, I-95, and I-495 have the most incidents, and they also have very high average daily volumes.

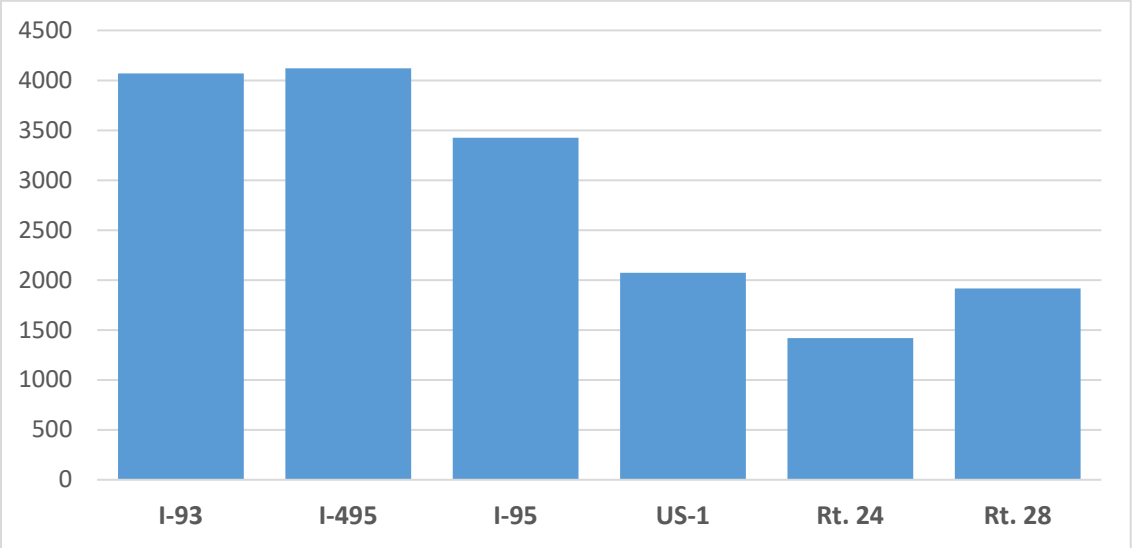

Figure 4.1: Incidents on the top six state routes

Selecting a corridor simply based on route incident frequency can lead to biased results, since longer routes often have more incidents. Therefore, the team took into consideration both route length and route incident frequency. The lengths of the six routes and their average numbers of incidents per mile per direction were calculated and are shown in Table 4.3 and Figure 4.2.

Table 4.3: Incidents per mile per direction for the top six routes

Route number	Number of incidents	Route length (mi)	Number of incidents/ mi/direction
I-93	4,070	46.4	43.9
I-495	4,121	120.6	17.1
I-95	3,425	90.1	19.0
US-1	2,073	85.9	12.1
Rt. 24	1,419	40.1	17.7
Rt. 28	1,914	150.4	6.4

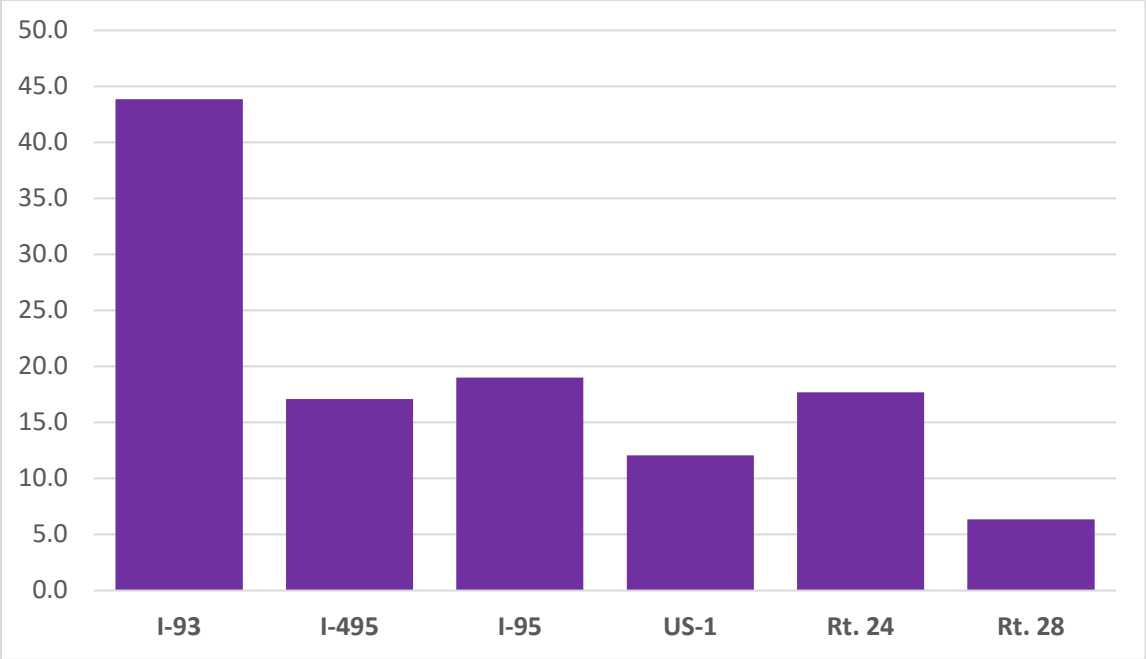

Figure 4.2: Incidents/mile/direction on the top six state routes

Interstate 93 has more than double the number of incidents of any other state route, therefore it is a good candidate as a test bed for developing and testing the incident detection strategy. The entire I-93 is too long to be used as a test bed for a pilot study; therefore, it was divided into two parts: (a) from its start at the Quincy split to Boston (segment of I-93 in District 6) and (b) from Boston to the New Hampshire border (segment of I-93 in District 4). The number of incidents in each segment and their lengths are: (a) 2,005 incidents over 10.4 miles and (b) 2,065 incidents over 36 miles, respectively. The average number of incidents per mile per direction with I-93 split into these two parts are shown in Figure 4.3, in which I-93 is split into District 6 and District 4 segments.

During the period considered (1/2017 to 4/2021), the segment of I-93 in District 6 (I-93-D6), shown in Figure 4.4 had about three times the number of incidents per mile per direction than any other state route. The high incident frequency for I-93-D6 is most likely due to the high traffic volumes carried by this freeway segment.

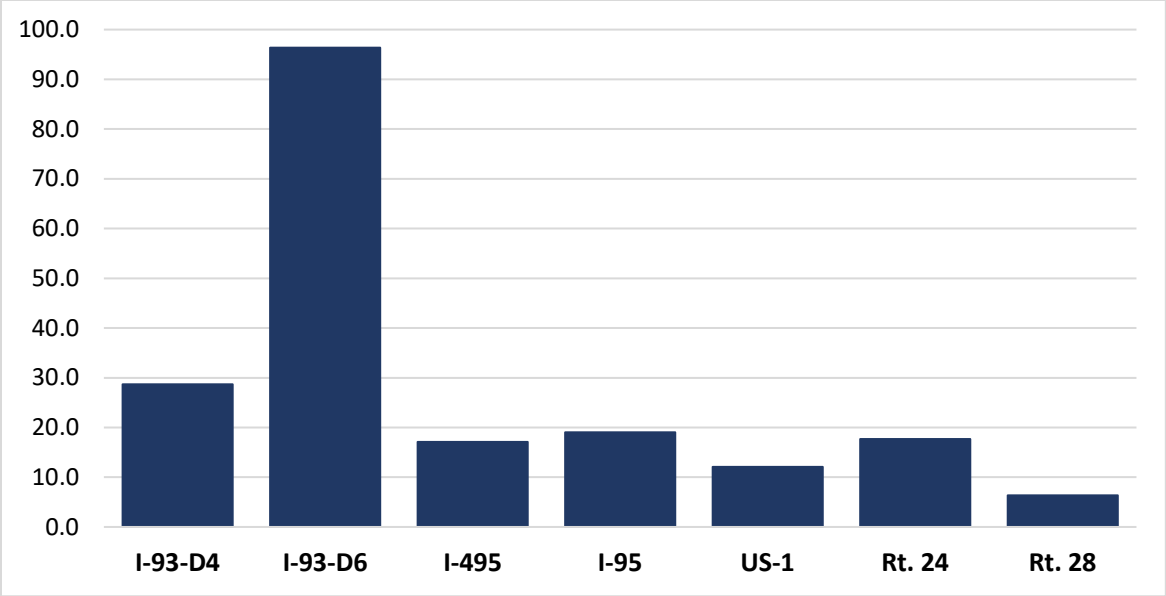

Figure 4.3: Incidents/mile/direction on the top six state routes

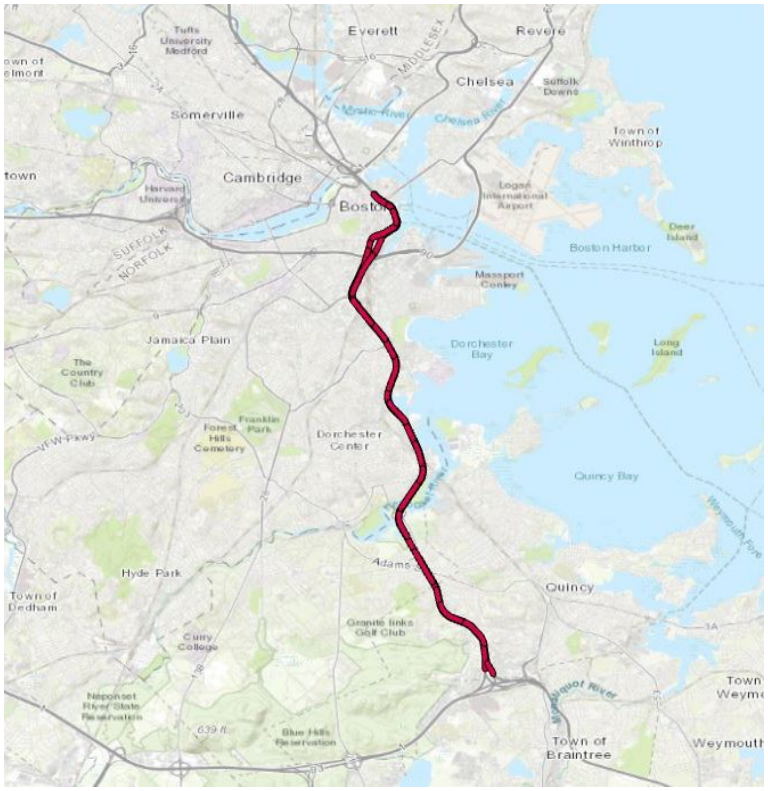

Figure 4.4: South segment of I-93 in District 6 (I-93-D6) from Boston to Quincy split

4.2 Distributions of Incidents on I-93-D6

In this section, various distributions of the incidents on I-93-D6 were prepared. For this purpose, we used the data during the calendar years from 2018 to 2020. The distributions considered are

- incidents in each month of the year,
- incidents in each day of the week,
- incidents in each hour of the day, and
- spatial distribution of incidents along the selected corridor.

This analysis was performed to ensure there is a sufficient number of incidents that can be used for developing and testing the incident detection strategy, comprising a variety of conditions, such as traffic, weather, light, and so forth. The number of incidents in each month of the year during the period of January 2018 through December 2020 is shown in Figure 4.4.

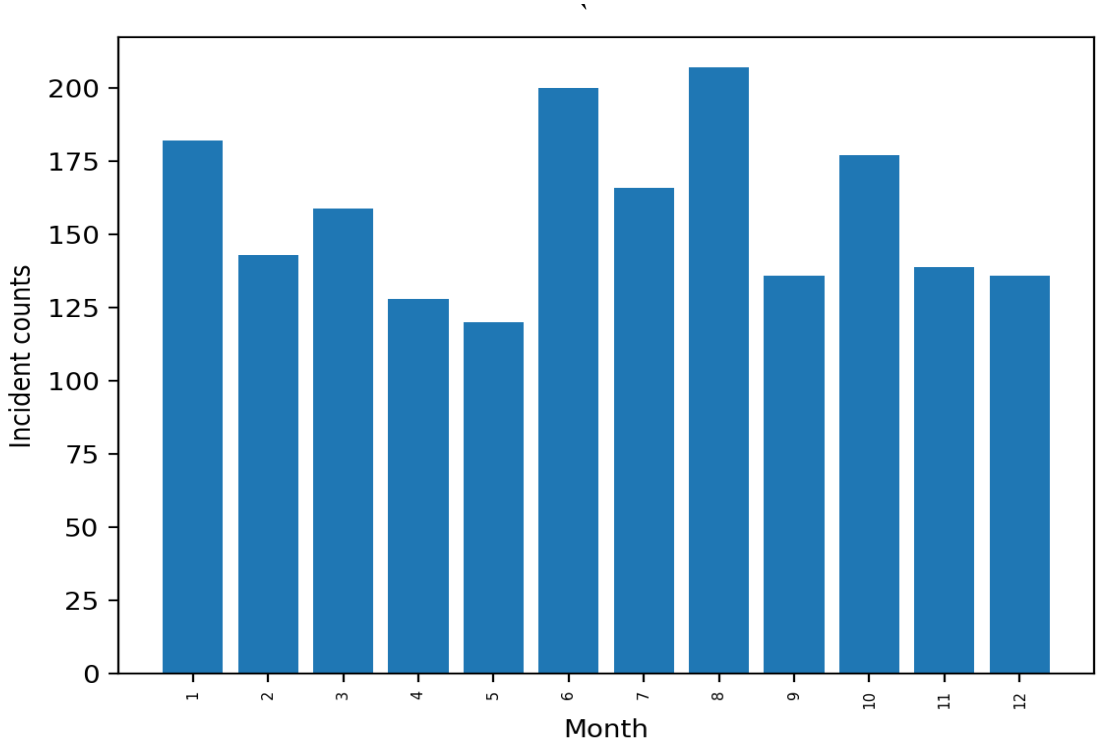

Figure 4.4: Incidents per month on I-93-D6

Figure 4.4 shows that each month has a significant number of incidents, with at least 120 recorded. The summer months of June to August display a peak, likely due to the surge in traffic toward the Cape and Islands. The ample number of incidents throughout the year guarantees that there are occurrences under diverse weather conditions that can be utilized for training and testing the incident detection model.

The number of incidents on each day of the week for the same period is shown in Figure 4.5, while the number of incidents in every hour of the day is shown in Figure 4.6. The number of

incidents follows the same pattern as the traffic volumes throughout the week. Higher traffic incident frequencies occur during the middle of the week, while lower frequencies are observed during the weekend when traffic volumes are also typically lower.

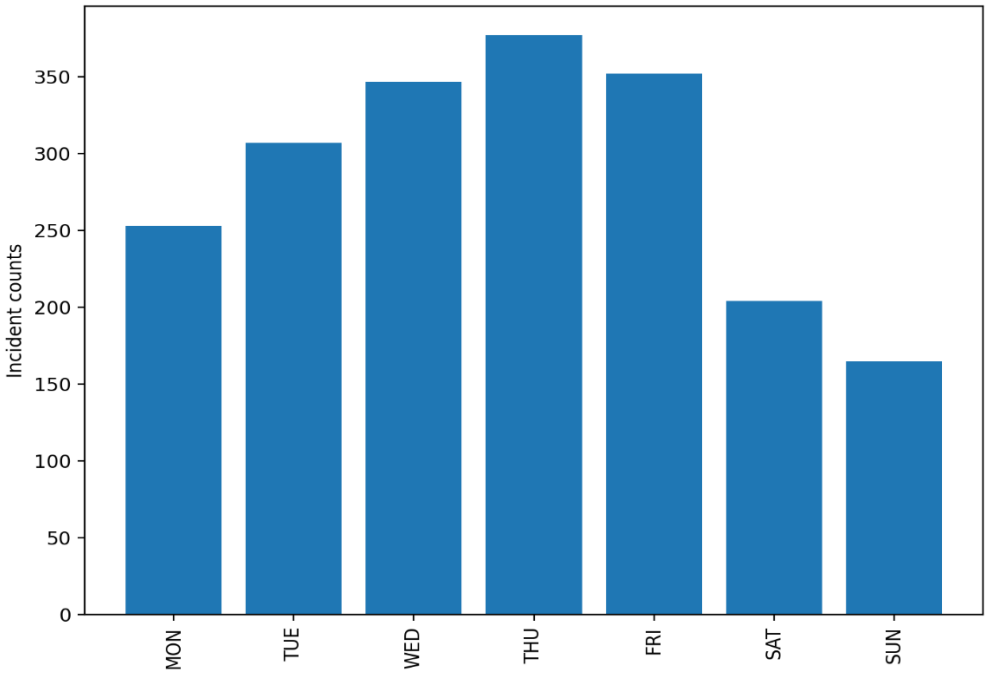

Figure 4.5: Incidents per day on I-93-D6

The same pattern is observed for the number of incidents during a day: there is an increase in incident frequency during the morning and afternoon peaks. A relatively high number of incidents (probably disproportional to the amount of traffic on the roadway) is observed during late-night hours between 10:00 p.m. and 1:00 a.m.

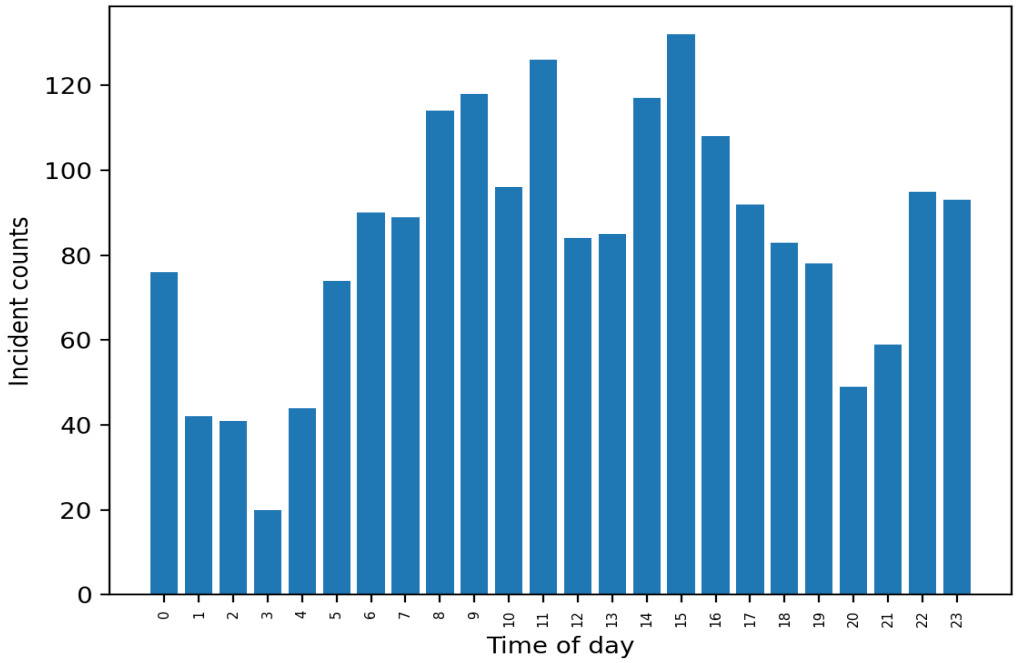

Figure 4.6: Incidents per hour of the day on I-93-D6

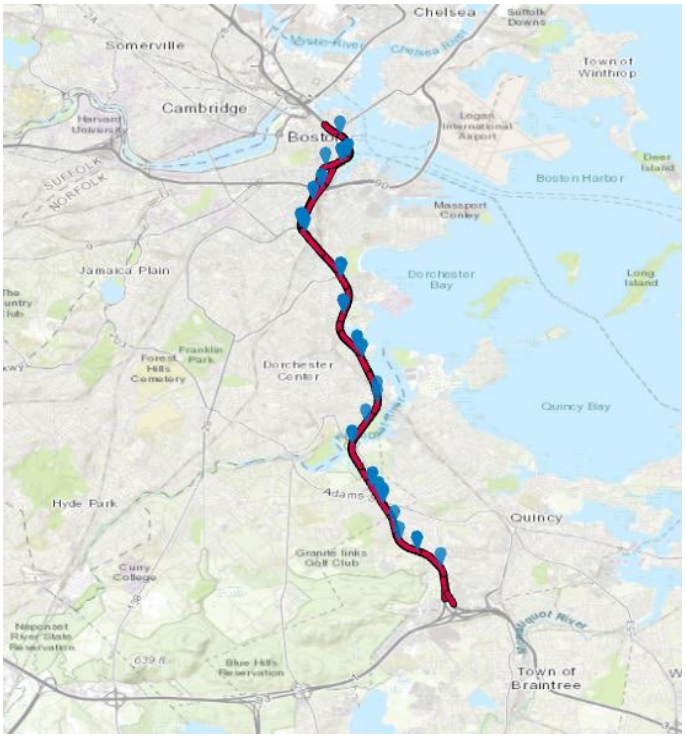

Figure 4.7: Incident locations on I-93-D6

The south segment of I-93 in District 6 consists of sections with different geometric characteristics, i.e., number of travel lanes, width of travel lanes and shoulders, and the presence of the HOV lane on a section of this south segment. The spatial distribution of incidents along this roadway for the period of January 2021 to April 2021 is shown in Figure 4.7. Incidents appear to be uniformly distributed, thus the geometric characteristics of different sections are not the predominant contributing factor in their occurrences.

Based on these observations, I-93-D6 has a sufficient number of incidents during different traffic and weather conditions and on sections with different geometric characteristics that enables the development and the testing of incident detection strategy. This analysis also provides insights into how historical incident data should be stratified for the establishment of base values for the activation of alarms.

Table 4.4 lists the 57 XD segments that are included in the section of I-93 in District 6. There are 24 XD segments in the northbound direction and 23 XD segments in the southbound direction. One-minute space-mean-speed data for the period 1/2018 to 12/2021 were downloaded from the RITIS platform for these XD segments. These records were used for the development of the base distributions of space mean speeds under normal conditions, so current observations can be characterized as inliers or as outliers indicating the presence of an incident leading to the activation of an alarm.

Table 4.4: XD segments on I-93-D6

Northbound	Southbound
128959360	386964859
386905455	386964865
386905454	440978614
386906636	1262964277
429056927	1262977162
1262968954	1262985447
1262974027	1262986958
1262974043	1263020045
1262986967	1263020294
1262988665	1263046143
1262993272	1263090316
1262993306	1263111350
1262993322	1263133715
1262997395	1263156327
1263011589	1263156342
1263047749	1263166971
1263071978	1263178282
1263156377	1263184372
1263162675	1263187978
1263166461	1263204379
1263166988	1263217624
1263226435	1263230448
1263231759	1263233170
1263232751	—

This page left blank intentionally.

5 Model Development and Implementation

Two models for detection of traffic incidents were developed and tested in this study. The first model is based on AI and the second is an empirical rule-based model. These models were applied for detection of traffic incidents on a segment of Interstate 93 southbound. The two models require the input data to be prepared in different ways. In this section, the two models and their corresponding input data preparation procedures are described in detail. Implementation results for the two models are also presented and compared.

5.1 AI Model

5.1.1 Description of AI Model and Model Inputs

AI has been widely used for solving regression and classification problems. Traffic incident detection essentially is a classification problem. The traffic state at a specific moment is characterized by a feature vector representing speed, occupancy, and so forth. This feature vector is then fed into a pretrained AI classifier and classified as either incident or non-incident. Two key elements for a successful AI-based classification application are choice of classifier and feature selection.

For any classification model (either AI, statistical, or other methods), selecting the right features is critical. Traditionally, occupancy, speed, and flow derived from point detectors such as inductive loops are used as input features for traffic incident detection. However, in many cases inductive loop detectors are available only at limited locations. Recently, data from in-vehicle navigation systems and mobile devices have been widely used by state DOTs. Such data has a much wider area coverage than traditional inductive loops and provides new opportunities for improving existing traffic incident detection practices. With these new data sources, the entire highway system is divided into small segments and the aggregated speeds of sampled vehicles on these segments within a short time interval (e.g., average speed for every 1-, 5-, or 10-minute interval) can be made available for incident detection purposes. INRIX data is used in this study. INRIX divides highways into small sections called XD segments. The input features include

1. lengths of the upstream, current, and downstream XD segments,
2. number of lanes of the current XD segment,
3. speed, average speed, and C-value of the upstream XD segment,
4. speed, average speed, and C-value of the current XD segment, and
5. speed, average speed, and C-value of the downstream XD segment.

To improve model performance, a 3-minute delay is introduced. For instance, the model makes a prediction at the end of 8:03 a.m. of what happened at 8:00 a.m. (i.e., three minutes ago) based on the 1-minute data points from 7:57 a.m. to 8:03 a.m. Therefore, for items 3 through 5 above, the speed, average speed, and C-value each refers to seven 1-minute observations. Each input feature in the data set is manually assigned a label (or target value) indicating whether it is an incident or not.

There are two main types of classifiers: supervised and unsupervised. Supervised classifiers require each input feature to be clearly labeled (e.g., as incident or non-incident). Labeling input features often is a very time-consuming process. Some recent methods such as deep learning typically require a large set of labeled input features to avoid model overfitting. On the other hand, unsupervised classifiers only need the input features and do not need labels. These methods can calculate the similarity/dissimilarity among the input features based on some distance metrics and automatically classify them into different categories.

A supervised learning method integrating LSTM [*40*] and variational autoencoders (VAE) [*41*] is adopted in this study. VAE is based on Autoencoder [*42*], which mainly consists of an encoder and a decoder. The encoder converts the input feature into a new feature in a latent space. This new feature is then decoded by the decoder. Through this encoding and decoding process, our goal is to reduce the noise or unwanted information in the data and reduce the dimensionality. A drawback of the original Autoencoder model is that the latent space depends heavily on the input data [*43*], making the model prone to overfitting. In the VAE model, the input features are encoded into a normal distribution over a latent space [*44*], which can help to mitigate the model overfitting issue.

Since the input features are time series in nature, we use an LSTM layer as the encoder. For the decoder, a multilayer perceptron (MLP) layer is used. The proposed algorithm samples a point from the encoded normal distribution and decodes it using the MLP layer. The decoder's job is to decode the hidden features and classify them as either incidents or non-incidents. More specifically, the decoded result is the probability for the input feature to be labeled as 1 (i.e., incident). A threshold can be chosen to further turn the probabilities into binary outcomes. For example, if the probability threshold is set to 0.9, input features with probability greater than (less than or equal to) 0.9 will be labeled as incidents (non-incidents).

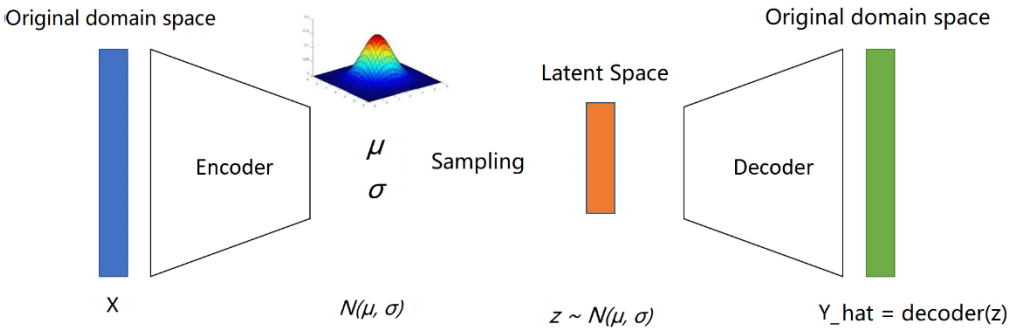

Figure 5.1: Structure of the proposed VAE model

Figure 5.1 [*45*] illustrates the proposed VAE model. Data samples (input features) in the original domain space are fed into an encoder. This encoder learns and generates a hidden normal distribution of the input features. From this learnable hidden distribution, the VAE model selects the same number (as the number of input features/records) of hidden representations in the latent space and sends them into the decoder to produce the classification labels, which are denoted as $\hat{Y}_i$ (Y_hat in Figure 5.1). At the end, the VAE model compares the generated labels with the ground-truth labels to calculate the loss and backpropagation.

In the backpropagation phase, both the standard binary cross-entropy (BCE) loss function and the focal loss function are evaluated. The focal loss function is an enhanced version of the cross-entropy loss function and is introduced to address the class imbalance problem. It gives more attention to samples in minor groups, which usually are more likely to be misclassified. This is achieved by assigning larger weights to those easily misclassified samples and smaller weights to samples that are typically classified correctly. However, our evaluation results suggest that the focal loss function does not perform any better than the BCE loss function shown in Eq. (5-1). Therefore, the BCE loss function is finally chosen in this study.

$$L_{BCE} - \frac{1}{n}\sum_{i=1}^{n}\left(Y_i \cdot log\widehat{Y}_i + (1 - Y_i) \cdot log\left(1 - \widehat{Y}_i\right)\right) \quad (5\text{-}1)$$

where

- n = the number of samples,
- Y_i = the ground-truth label of the ith sample, and
- $\widehat{Y}_i$ = the predicted probability for the ith sample to be 1.

The BCE loss function measures how well a machine learning model predicts the likelihood of a binary outcome. It is calculated by taking the average of the cross-entropy loss over all the training samples, where the cross-entropy loss is defined as the sum of the negative log likelihoods of all the correct predictions. The BCE loss function is widely used when training models for binary classification tasks. Figure 5.2 is an example showing how the BCE loss function value decreases as the number of epochs increases.

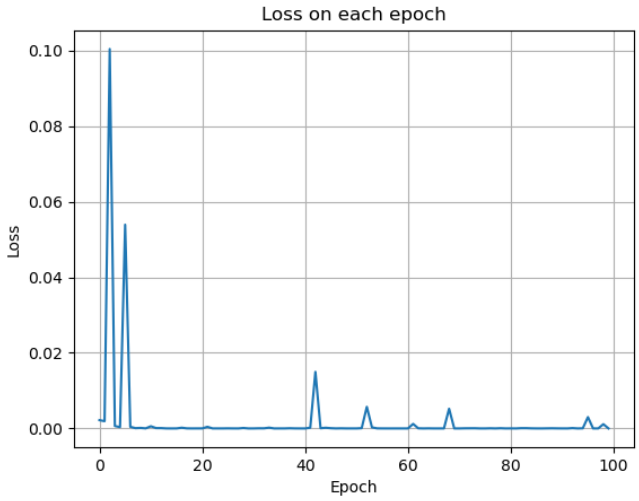

Figure 5.2: Structure of the proposed VAE model

LSTM is one of the well-known recurrent neural networks and a typical LSTM model is illustrated in Figure 5.3 [*40*]. It consists of four main components: a cell, an input gate, an output gate, and a forget gate. The cell remembers the values over time and the three gates update the cell values. The input gate embeds and determines the input information and updates the cell state. The forget gate decides whether information should be passed into the next layer or

forgotten at this stage. The output gate is to aggregate the information for the next layer of the LSTM model.

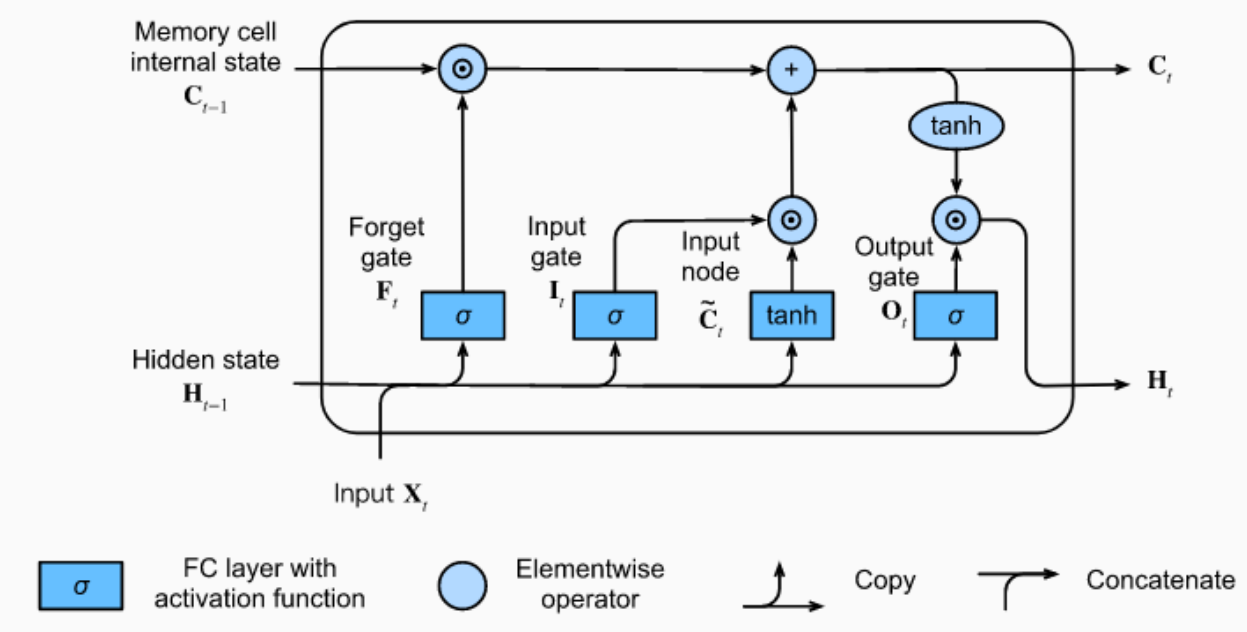

Figure 5.3: Structure of a typical LSTM model [*40*]

5.1.2 Data Preparation

Since a supervised learning model is used as the classifier in this study, a critical step is to identify traffic incidents from historical data and label them. The project team was provided with two sets of historical data: traffic incident records from the MassDOT HOC and the speed and travel time data made available through the RITIS platform.

From the HOC incident records, we can obtain the locations, start times, and durations of individual traffic incidents based on attribute fields "STARTED DATE," "END DATE," and "PRIMARY COORDINATE." Because such data was manually entered into the incident database, errors were difficult to avoid. In some cases, we found the incident locations were not on any highways. In other cases, we checked the start and end times of some incidents and could not find any matching signs of traffic congestion in the RITIS data. A possible explanation for the second issue is that some minor incidents did not cause any noticeable congestion. The RITIS data also includes the incidents reported by Waze App users. Again, the Waze incident reports do not always match the HOC incident records or the RITIS data. Some Waze reported incidents (e.g., a speed trap) are not associated with any traffic slowdowns manifested by the RITIS speed data. Since this study relies on RITIS speed and travel time data to detect traffic incidents, the developed algorithms cannot detect minor events that do not cause any speed disturbances.

The RITIS data is organized using two geographic units: TMC and XD segments. RITIS provides the speed, average speed, and C-value information for individual TMC or XD

segments. Each XD segment is usually less than 1 mile long. For XD segments near interchanges, where roadway geometry (e.g., number of lanes) changes frequently, their lengths are much shorter so that the resultant XD segments are homogenous. XD segments in general are shorter than TMC segments and provide more granular information. Shorter segments are also helpful in more accurately determining incident locations. Therefore, the XD segment data is used in this research instead of the TMC data.

To prepare the data needed for developing and testing our models, we started with selecting a highway segment. All incidents on this segment in the HOC database were identified. Based on the locations of such incidents, their XD segments (including upstream and downstream XD segments) were determined. The corresponding traffic data for these XD segments were extracted from the RITIS platform. Specifically, a segment of I-93 (shown in Figure 5.4) between Downtown Boston and Quincy was selected, which consists of 55 XD segments. Incident records for these XD segments between January 2021 to April 2021 were extracted from the HOC database. The RITIS data in 1-minute interval was considered. Although the data is also available in 5-minute and 15-minute intervals, a shorter interval will allow us to detect incidents more quickly.

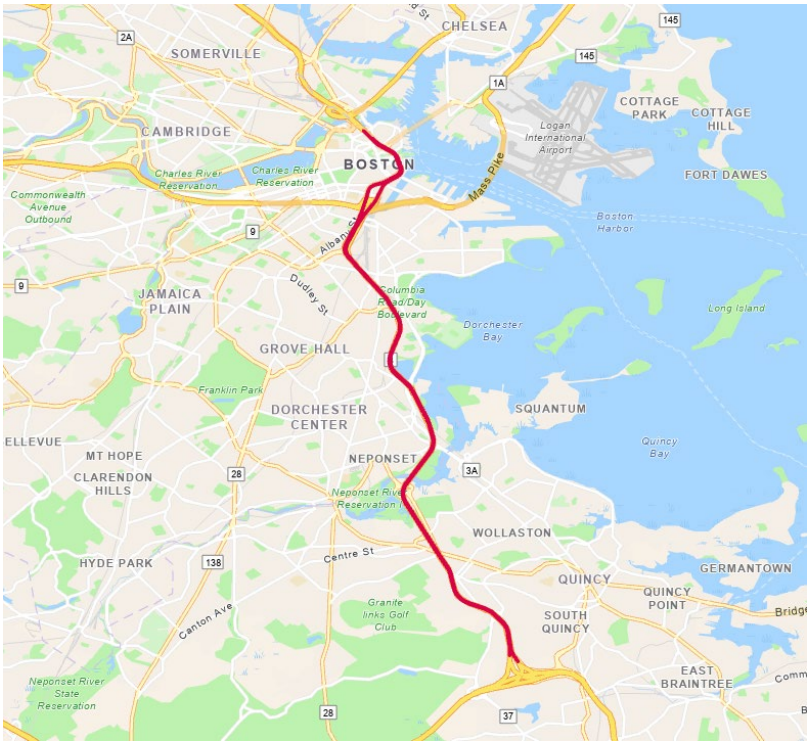

Figure 5.4: Segment of I-93 selected for this study

To develop incident detection models, an important step is to prepare the input features and label each one of them appropriately. This was done by manually correlating the HOC incident records to the RITIS data. Based on the start time, duration, and location of an incident in the HOC database, we checked the RITIS data to find the best matching XD segment. As discussed before, we considered the speed data 3 minutes before and 3 minutes after an incident. In other

words, a 7-minute time window was considered to generate the input features. We also included the speed data from neighboring XD segments immediately upstream and downstream of the incident. This is because incidents typically result in a pattern of increased downstream XD segment speed and decreased upstream XD segment speed. Finally, the 1-minute speeds, average speeds, and C-values of the three XD segments 3 minutes before and after the incident start time were used to form one input feature and this feature was labeled as "incident." Following the same approach, many "non-incident" input features were also generated. In total, we obtained about 1,500 labeled incident features and more than 2 million labeled non-incident features.

While the preceding procedure to prepare and label input features is seemingly straightforward, in general, several issues were encountered when implementing it. For example, for some incidents in the HOC database the RITIS speed data do not show any signs of congestion; speed reductions happen significantly before or after the incident start time recorded in the HOC database; and the upstream speed goes down earlier than the speed of the subject XD segment where the incident occurs, or the speed goes up and down without a clear pattern. These events were not used in our model development and testing. These examples indicate that preparing and labeling the input data is not straightforward, but rather a time-consuming and complicated process. It is significantly affected by the quality of the input data. For example, the HOC database suggests there were seven major incident-free periods between January 2021 and April 2021. Therefore, based on the HOC data, many non-incident features were generated for this period. Later, using the Congestion Scan tool in RITIS we found a major congestion event (not during rush hours due to recurring congestion) in one of the seven incident-free periods. Therefore, we had to go back and exclude all the corresponding input features.

5.1.3 Results of AI Method

Two performance metrics are used in this study, which are detection rate (DR) and FAR [Eqs. 2-1 and 2-1]. As the definitions [*46*] of FAR and DR suggest, smaller FAR and larger DR values are more desirable.

Various VAE model configurations have been evaluated in this study. The results of the best performing VAE model are FAR = 0.0069% and DR = 91.70%. This model considers the following hyperparameters: two LSTM layers, batch size = 1,024, learning rate = 0.01, and no focal loss.

Hyperparameters can have significant impacts on the VAE model results. For example, the number of LSTM layers affects the overall VAE model complicity and training time. The batch size also affects the time needed to train a VAE model. Properly choosing the batch size together with the learning rate can help to prevent the overfitting problem.

Besides the hyperparameters, choosing the right variables for the input features is critical for the model performance. Different variables were considered and evaluated. Among them, the 3+3 strategy (3 minutes before and after a decision point) appears to be the best one. We also examined other strategies such as 5+3, 4+4, and the 3+3 strategy with additional temporal and spatial features. As the name suggests, the $m + n$ strategy means we consider the speed, average speed, C-value of the upstream, current, and downstream XD segments m minutes before and n minutes after a decision point.

Based on the 3+3 strategy, additional temporal and spatial features were also explored. For the spatial features, we added the number of lanes for the upstream and downstream XD segments. For the temporal features, we encoded the timestamps by using cyclical encoding. The purpose of encoding the timestamps is to find out if the time stamp information is associated with traffic congestion. One day is equivalent to 1,440 minutes, and each minute was coded using a sine and a cosine value. Although we spent a lot of time exploring all these strategies, it was found that the original 3+3 strategy worked the best.

In addition, some data augmentation methods have been tried to address the imbalanced data set issue. One of the most popular methods for this purpose is the SMOTE [*47*]. In this research, an extension of the SMOTE called adaptive synthetic sampling (ADASYN) [*48*] was adopted, since some researchers [*48*] showed that ADASYN performed better than SMOTE. The evaluation results in this study show that ADASYN does not lead to better FAR and DR values.

As discussed earlier in this section, a threshold value is needed to turn the generated probabilities into incidents and non-incidents. Four candidate threshold values are experimented with in this study, which are 0.9990, 0.9985, 0.9980, 0.9975, and 0.9970. We select one day from each month between January and June to evaluate these candidate threshold values and try to find the best one. The evaluation results are presented in Figure 5.5 through Figure 5.14. There is a description at the top of each of these figures. For example, Figure 5.5 has "2021_0115_0.999_SB" at its top, which means this figure is for the results on 01/15/2021 using a threshold value of 0.999. "SB" at the end suggests that this figure is for the southbound of the selected corridor in Figure 5.4. The *x*-axis is time, and the *y*-axis is the distance from the beginning of the corridor. Note that due to missing values in RITIS, the *x*-axis intervals sometimes are not equal to 30 minutes. Figures 5.5 through 5.10 show results for January 15, 2021, and Figures 5.11 through 5.14 show results for March 15, 2021. All figures show southbound traffic.

As can be seen in Figure 5.5 through Figure 5.14, 0.9990 and 0.9985 seem to be better choices. Starting from 0.9980, the detection seems more reliable. By further decreasing the threshold value, the detection results become increasingly noisy especially when its value reaches 0.9970.

It is found that the optimal threshold value varies in different months. For March, it is clear that 0.9980 is not good enough to detect traffic incidents, while 0.9975 and 0.9970 perform better. This is evidenced by the congestion scan results for March 15 in Figure 5.14. When a threshold of 0.9980 is used, it is difficult to match the incident beginning location and time in Figure 5.11 with those in Figure 5.14, but under 0.9975 (Figure 5.12) and 0.9970 (Figure 5.13), we can find a better match with the incident start time and location in the congestion scan map in Figure 5.14.

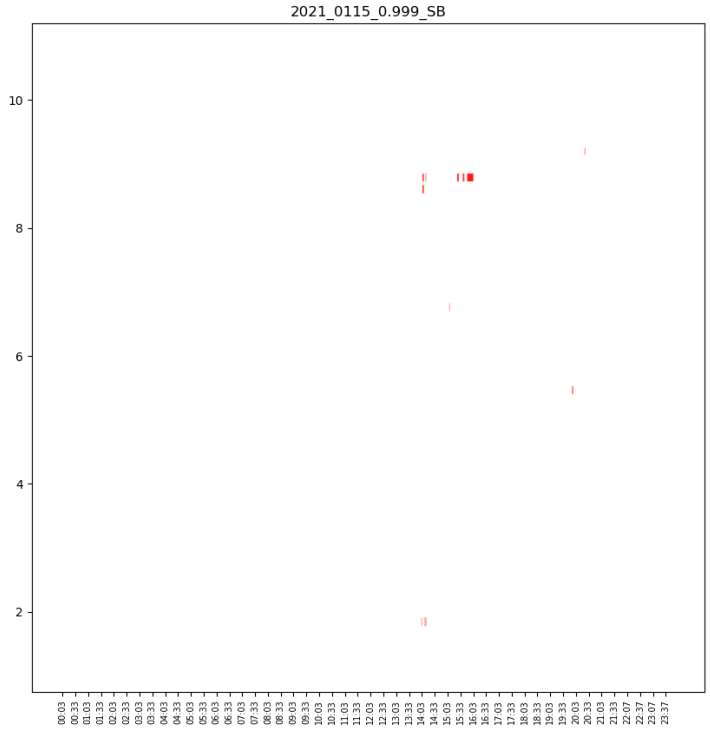

Figure 5.5: AI model incident detection results using a threshold value of 0.9990

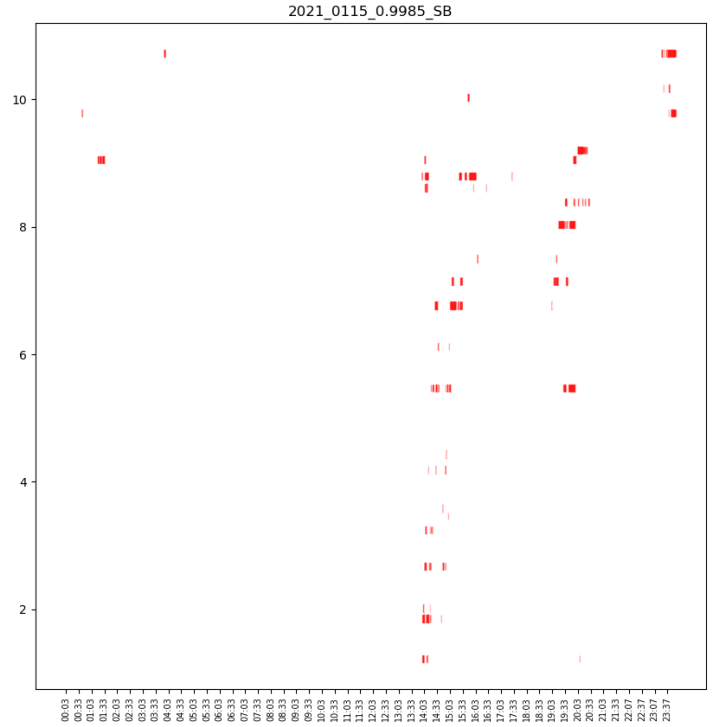

Figure 5.6: AI model incident detection results using a threshold value of 0.9985

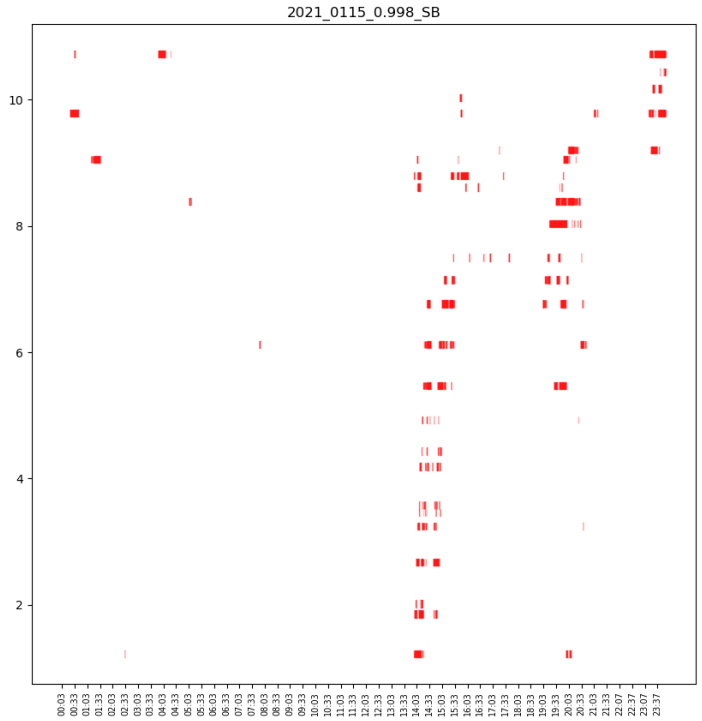

Figure 5.7: AI model incident detection results using a threshold value of 0.9980

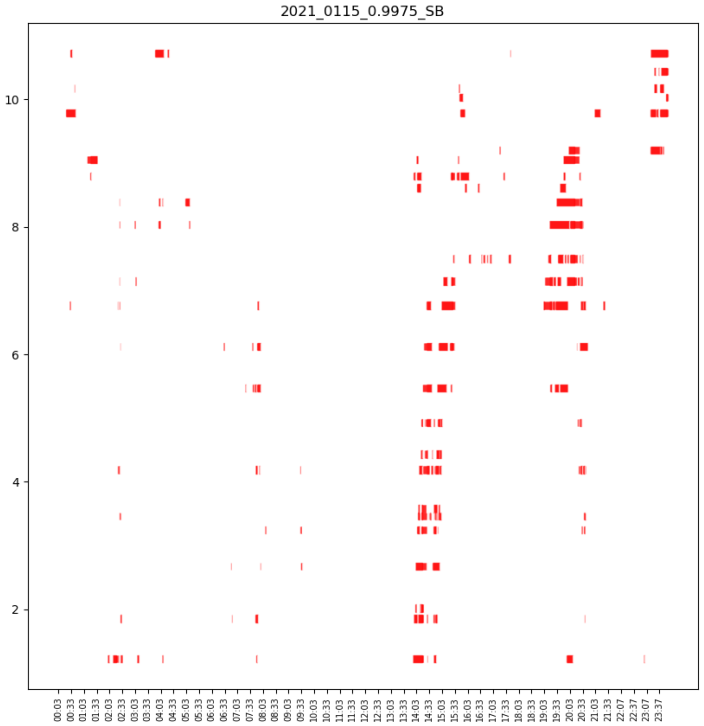

Figure 5.8: AI model incident detection results using a threshold value of 0.9975

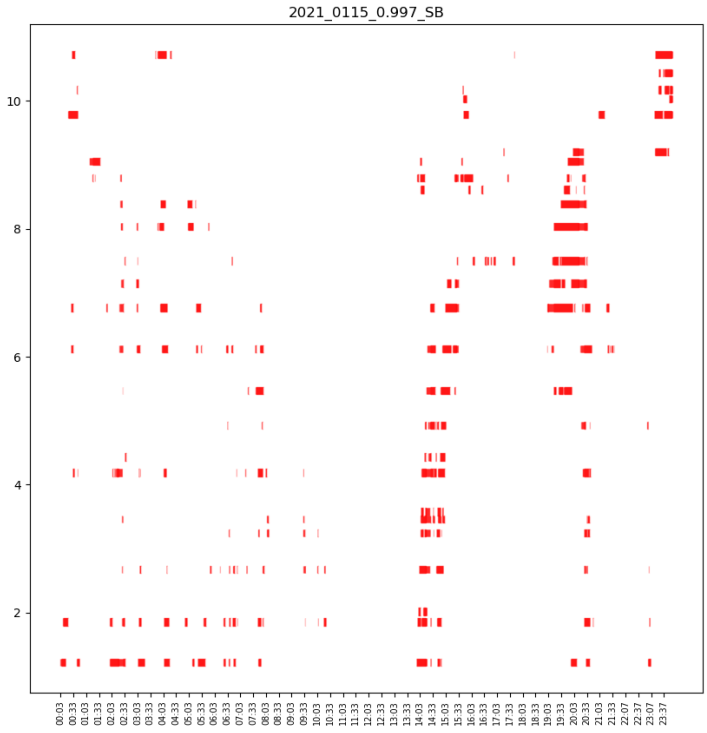

Figure 5.9: AI model incident detection results using a threshold value of 0.9970

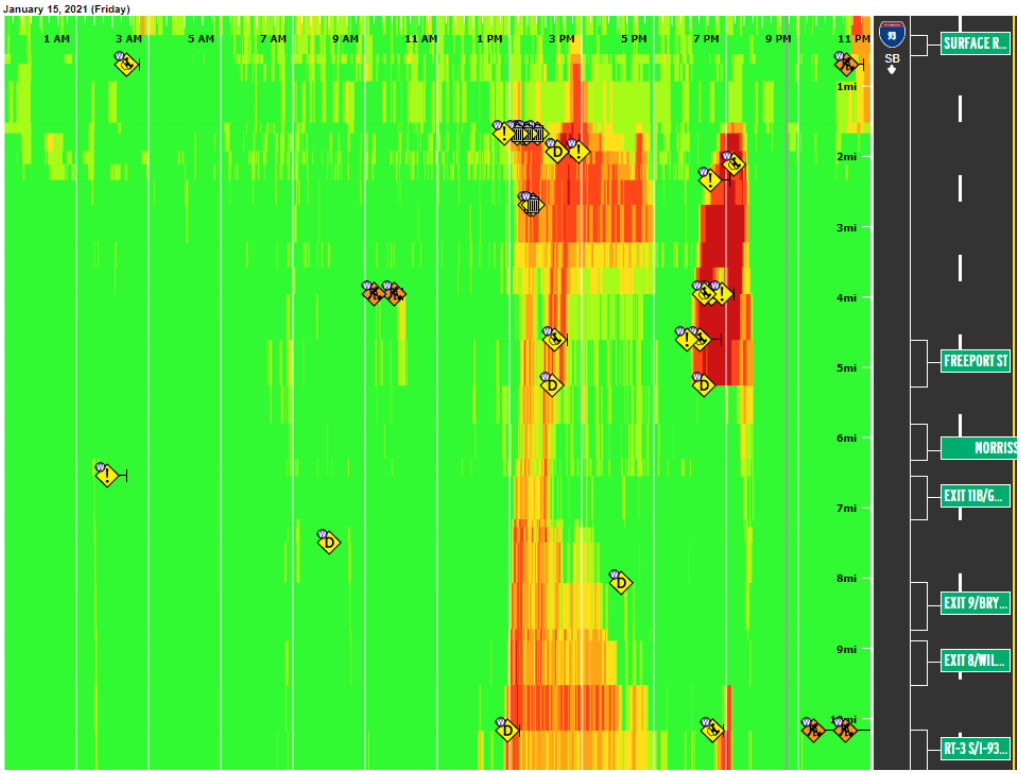

Figure 5.10: Congestion scan results for southbound traffic

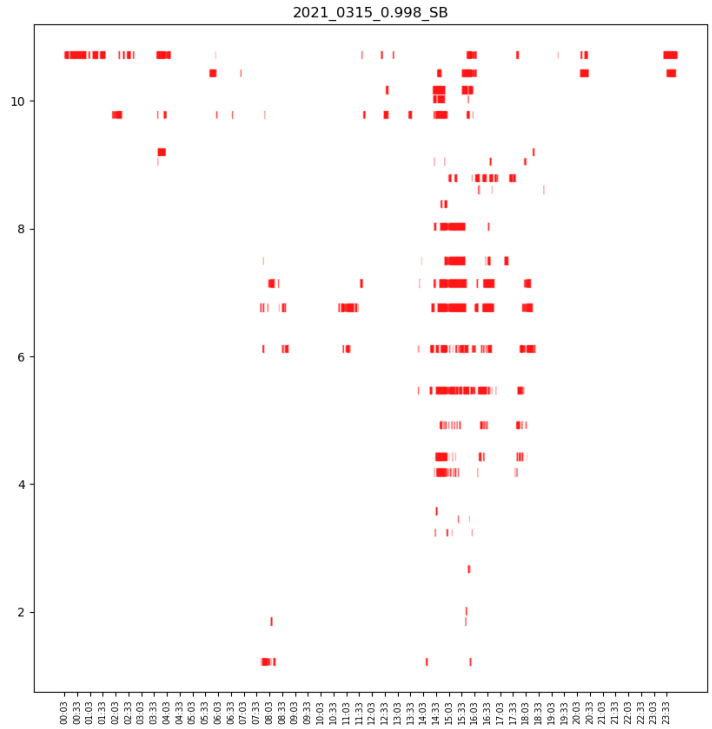

Figure 5.11: AI model incident detection results using a threshold value of 0.9980

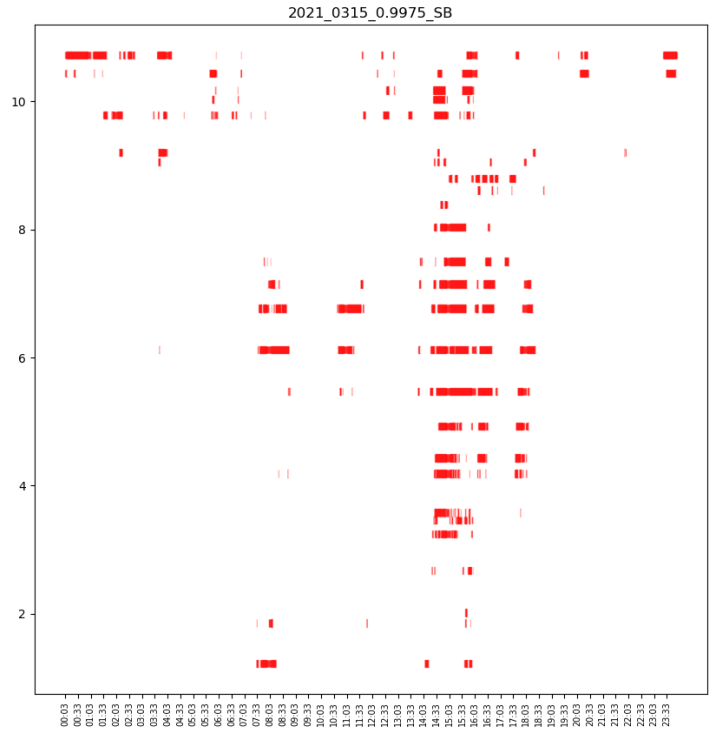

Figure 5.12: AI model incident detection results using a threshold value of 0.9975

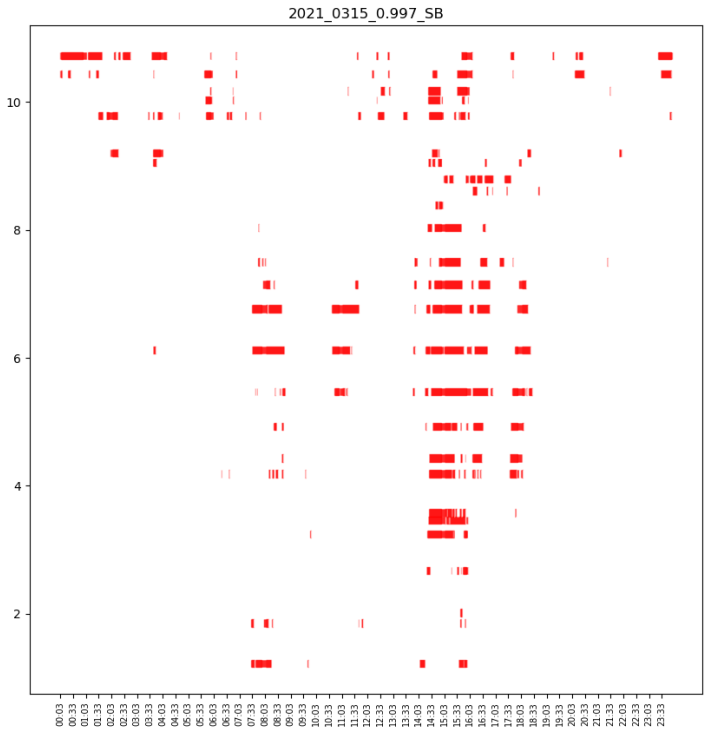

Figure 5.13: AI model incident detection results using a threshold value of 0.9970

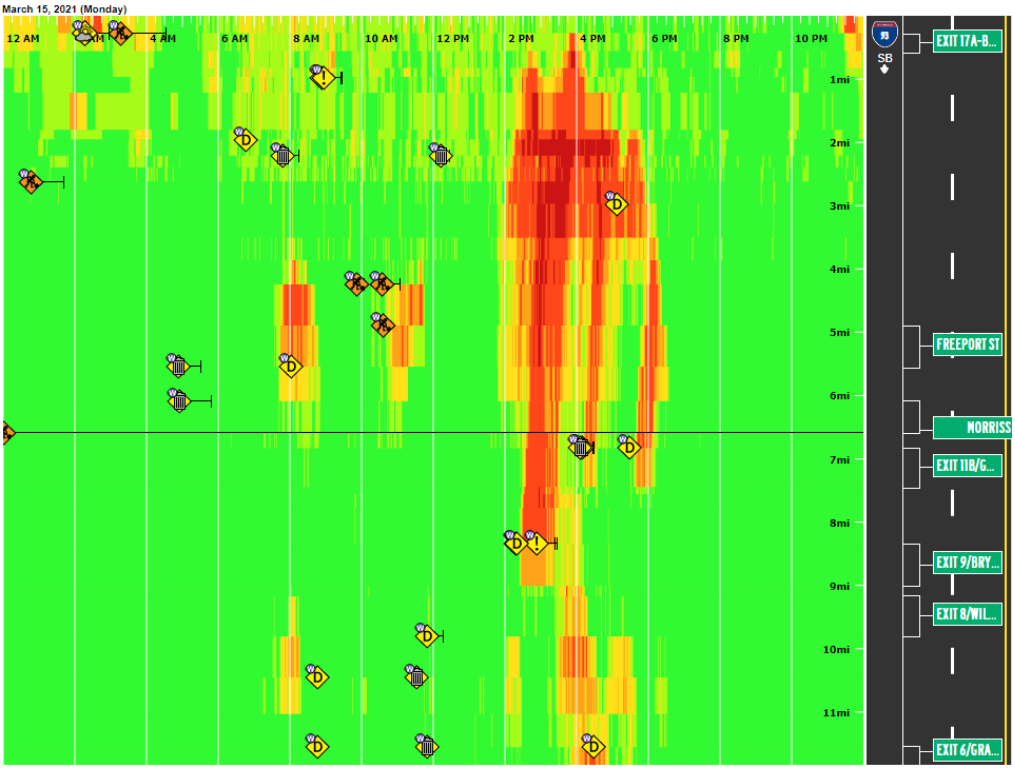

Figure 5.14: Congestion scan results for southbound traffic

5.2 Empirical Rule-Based Methods

5.2.1 Overview of the Rule-Based Methods

The AI method in the previous section is a Blackbox solution. Although it works, we do not know exactly the underlying mechanism. For transportation agencies, knowing how the system works is also important. Therefore, we also develop an empirical rule-based method. This method uses threshold values on the observed traffic parameters, i.e., space mean speeds along with their corresponding confidence parameters, available through the RITIS platform. When the currently observed speed on a road segment drops below the selected threshold value an alarm will be issued, requiring the HOC operator's attention. For this purpose, first the distributions of speeds at different time periods and different locations must be developed, and then various percentile values of speed, to be set as thresholds, can be tested for their effectiveness in detecting incidents.

5.2.2 Data

The same corridor (Figure 5.4) for developing the AI method is also considered here. This corridor consists of 55 XD segments. Figure 5.15 shows how the speeds of adjacent XD segments change over time due to an incident that occurred around 5:06 p.m. on 3/8/2021 in XD segment 1263231759. The corresponding congestion scan map generated by RITIS is shown in Figure 5.16. The top half of Figure 5.15 is for speed changes and its *y*-axis measures miles per hour. The bottom half shows the confidence values of those speeds, and its *y*-axis values are between 0 and 100, with 100 being the most confident. The two vertical yellow lines represent the reported incident start time, which was obtained from the MassDOT HOC database. Figure 5.15 shows that the speeds of all three XD segments decreased before the reported incident start time, suggesting there was a delay between when the incident occurred and when it was documented. Among the three XD segments, the current XD segment speed (continous line) went down more quickly than the other two, since vehicles in that segment were affected immediately by the incident. The downstream XD segment speed dashed line) also went down significantly. This probably was because the incident location was close to the beginning of the downstream segment, and it took drivers some time to speed up. Note that the downstream XD segment speed recovered earlier than the other two XD segments, which is reasonable.

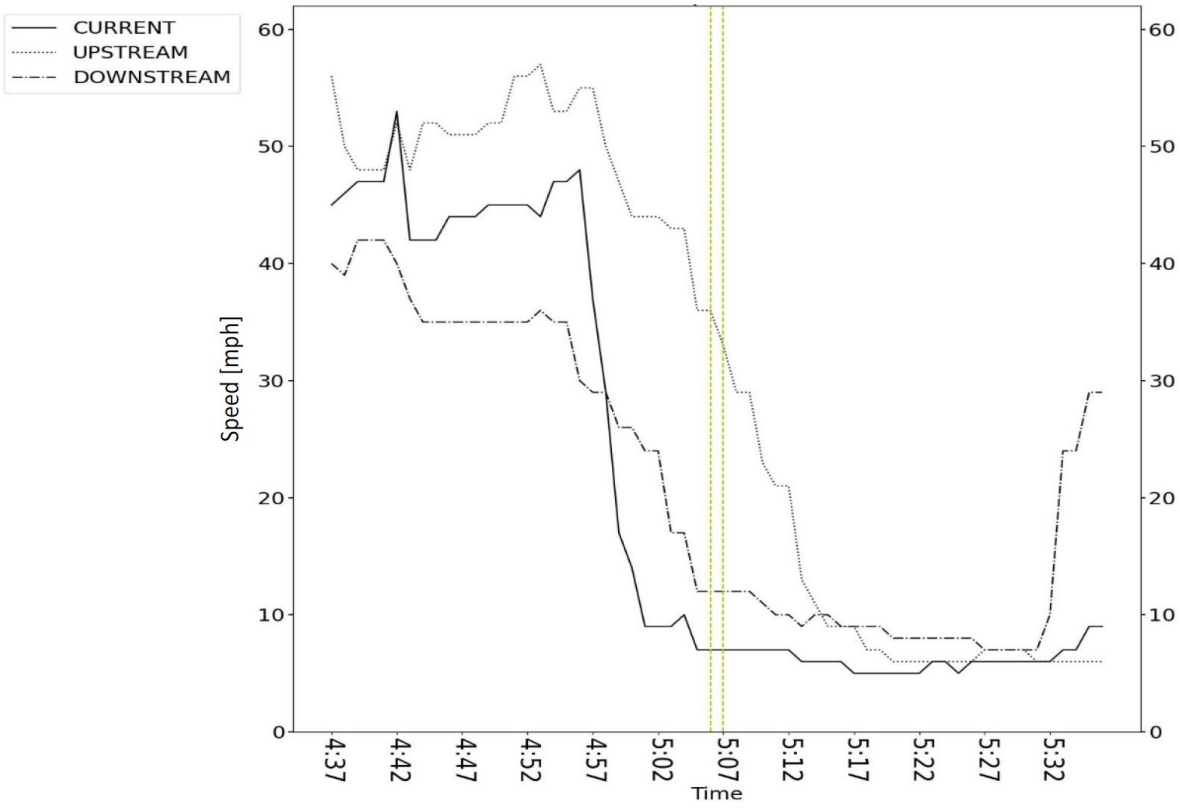

Figure 5.15: Speed changes on consecutive XD segments due to an incident

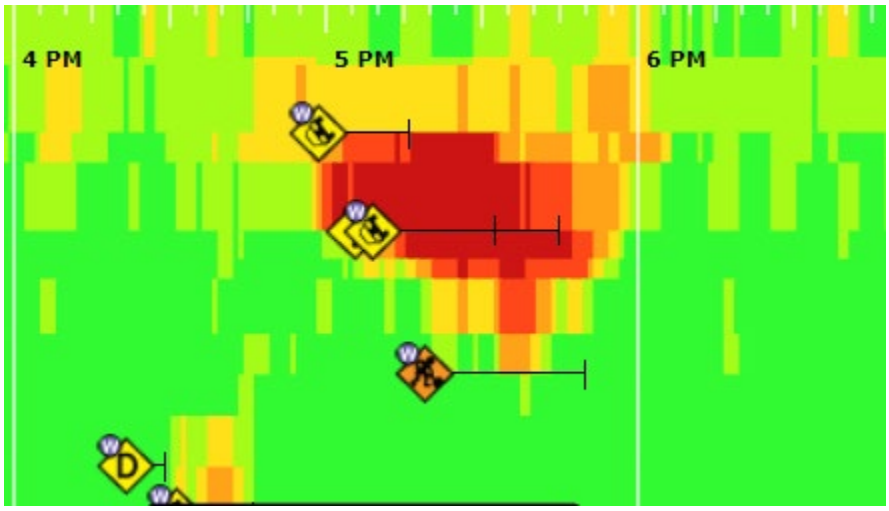

Figure 5.16: Congestion scan results for an incident in XD segment 1263231759

5.2.3 Speed Distributions

The RITIS platform provides speed data for every one-minute time interval for each XD segment. The records used in the following analysis are from January to December 2019 and

2021 and January to October 2022. Records during 2020 were omitted due to the impacts of the pandemic that may have caused the data to be biased—observed space mean speeds were generally higher than normal. The time stamp of each speed data record provides information such as year, month, weekday versus weekend, exact time, and so forth. Such information allows us to generate speed distributions for a specific time frame (e.g., a month, winter, summer, weekdays, weekends) or exclude the impacts of holidays.

To establish the distributions of speeds at different time periods and different locations certain levels of data aggregation must be applied. This is necessary, so the distributions can be developed by using a reasonable number of observed values. Therefore, time periods when traffic patterns are expected to be similar must be identified and grouped together. The following procedures were used:

- It is reasonable to assume that traffic patterns (and speeds) are similar during weekdays but different during weekends; therefore, records were grouped based on weekdays and weekends.
- To take into consideration seasonal effects, observed speed records were grouped for each two consecutive months (January and February, March and April, etc.) for the three years the data were used.

Based on this, for each XD segment there are 17,280 distributions (60 minutes/hour × 24 hours/day × 2 types of days × 6 two-month-periods/year); and each distribution is constructed based on 130 speed observations for weekday distributions and 52 speed observations for weekend distributions (on average; the exact number depends on the numbers of weekdays and weekends in each 2-month period). Figure 5.17 shows these distributions for the XD segment 1263156377 (I-93 northbound) for weekdays and for the June to July period (a total of 1,440 distributions). Each graph includes 60 such distributions for each hour of the day. The *x*-axis is for speed, the *y*-axis is for minutes in an hour, and the *z*-axis is for speed frequency.

Figure 5.18 shows more clearly these speed distributions for the period of 5:00 a.m. to 6:00 a.m. It can be seen that their shapes are quite irregular, mostly due to the limited number of observations.

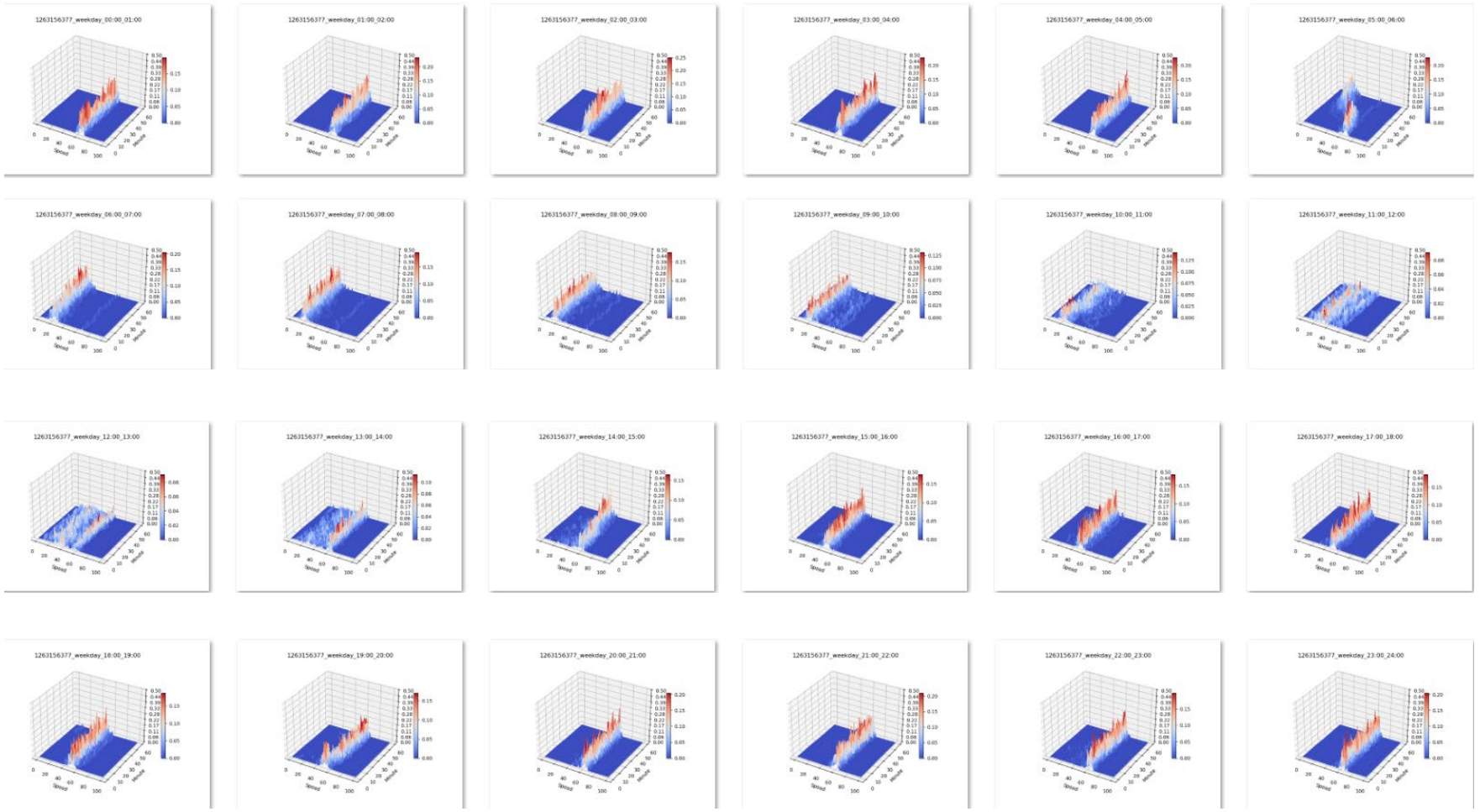

Figure 5.17: One-minute distributions of observed speeds

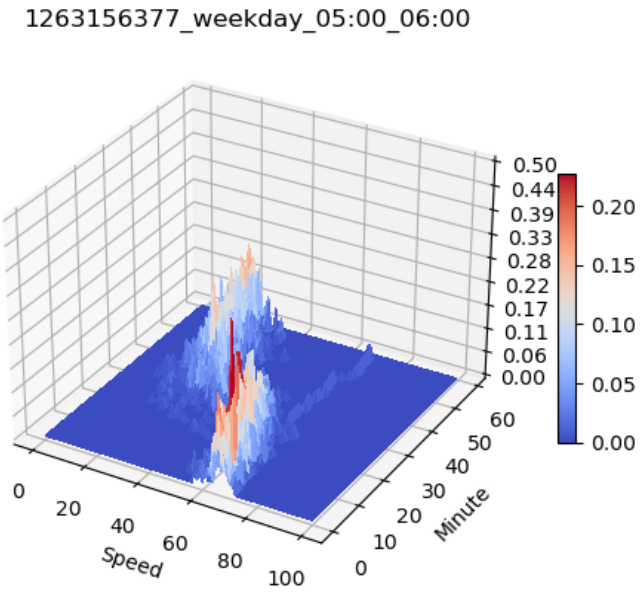

Figure 5.18: One-minute distributions of observed speeds, 5:00–6:00 a.m.

To improve the shape of these distributions, a two-step strategy is used which includes averaging and kernel density estimation (KDE) smoothing steps.

- RITIS provides average speeds using 1-minute as well as 5-minute intervals. Instead of the 1-minute speed values that exhibit too much randomness, the 5-minute average speeds are used since this data is less noisy. In the averaging step, we further consider the average speeds of the previous, current, and next 5-minute intervals. These three 5-minute average speeds are averaged again, and the mean value is then assigned to the current 5-minute interval. In other words, for every 5-minute interval, its average speed is calculated from a 15-minute time window. The 5-minute speed distribution for the same XD segment and period as in Figure 5.18 (i.e., 1263156377) is shown in Figure 5.19. The new distribution clearly looks smoother, but still, they look like discrete histograms, with the height of each bar representing the percentage of points in each 1 mi/h speed increment.

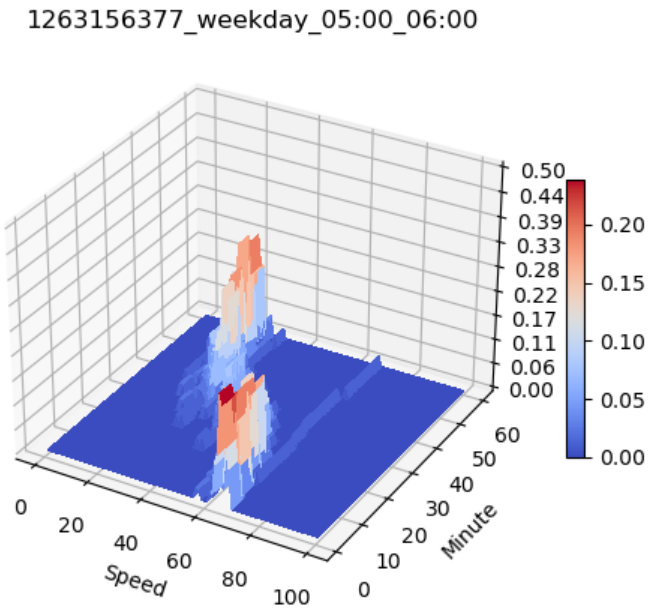

Figure 5.19: Five-min. distributions of observed speeds, 5:00–6:00 a.m.

- To convert the histogram to a continuous curve, the KDE is used. KDE is a non-parametric method for estimating the probability density function of the speeds, based on the limited data sample obtained through the previous step. KDE uses the normal distribution kernel to represent the points, then all the kernels are summed up to generate the final distribution.

The results of this two-step approach, for the same period and same XD segment as in Figure 5.19, are shown in Figure 5.20. By using 5-minute distributions, instead of 1 minute, for each XD segment the number of distributions is reduced to 3,456. For comparison purposes Figure 5.21.a and Figure 5.21.b show the speed distributions for the same XD segment (XD 1263156377) and the same time period (5:00–6:00 a.m.), but for the months of January and February and for weekdays (Figure 5.21.a) and weekends (Figure 5.21.b).

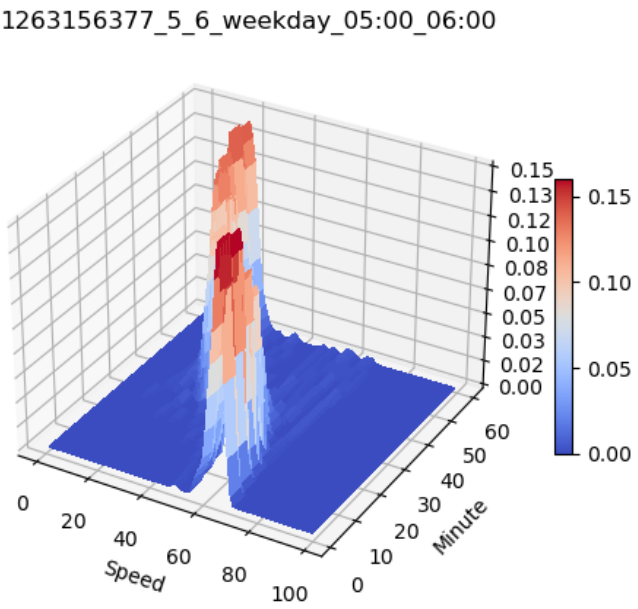

Figure 5.20: Smoothed 5-minute speed distributions, 5:00–6:00 a.m.

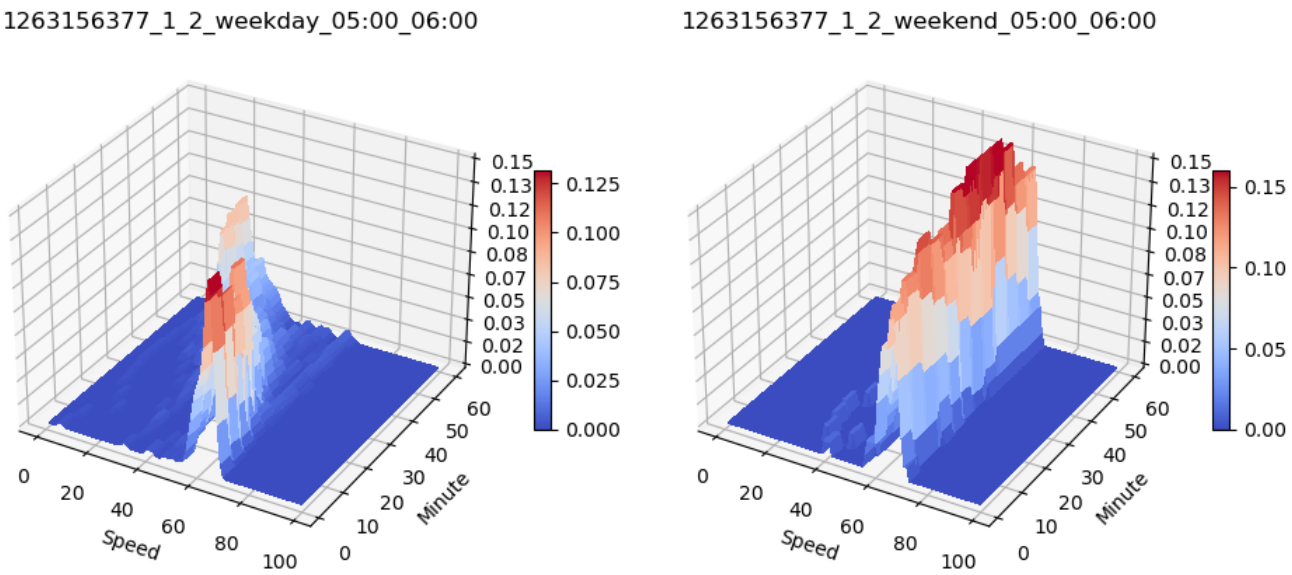

(a) (b)

Figure 5.21: Smoothed 5-minute speed distributions: (a) weekdays; (b)weekends

5.2.4 Establishment of Threshold Values

Once the distributions for all XD segments in the test corridor and for all time periods were developed, the threshold values of speeds observed in these segments for non-incident conditions must be established. If the speed observed in a segment falls below the threshold value, an alarm will be issued requiring the operator's attention to verify that there is an incident or cancel the alarm.

As a first approach for establishing effective thresholds, for each of these distributions the mean μ and the standard deviation σ are calculated. The threshold value $V_{t,s}^{T}$ for segment s at time t is calculated as:

$$V_{t,s}^{T} = \mu_{t,s} - \beta * \sigma_{t,s} \quad (5\text{-}2)$$

where β is the number of standard deviations the threshold is set below the mean value.

We tested four different values for β, 1.5, 1.75, 2.0 and 2.25. If the current speed is higher or equal to the threshold, then this record is labeled as 0, which implies normal conditions. On the contrary, if the current speed is lower than the threshold, the record is labeled as 1, which indicates non-normal conditions, and an alarm is issued.

We tested this approach on the 1-minute records downloaded from the RITIS platform. The records were not prelabeled before the run of the tests, because of the difficulties described in 5.2.2. The performance of the selected thresholds is done by comparing the labeling of records (0 or 1) against congestions scans available in RITIS.

An example of this analysis is shown in Figure 5.22 through Figure 5.25. The congestion scan for Friday, January 15, 2021, for the entire test corridor in the southbound direction is shown in Figure 5.10. It should be noted that on that date, there were no events reported in the data provided by MassDOT HOC.

Figure 5.22 through Figure 5.25 show the results of labeling the 1-minute records based on the thresholds described in Eq. (5-2) for β =1.5, 1.75, 2.0, and 2.25. The horizontal axis in these graphs is the time of the day (24 hours), while the vertical axis is the length of the corridor. The bars in these figures, indicate speeds below the corresponding threshold value. Note that the bars are not drawn to be equal to the length of the XD segment, resulting in some locations along the corridor being in gaps between the rows of markers. Each graph includes 23 rows of markers, one for each XD segment along the southbound of the test corridor.

The smaller the value of β, the more records are identified as abnormal operational conditions leading to several false alarms. For higher values of β, i.e., β=2.25, small fluctuations of speeds do not trigger an alarm, while significant events, such as the slow speeds on XD segments 1263046143 (Freeport St.) to 1263020045 (Purchase St./Summer St./Congress St./Pearl St.) are detected. The slow speeds between 1:00 p.m. and 4:00 p.m., especially in the northern part of the corridor, are similar to what is experienced on the corridor at that location on a daily basis due to recurring congestion, thus no alarms are issued. Such recurring congestion can be seen in Figure 5.26 and Figure 5.27, showing the congestion scans for two Fridays, January 8 and 22, 2021.

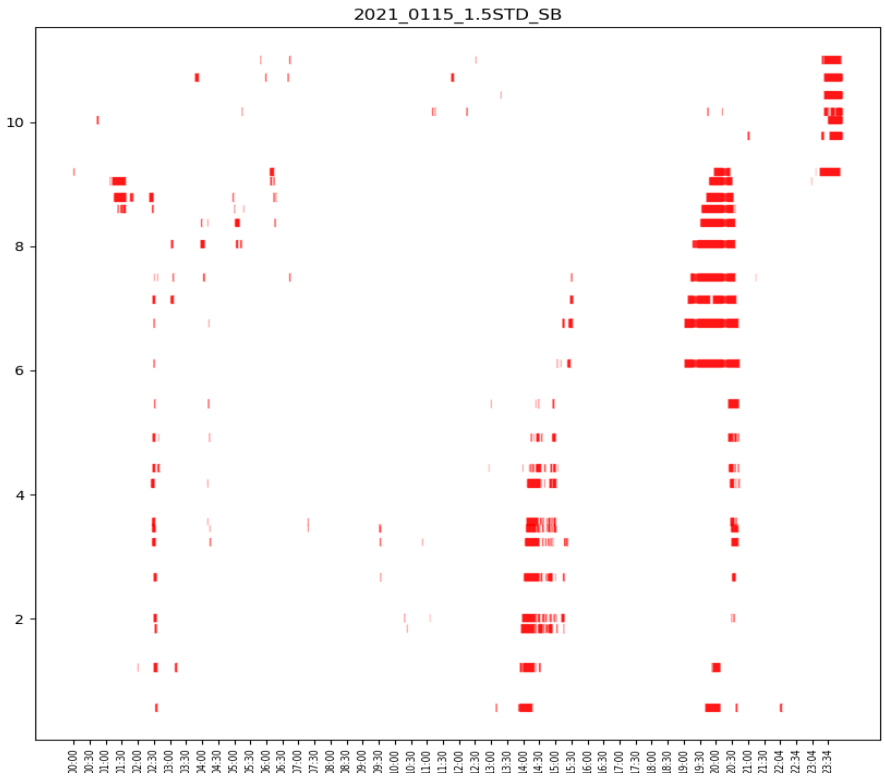

Figure 5.22: Incident detection results on 01/15/2021 using a β=1.5 for SB I-93

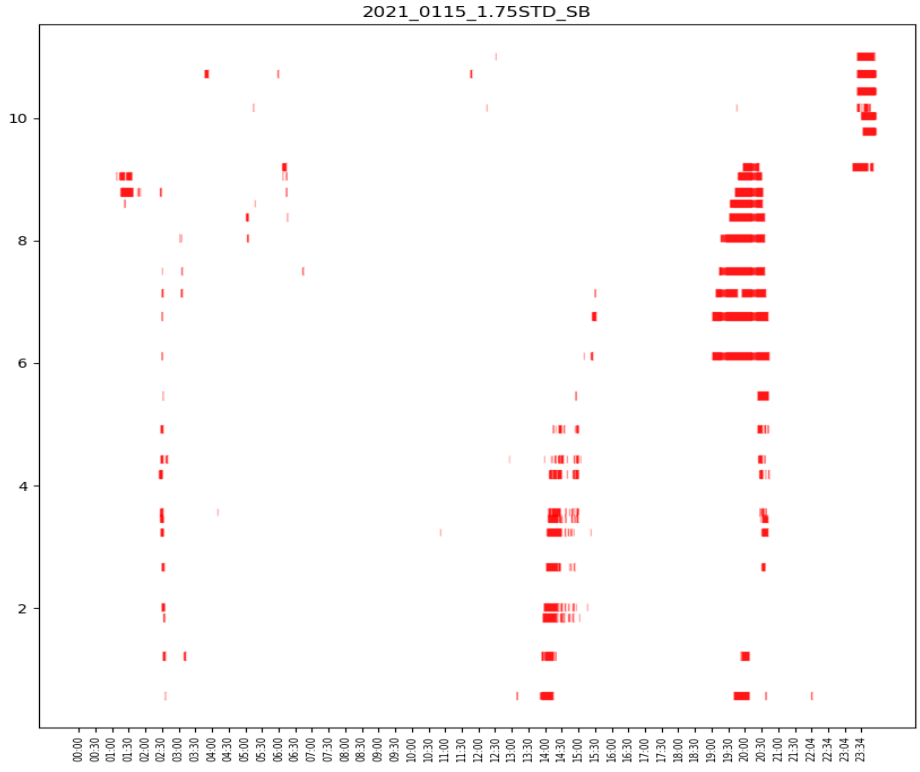

Figure 5.23: Incident detection results on 01/15/2021 with β=1.75 for SB I-93

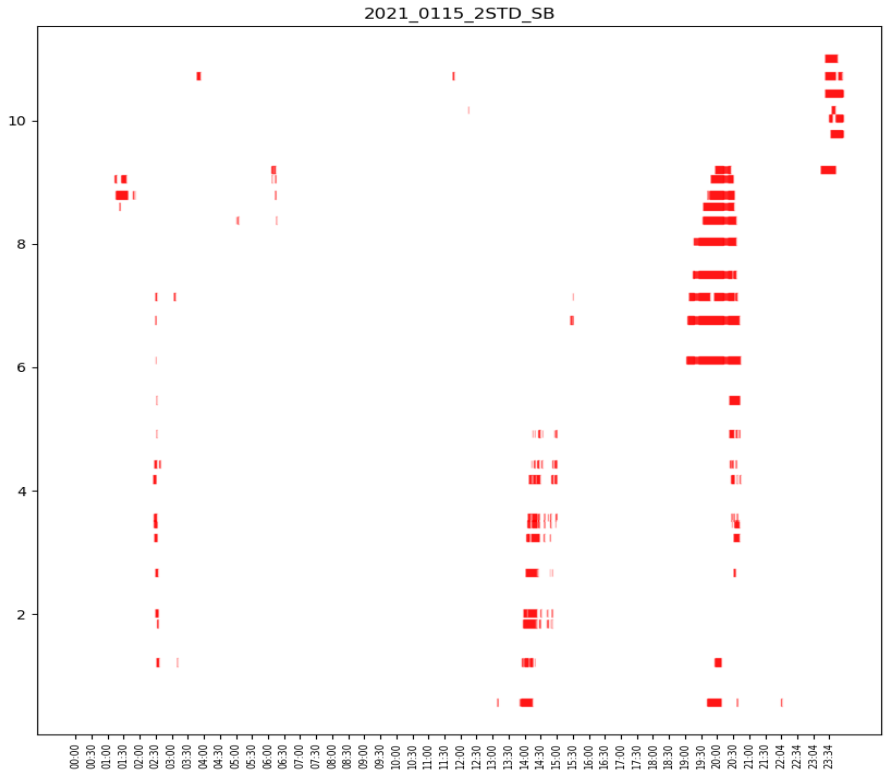

Figure 5.24: Incident detection results on 01/15/2021 with β=2 for SB I-93

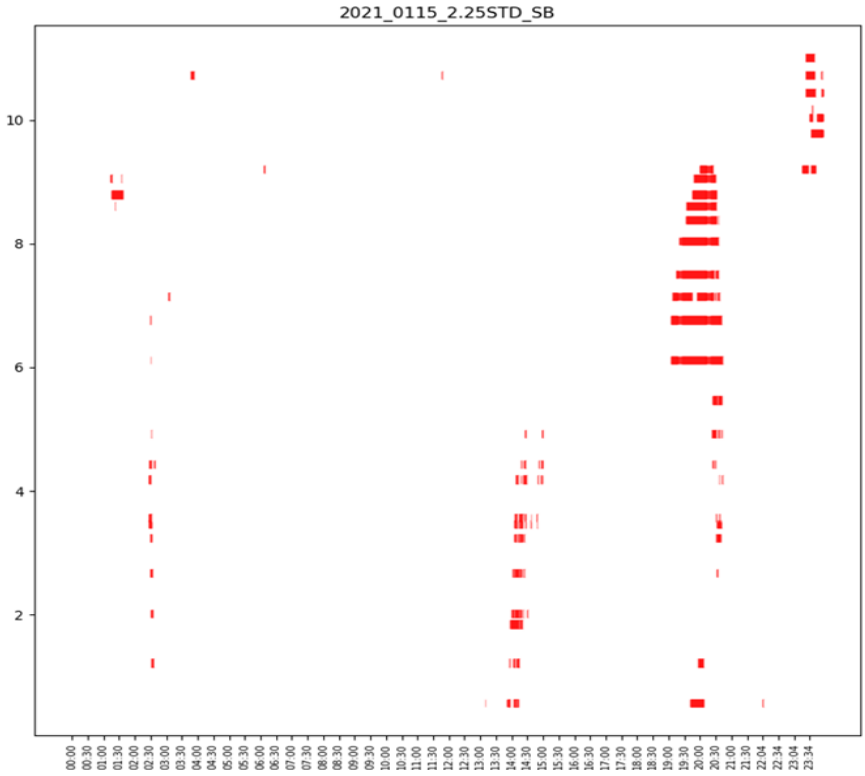

Figure 5.25: Incident detection results on 01/15/2021 with β=2.25 for SB I-93

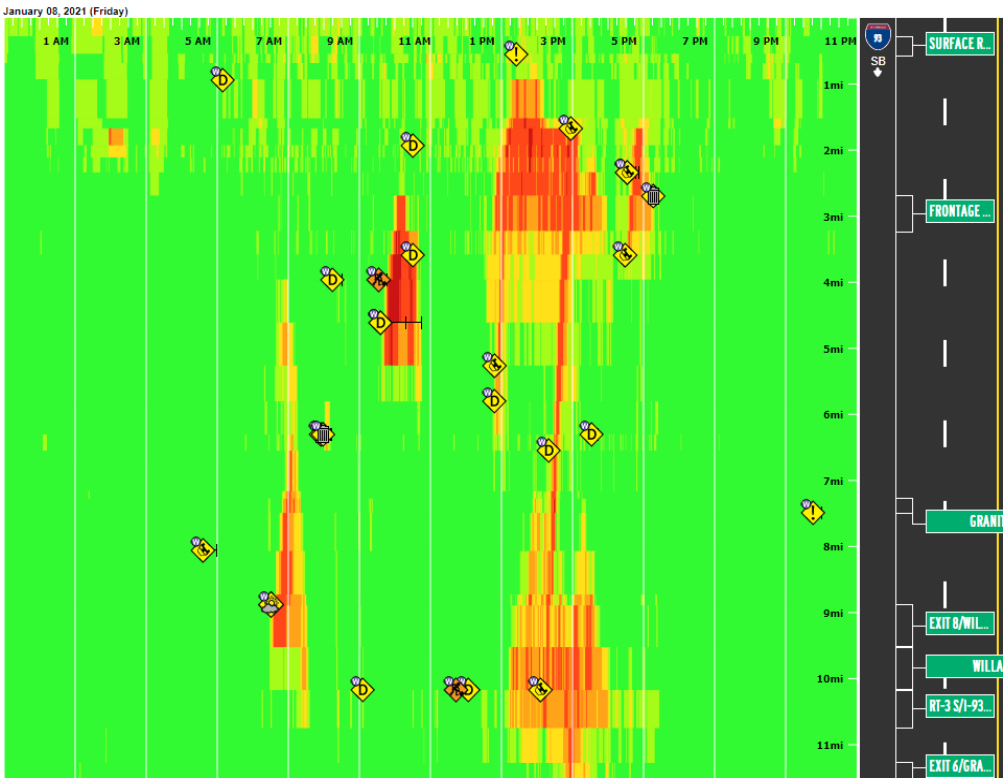

Figure 5.26: Congestion map for SB I-93, Friday, January 08, 2021

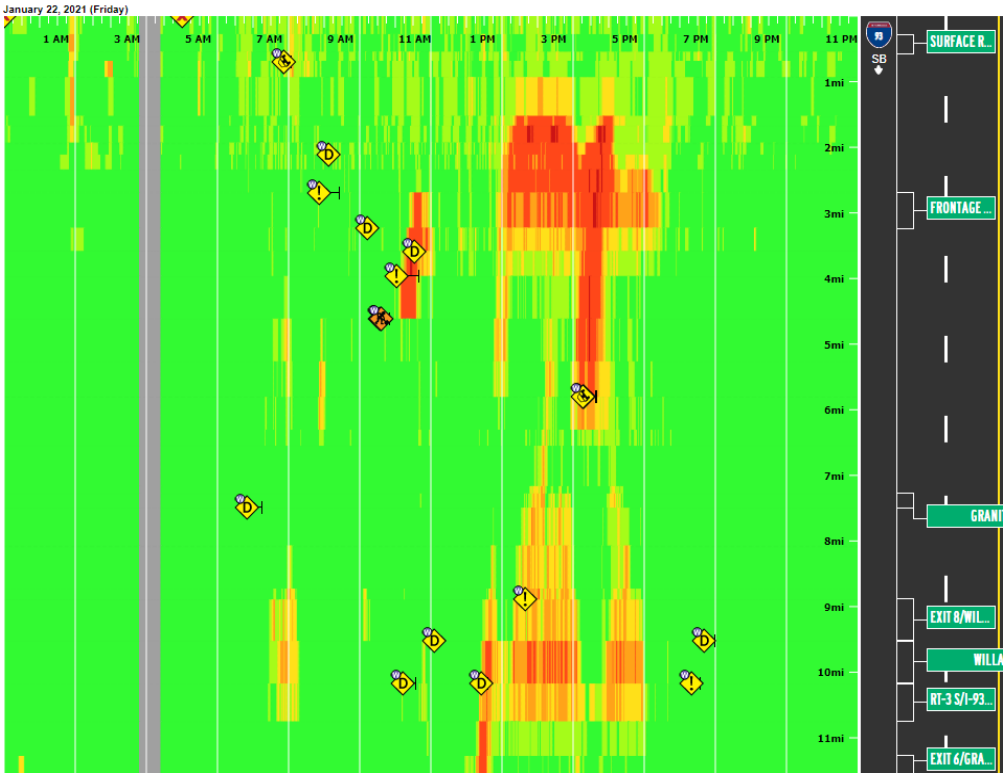

Figure 5.27: Congestion scan for SB I-93, Friday, January 22, 2021

5.2.5 Threshold by persisting speed differences on current and adjacent XD segments

To reduce false alarms that appear in the results obtained by considering instantaneous speed differences only on the XD segment under consideration, the rule for issuing an alert, described in the previous section, is expanded as follows:

$$\text{if } \begin{Bmatrix} V_{t-2,s} < \mu_{t-2,s} - \beta * \sigma_{t-2,s} \\ V_{t-1,s} < \mu_{t-1,s} - \beta * \sigma_{t-1,s} \\ V_{t,s} < \mu_{t,s} - \beta * \sigma_{t,s} \end{Bmatrix} \text{ and } \{V_{t,s-1} < \mu_{t,s-1} - \beta * \sigma_{t,s-1}\} \Rightarrow \text{label} = 1 \quad (5\text{-}3)$$

where $V_{t-2,s}$, $V_{t-1,s}$ are the speed values observed two and one minute earlier than the current speed observation $V_{t,s}$. $V_{t,s-1}$ is the speed observed currently on the upstream XD segment, and $\mu_{t,s}$ and $\sigma_{t,s}$ are the corresponding mean and standard deviation values. To label a record as a abnormal record (label 1) all these conditions must be satisfied: the speed on the segment under consideration must be lower than the mean value by β standard deviations at least for three consecutive minutes, and the current speed on the upstream segment must be also lower than the mean value by β standard deviations. If any of these conditions is not satisfied the record is labeled as 0, which indicates normal conditions, and no alarm is issued. Note that the implication of this is that the labeling of a record is not based on a single threshold value but rather four values considered simultaneously.

The results of this set of rules [Eq. (5-3)], for β = 1.5, 1.75, 2.0 and 2.25, for Friday, January 15, 2021, for the entire test corridor in the southbound direction (same day as in previous example), are shown in Figure 5.28 to Figure 5.31.

Short duration reductions of speed (less than three minutes) do not generate an alarm. Reduced speeds, and therefore queues, must have propagated to the upstream segment. This reduces the number of false alarms but increases unavoidably the detection time by at least two minutes, plus the time it takes for queues to propagate to the upstream segment and affect its speed. Generally, the length of the XD segments is very short, so queues should transfer quickly to the upstream segment. However, for minor incidents and during low traffic conditions queues may not propagate upstream, or if they do it may take more than two minutes. Therefore, the disadvantage of this approach is that incidents that affect only the segment where they occurred may not be detectable or if they are, they have longer detection times. Generally, using this set of rules for labeling speed records results in less noise, alarms lasting only a few minutes and scattered at disjoint XD segments.

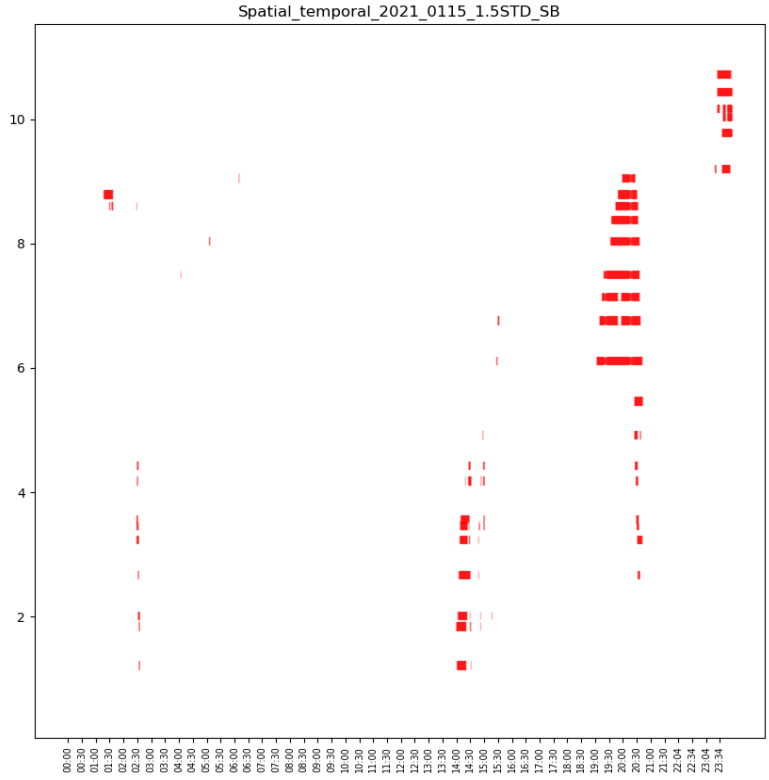

Figure 5.28: Incident detection results with Eq. (5-3) and β=1.5 for SB I-93

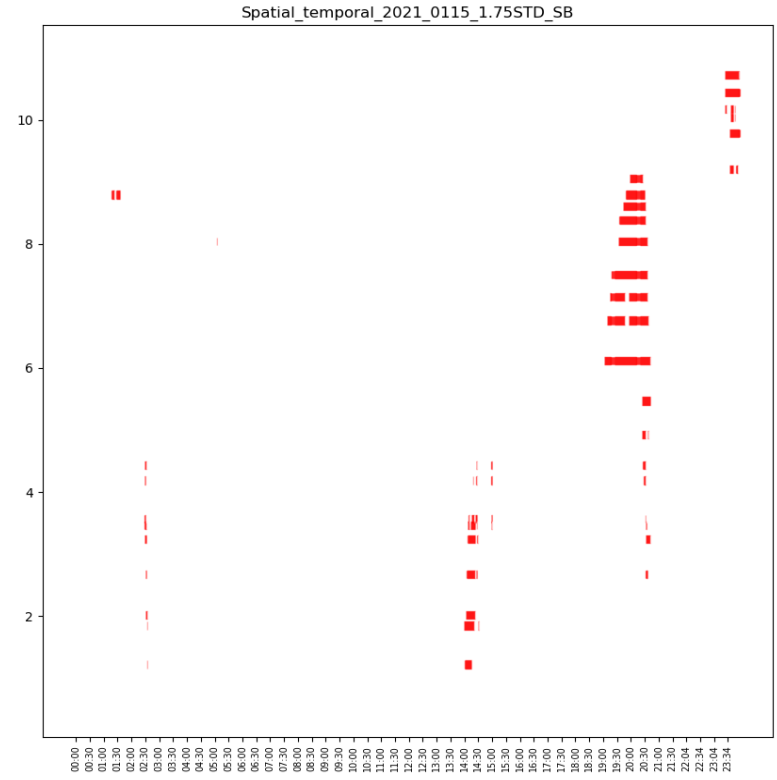

Figure 5.29: Incident detection results with Eq. (5-3) and β=1.75 for SB I-93

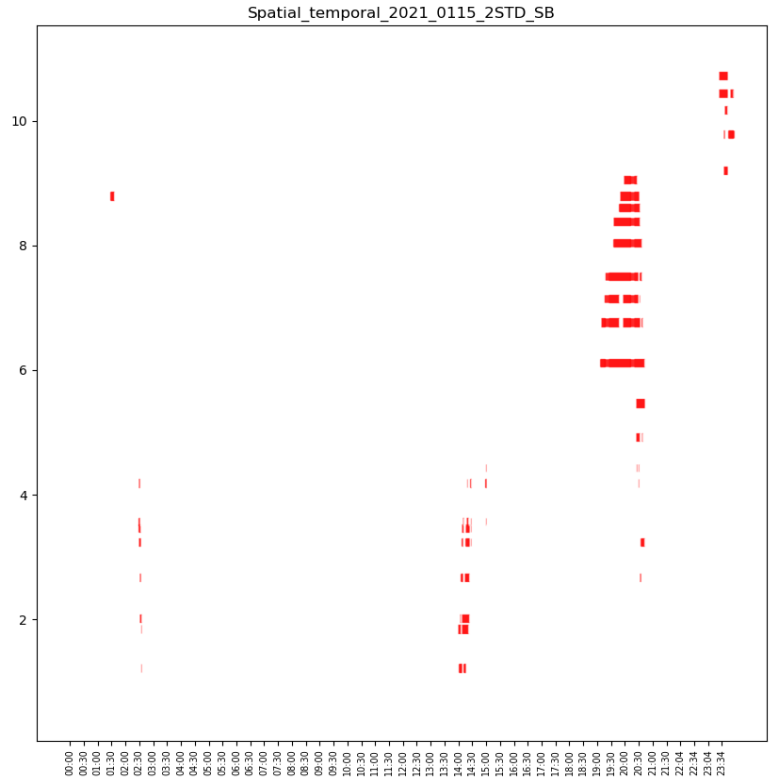

Figure 5.30: Incident detection results with Eq. (5-3) and β=2.0 for SB I-93

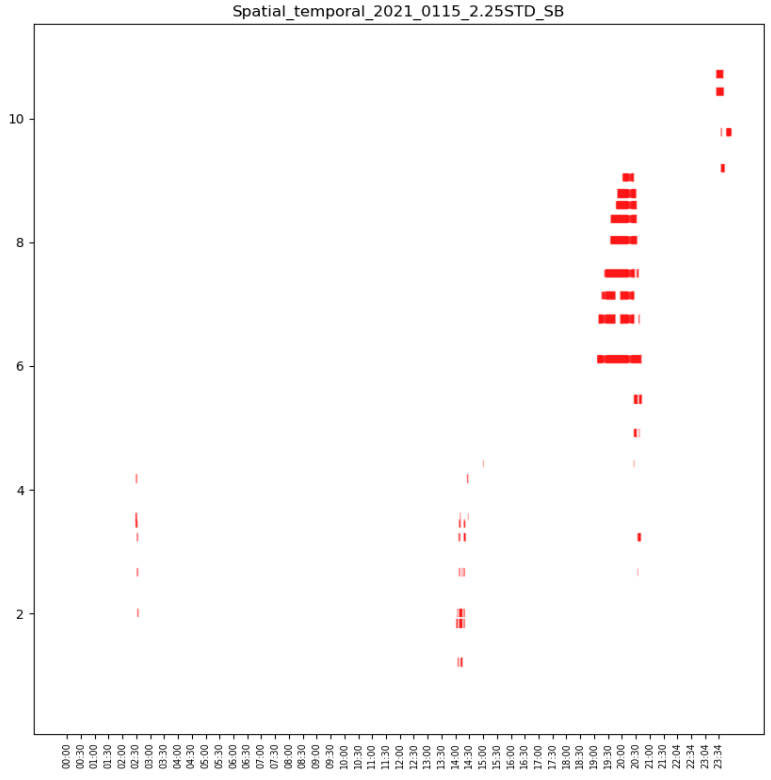

Figure 5.31: Incident detection results with Eq. (5-3) and β=2.25 for SB I-93.

A variation of the previous set of rules is to consider the traffic conditions on the downstream XD segment. When an incident occurs, it creates a bottleneck to the flow of traffic, resulting in reduced speeds on the segments where it occurred and possibly on upstream segments as well. Downstream segments should be unaffected. The modified set of rules is presented in Eq. (5-4):

$$\text{if } \left\{ \begin{array}{l} \dfrac{\mu_{t-2,s} - V_{t-2,s}}{\sigma_{t-2,s}} - \dfrac{\mu_{t-2,s+1} - V_{t-2,s+1}}{\sigma_{t-2,s+1}} > \beta \\ \dfrac{\mu_{t-1,s} - V_{t-1,s}}{\sigma_{t-1,s}} - \dfrac{\mu_{t-1,s+1} - V_{t,s+1}}{\sigma_{t-1,s+1}} > \beta \\ \dfrac{\mu_{t,s} - V_{t-1,s}}{\sigma_{t,s}} - \dfrac{\mu_{t,s+1} - V_{t,s+1}}{\sigma_{t,s+1}} > \beta \end{array} \right\} \Rightarrow \text{ label} = 1 \qquad (5\text{-}1)$$

To compare the speed on the segment under consideration to the speed on the downstream segment, the values must be "normalized," and the difference of the normalized values must be greater than β standard deviations of the standard normal distribution (which is equal to 1). The time subscripts $t, t-1, t-2$, correspond to current, one-minute earlier and two minutes earlier speed observation and corresponding distribution parameters, while the segment subscripts $s, s+1$, correspond to the XD segment under consideration and the downstream segment. If the difference of these "normalized" speeds are greater than or equal to β for three consecutive minutes the current record is labeled 1, which indicates abnormal conditions, and an alarm is issued.

The results of using this set of rules [Eq. (5-4)], for β =1.5, 1.75, 2.0 and 2.25, for Friday, January 15, 2021, for the entire test corridor in the southbound direction (same day as in previous example), are shown in Figure 5.32 to Figure 5.35.

Notice that for the event that occurs at 7:00 p.m. only the first XD segment is flagged, since for segments further upstream speeds may be lower than normal but the differences of their normalized values will be smaller than β, as both the segment under consideration and the immediate downstream segment are experiencing low speeds. This may be advantageous, since the operators will not have to deal with multiple alarms for the same incident. For larger values of β, i.e., 2.0 and 2.25, there is very little noise and only major events are identified.

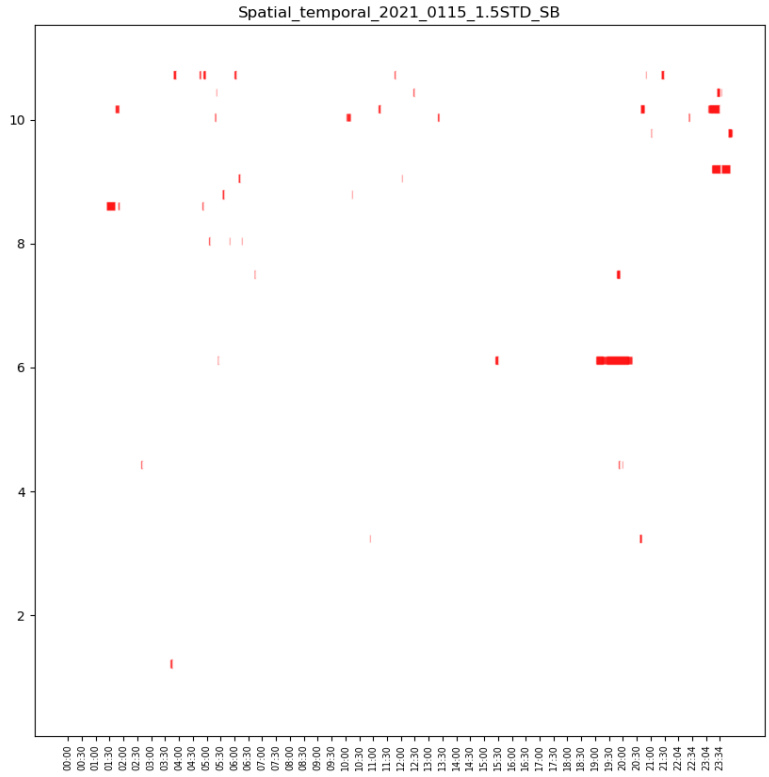

Figure 5.32: Incident detection results with Eq. (5-4) and β=1.5 for SB I-93

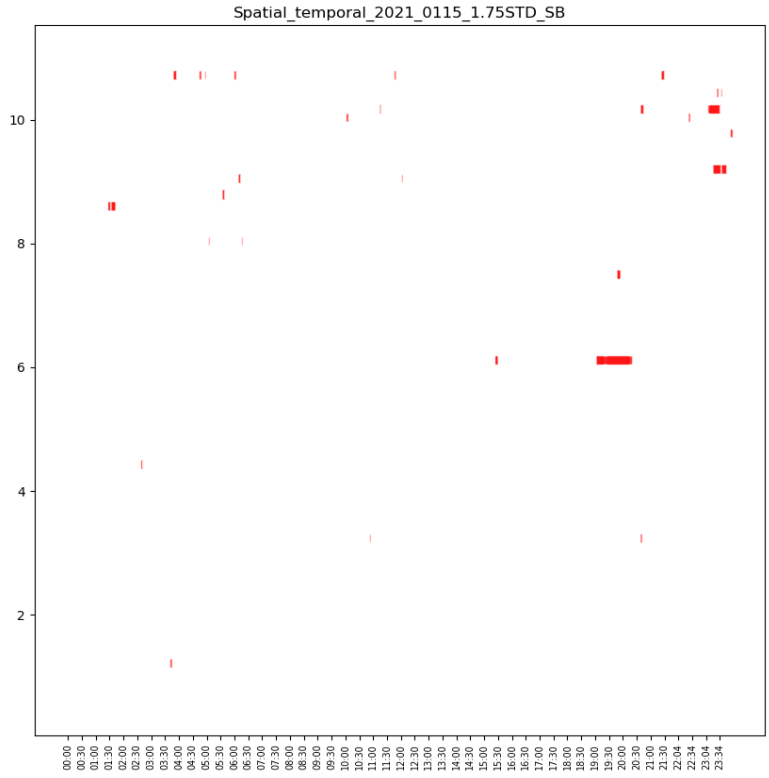

Figure 5.33: Incident detection results with Eq. (5-4) and β=1.75 for SB I-93

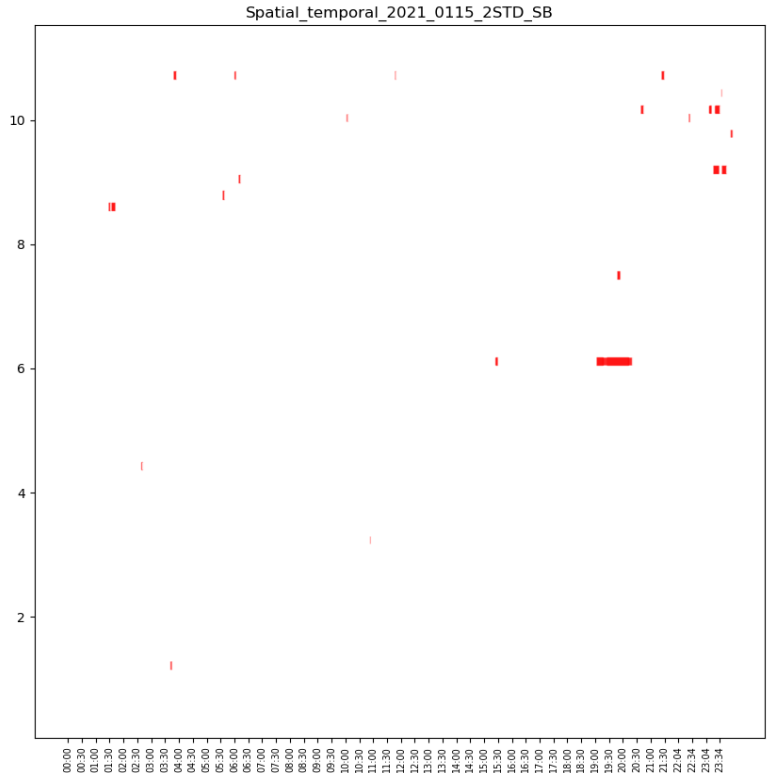

Figure 5.34: Incident detection results with Eq. (5-4) and β=2.0 for SB I-93

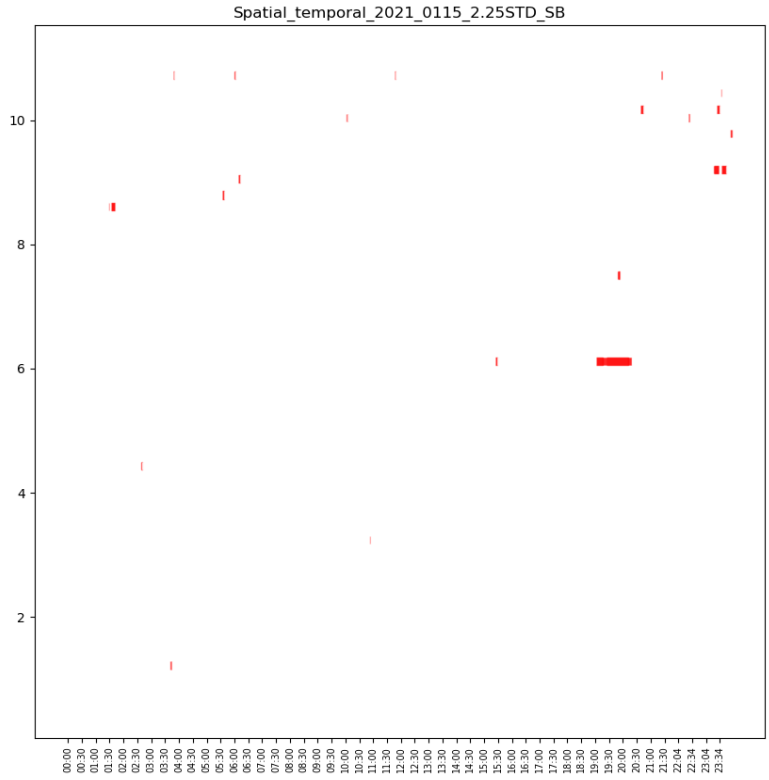

Figure 5.35: Incident detection results with Eq. (5-4) and β=2.25 for SB I-93

5.2.6 Beta Distribution

In the analysis performed so far, the implicit assumption was that under normal operational conditions, for any time period and at any XD segment, the distribution of observed speeds follows a normal distribution. An alternative distribution that can be used to describe the speed data is the Beta distribution, which is actually a family of distributions defined in the interval [0, 1] in terms of two positive parameters, α and β. Since speeds are non-negative, using a Beta distribution is more reasonable than a normal distribution.

The parameters α and β can be estimated from the values of the observed speeds, and the Beta distribution can be shifted and scaled, to fit the range of these observed speeds [*49*]. To establish these parameters with greater reliability, 5-minute speed observations are grouped together for every hour of the day (thus 24 distributions for each day). Similar to the analysis performed before, different Beta distributions are developed for each hour of the day, for weekdays and weekends, for every two-month season and for every XD segment.

With the Beta distribution, we can simply choose the 1st, 1.25th, 1.5th, 1.75th, 2nd, or 2.25th percentile as the threshold for incident detection. If the newly observed 1-minute speed is below the threshold, an alert can be triggered. To fit the speed data using the Beta distribution, the SciPy Python package [*50*] can be used This package generates four parameters for the Beta distribution, which are α, β, shift, and scale.

Figure 5.36 and Figure 5.37 show the fitted Beta probability density functions (PDF) for XD segment 1262993306 for two 1-hour time periods on weekdays. The 1st, 1.25th, 1.5th, 1.75th, 2nd, or 2.25th percentiles during 11:00 a.m. to 12 noon are 37.4, 38.5, 39.4, 40.2, 40.9, and 40.6 mi/h, respectively. The same percentiles during 15:00 p.m. to 16:00 p.m. are much lower: 8.1, 8.6, 9.0, 9.5, 9.9, and 10.3 mi/h, respectively.

The results of using the Beta distribution for the 1st, 1.25th, 1.5th, 1.75th, 2nd, and 2.25th percentiles, for Friday, January 15, 2021, for the entire test corridor in the southbound direction (same day as in previous examples), are shown in Figure 5.38 to Figure 5.43. In these tests, information only from the current XD segment and during the current time interval is considered. Generally, the smaller the percentile (i.e., 1st or 1.25th percentiles) the lower the threshold value for the observed speeds to indicate abnormal conditions. Compared to the results using the normal distribution (Figure 5.22 to Figure 5.25), using the Beta distribution results in less noise, i.e., false alarms.

The Beta distribution theoretically is more reasonable since the random variable is assumed to be non-negative. Therefore, considering the Beta distribution is still a very promising direction for future work.

Another method to estimate α and β is the Method of Moments [*51*]. To apply the Method of Moments, we need first to normalize the input speeds and convert them to a range between 0 and 1. In this way, the shift and scale coefficients of the Beta distribution are 0 and 1, respectively. We only need to focus on estimating α and β. Once Beta distributions are fitted based on the observed speed data, the speed thresholds can be calculated and further used for incident detection. Given the limited time for this study, the Beta distribution approach has not been evaluated thoroughly and should be further explored in future research.

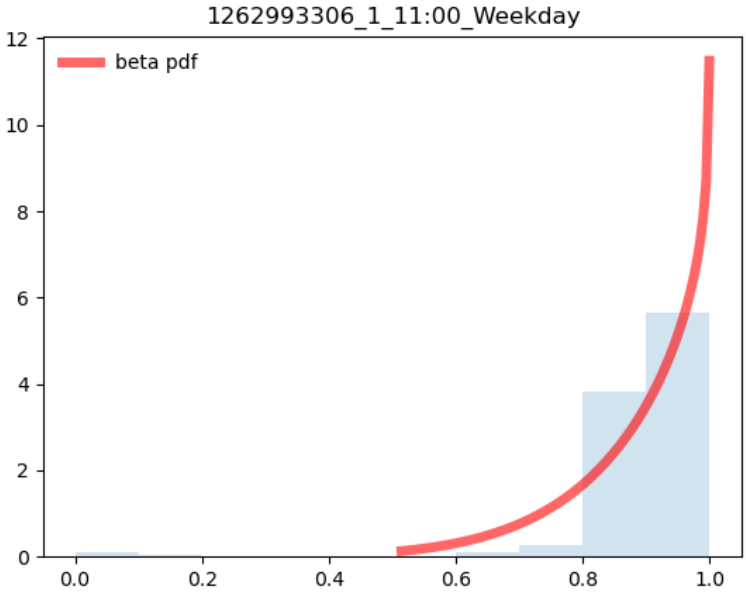

Figure 5.36: Beta probability density functions 11:00 a.m. to 12:00 noon weekdays

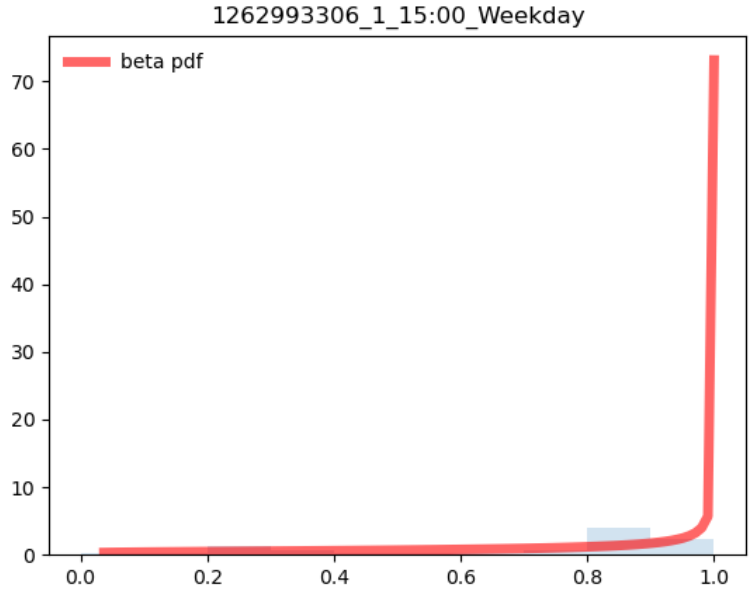

Figure 5.37: Beta probability density functions 3:00 p.m. to 4:00 p.m. weekdays

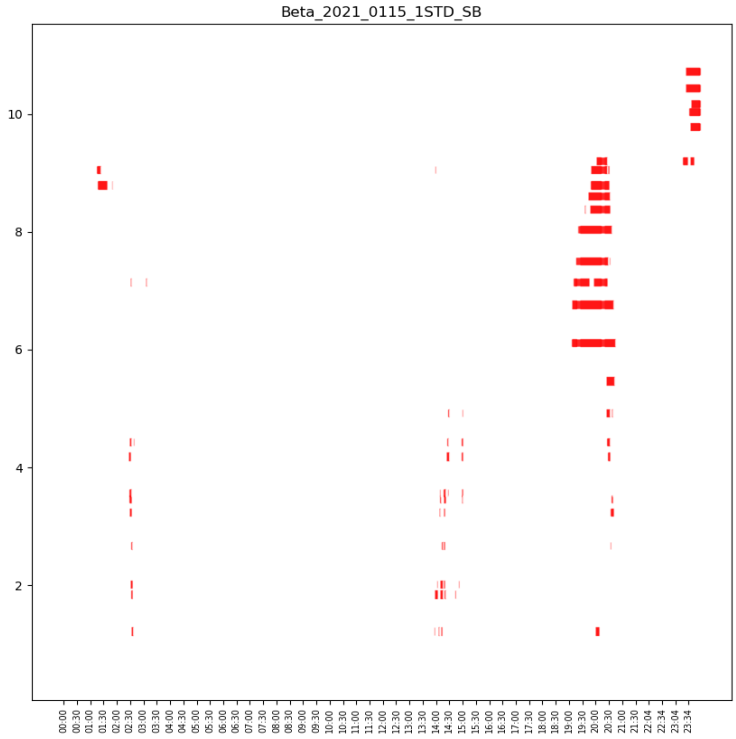

Figure 5.38: Incident detection results using Beta distribution, 1st percentile

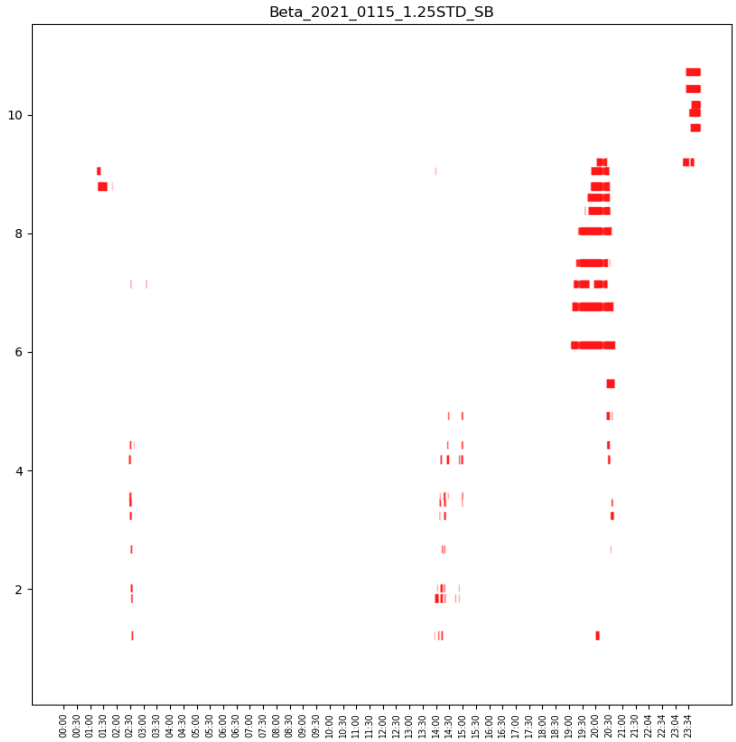

Figure 5.39: Incident detection results using Beta distribution, 1.25th percentile

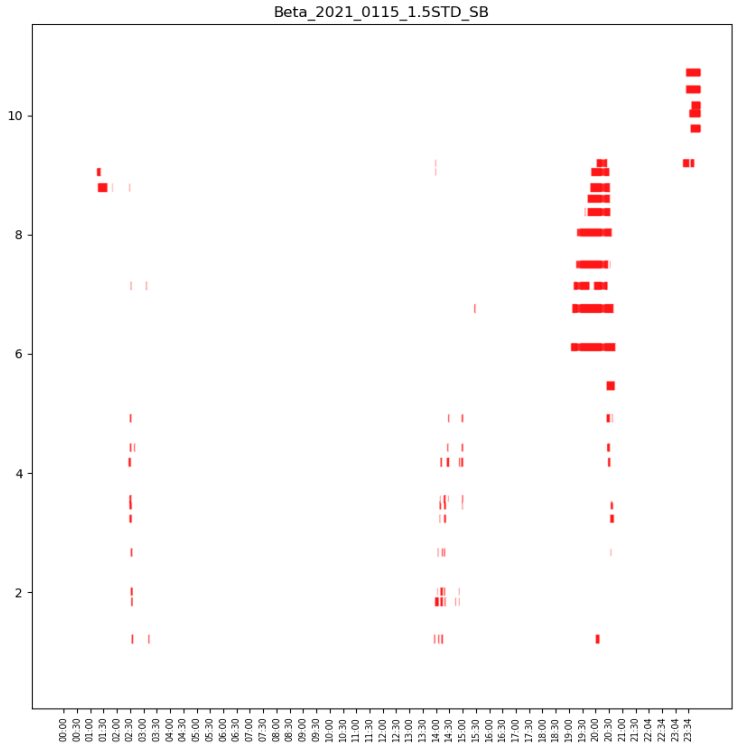

Figure 5.40: Incident detection results using Beta distribution, 1.5th percentile

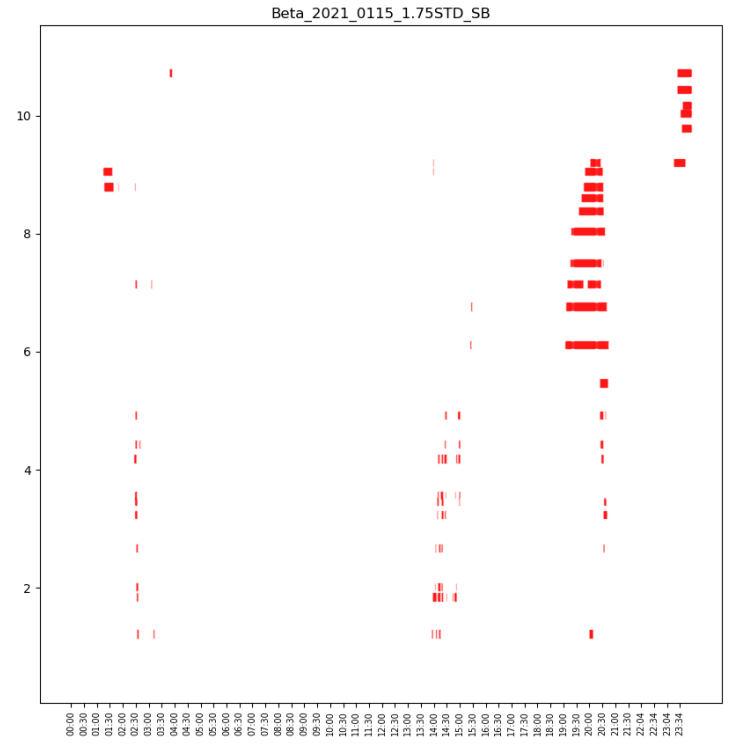

Figure 5.41: Incident detection results using Beta distribution, 1.75th percentile

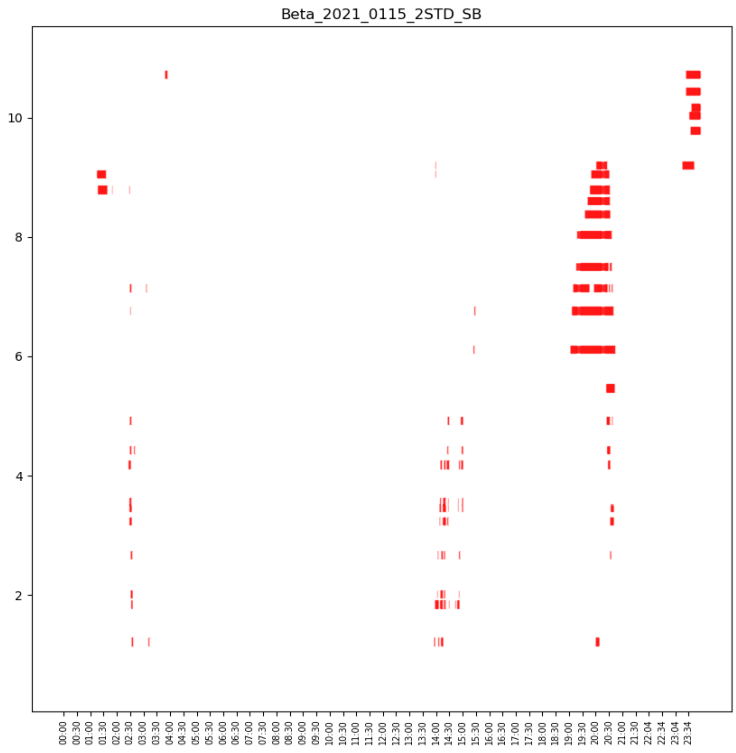

Figure 5.42: Incident detection results using Beta distribution, 2nd percentile

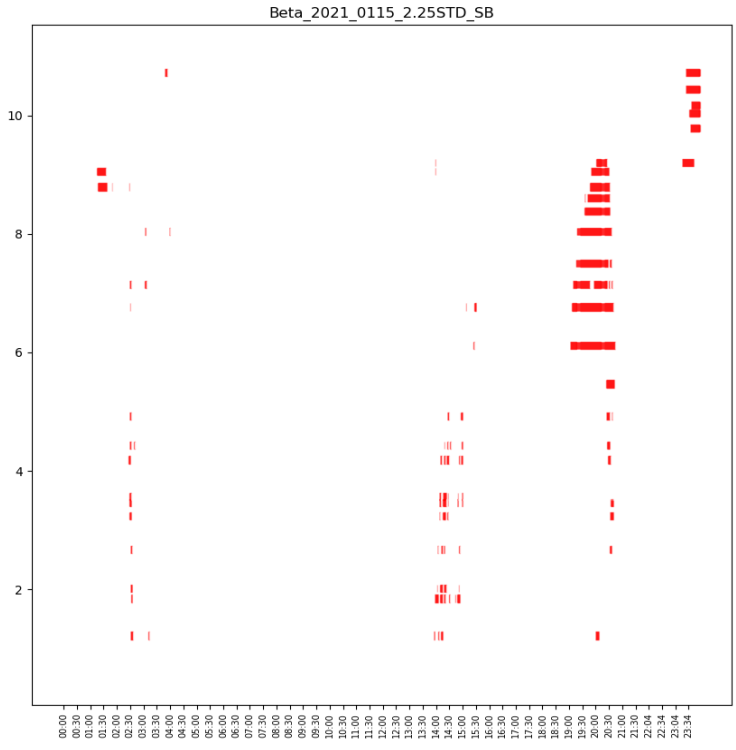

Figure 5.43: Incident detection results using Beta distribution, 2.25th percentile

5.3 Comparison of AI and Rule-Based Methods

The AI model appears to be able to detect more incidents than the rule-based methods in some cases. However, it is difficult to understand how the AI model works. On the other hand, the various rule-based methods also perform well. An important benefit of the rule-based methods is that users can adjust the parameters based on experience. The effects of these parameters are easy to understand.

Two examples for comparing the AI and rule-based methods are provided in Figure 5.44 through Figure 5.49. The first example is for the northbound direction of the corridor on 01/15/2021 (Figures 5.44 through 5.46). The AI model threshold is 0.998 and the rule-based model threshold is 2 (only the beta threshold is considered, no other criteria). The entire event marked by the black dashed rectangle in Figure 5.44 is missed by the rule-based model (see Figure 5.45). However, the AI model can detect some parts of it as shown in Figure 5.46. In addition, the event marked by the black oval in Figure 5.44 is again missed by the rule-based model, while the entire event is mostly captured by the AI model.

The second example (Figures 5.47 through 5.49) is for the southbound direction of the corridor on 05/15/2021. Two major incidents occurred on that day at different locations. The same threshold values used in the first example are considered here. The incident in the black oval in Figure 5.47 is largely missed by the rule-based method but mostly captured by the AI model.

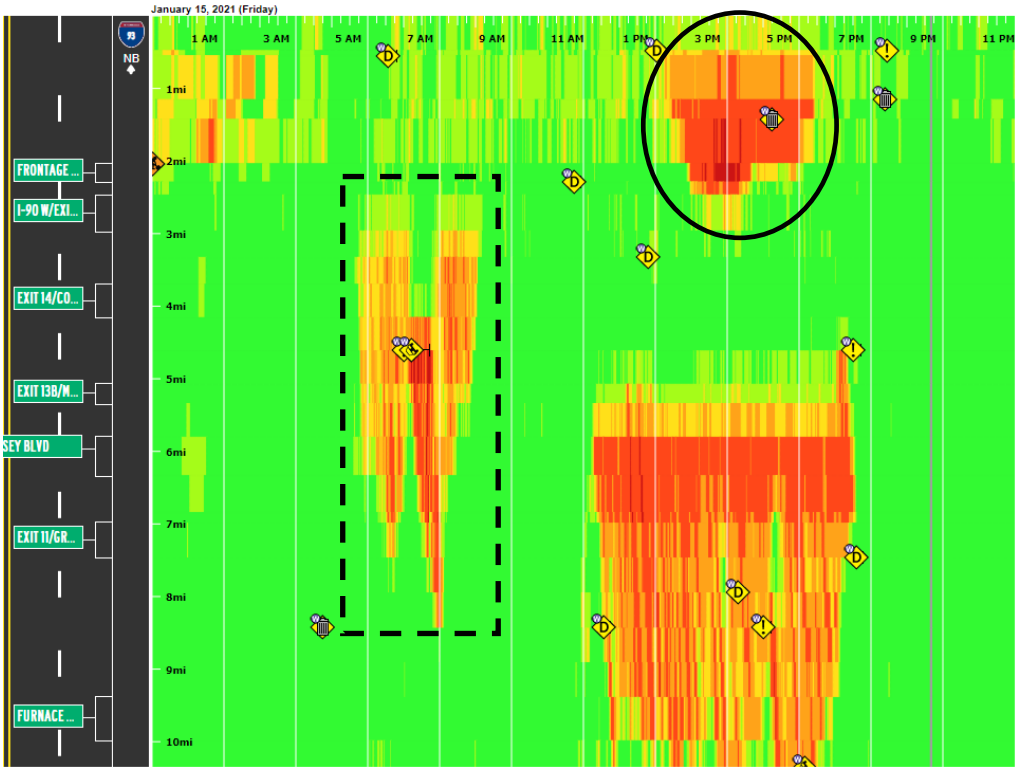

Figure 5.44: Congestion scan results for NB traffic on 01/15/2021

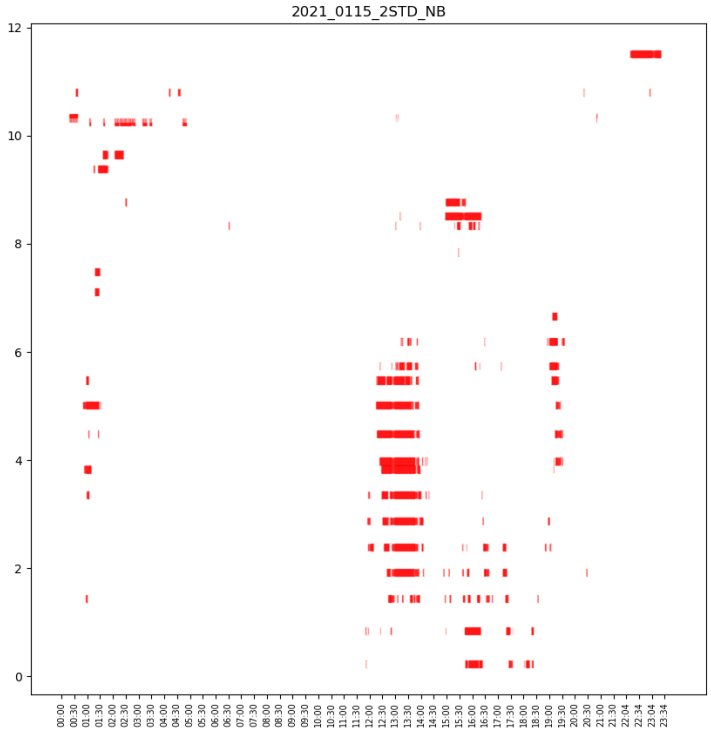

Figure 5.45: Incident detection results using a beta threshold value of 2.0 for NB traffic

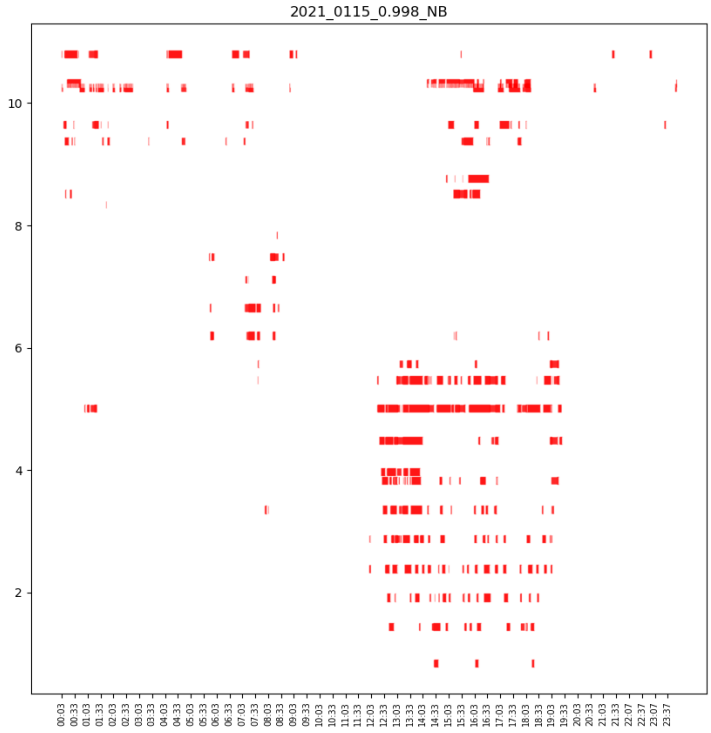

Figure 5.46: AI model incident detection results using a threshold value of 0.9980 for NB traffic

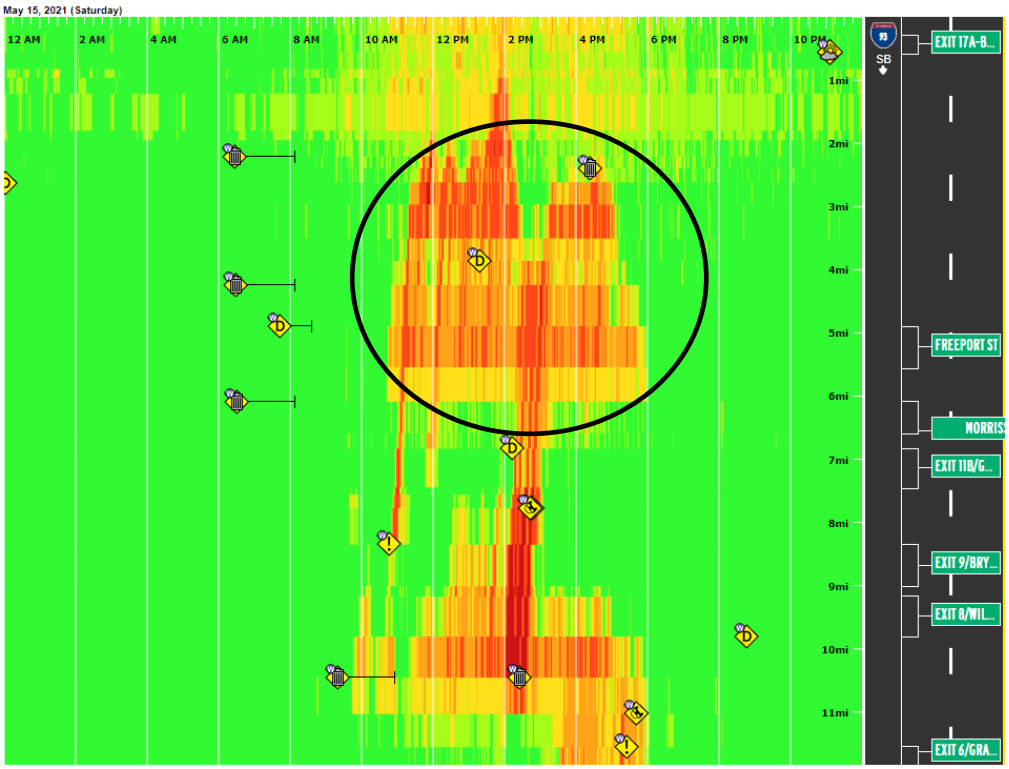

Figure 5.47: Congestion scan results for SB traffic on 05/15/2021

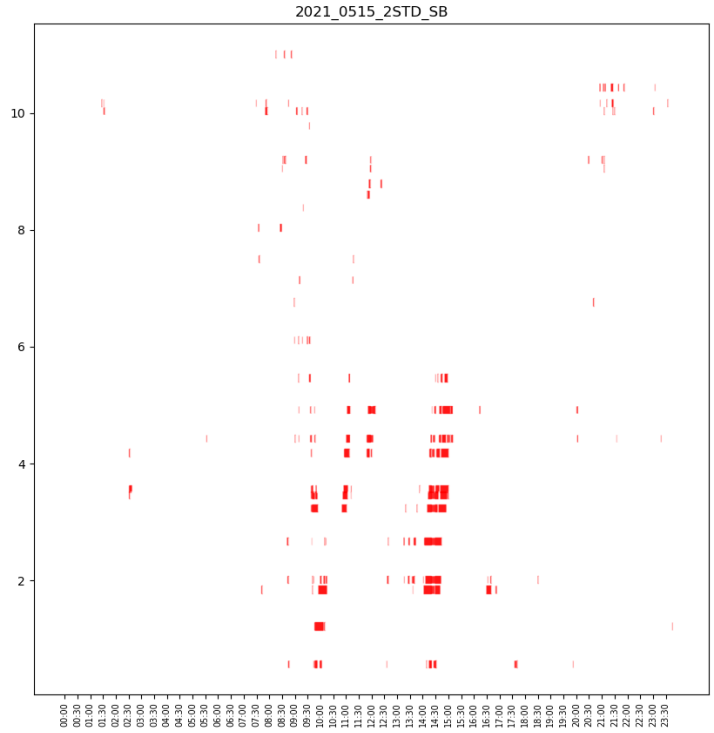

Figure 5.48: Incident detection results using a beta threshold value of 2.0 for SB traffic

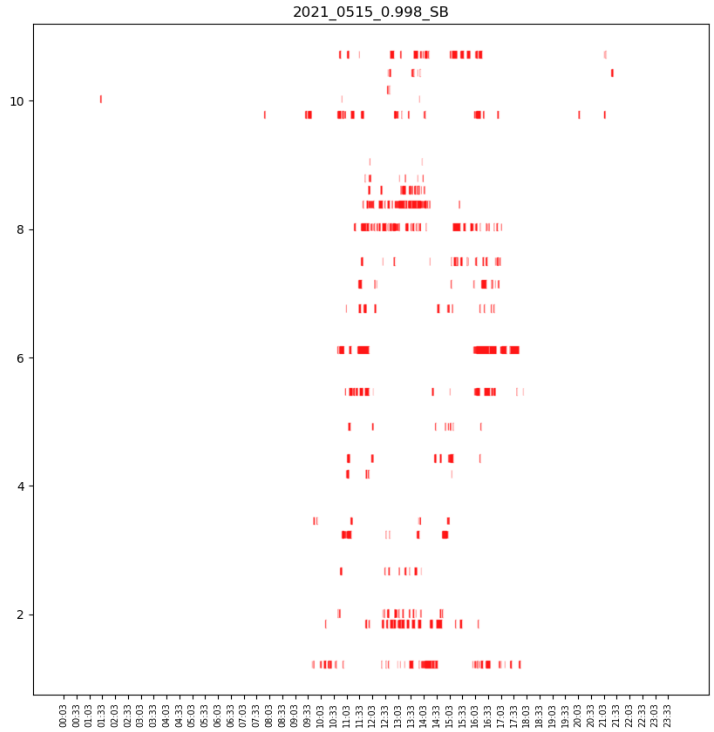

Figure 5.49: AI model incident detection results using a threshold value of 0.9980 for SB traffic

5.4 Other Modeling Efforts

Several other methods have been evaluated in this research. One of them is PyCaret [*52*], which is an open-source machine learning library for classification, regression, etc. A small data set with only one incident on 02/04/2021 was used to evaluate the methods in this library. The methods evaluated were Angle base Outlier Detection, Clustering-Based Local Outlier, Connectivity-Based Local Outlier, Isolation Forest, Histogram-based Outlier Detection, K-Nearest Neighbors Detector, Local Outlier Factor, One-class SVM detector, Principal Component Analysis, Minimum, Covariance Determinant, Subspace Outlier Detection, and Stochastic Outlier Selection. Overall, the results were unsatisfactory. As can be seen in Figure 5.50, the red dots indicate the abnormal events detected by the methods in the PyCaret library, which are all over the place. When applying the methods in PyCaret, the input data was simply treated as time series without considering upstream and downstream XD segment speeds. This might be one of the reasons for the poor performance.

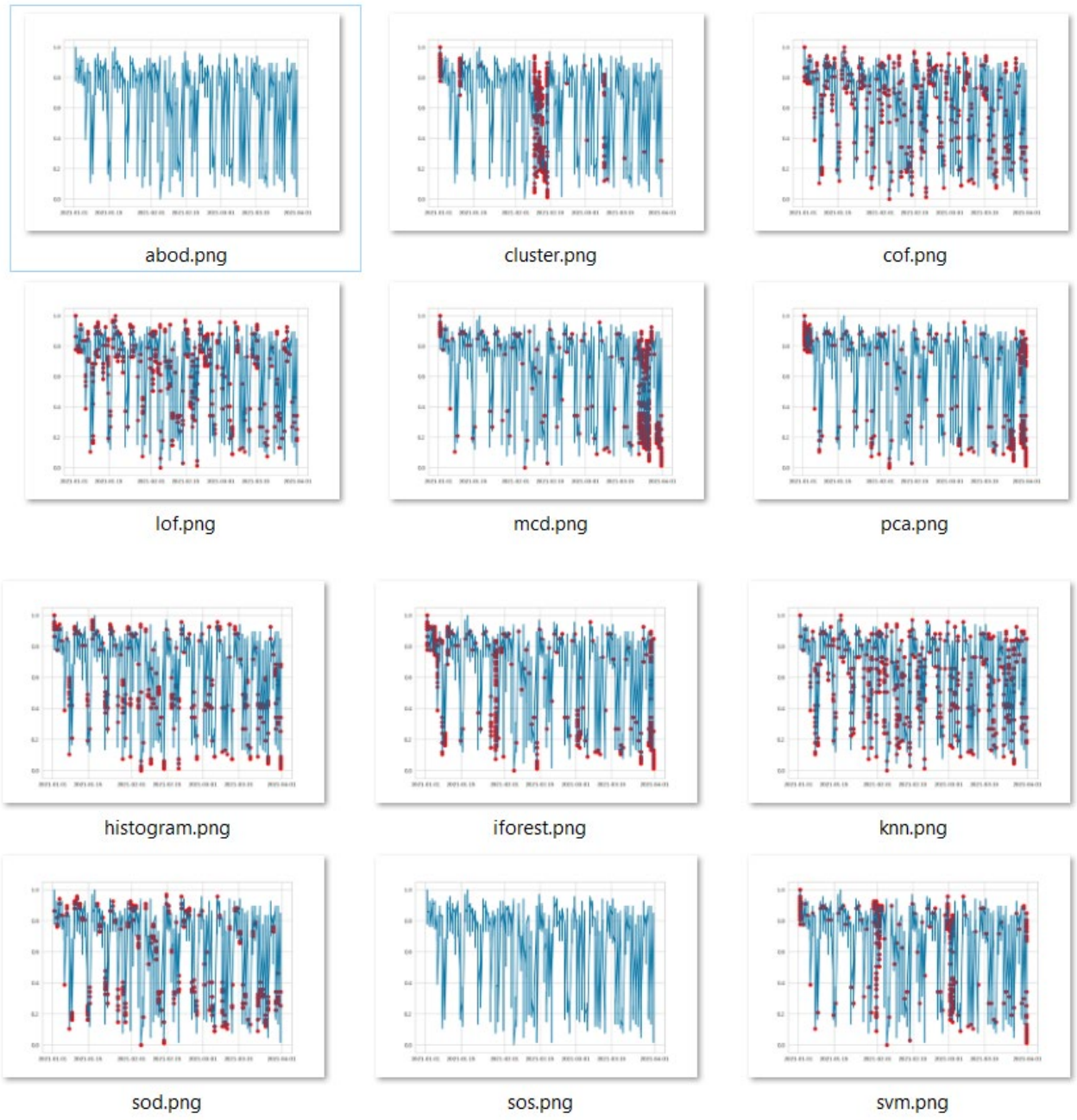

Figure 5.50: PyCaret evaluation results

We also investigated the applicability of two other models: Deep SAD [*5351*] and Unsupervised Data Augmentation (UDA) [*5452*]. Given the difficulties in labeling incident data, exploring unsupervised and semisupervised methods for detecting traffic incidents appears to be a promising direction. Although we were unsuccessful in obtaining good results from these models, these and similar unsupervised and semisupervised methods are worth exploring in the future.

This page left blank intentionally.

6 Field Testing

To further test the incident detection methodologies described above, under a variety of situations, selected strategies were applied to both the northbound and southbound directions of the test corridor over a continuous 30-day period. The period used was between June 1 and June 30, 2021. To keep the calculation of the threshold values as simple as possible, so that the selected procedure can be applied easily on different roadways, the procedures discussed in 5.2.4 and 5.2.5 were used. Although the beta distribution approach also generates good incident detection results, calculating its thresholds is less straightforward and involves the estimation of distribution parameters and various percentile values. Therefore, the beta distribution approach was not used in this field test.

When the incident detection strategy described in 5.2.5 was applied [i.e., using the speed of the downstream segment as defined by the rule in Eq. (5-4)], the detection rate was rather poor. This is because such a rule can only capture events that result in significant differences in the speeds of the current and downstream XD segments, which would be observed in the case of an incident occurrence during off-peak periods. During the test period, the test corridor has long periods of recurring congestion on all its segments. As a result of this, in the event of a traffic incident, the downstream segment is also congested due to recurring congestion. Therefore, the difference between the speed on the incident segment and the speed on the downstream segment is not large enough to satisfy the rule described by Eq. (5-4).

Based on these results it was decided that the second incident detection strategy should be tested, which is described in Eq. (5-2) considering a $\beta = 2.25$ standard deviation. Before an incident alert is generated, the condition in Eq. (5-2) should be valid for at least three consecutive minutes. Generally, the relatively large value of β and the three-minute rule kept the false alarm rate low and resulted in fast detections of speed anomalies.

A problem identified during these tests was that congested periods often have large standard deviations and low mean values for speed. In these cases, using the normal distribution often resulted in extremely low or even negative (in which case it was set to 0) threshold speed values. For example, the average speed for northbound XD segment 1263148464 during weekdays and around 2:25 pm drops to about 14 mi/h and the corresponding standard deviation is around 11 mi/h (Table 6.1). Using the rule in Eq. (5-2) and $\beta = 2.25$, the resultant threshold value is 0 mi/h. In this case, even very low observed speeds (e.g., 3 or 4 mi/h) do not trigger an alarm (Table 6.2).

Table 6.1: Mean and standard deviation of speed distributions on XD 1263148464

XDID	Month 1	Month 2	Weekday	Time	Mean	Std. Dev.
1263148464	5	6	1	2:00 PM	27.18	16.34
1263148464	5	6	1	2:05 PM	23.95	15.64
1263148464	5	6	1	2:10 PM	20.62	14.02
1263148464	5	6	1	2:15 PM	17.80	12.73
1263148464	5	6	1	2:20 PM	15.51	11.85
1263148464	5	6	1	2:25 PM	13.89	10.94
1263148464	5	6	1	2:30 PM	12.73	10.29
1263148464	5	6	1	2:35 PM	12.04	9.68
1263148464	5	6	1	2:40 PM	11.84	9.80
1263148464	5	6	1	2:45 PM	11.58	9.60
1263148464	5	6	1	2:50 PM	11.38	9.19
1263148464	5	6	1	2:55 PM	11.12	8.99

Table 6.2: One-minute speed observations on XD 1263148464

XDID	Time stamp	Speed	Prediction
1263148464	6/1/2021 2:02 PM	48	0
1263148464	6/1/2021 2:03 PM	48	0
1263148464	6/1/2021 2:04 PM	47	0
1263148464	6/1/2021 2:05 PM	47	0
1263148464	6/1/2021 2:06 PM	47	0
1263148464	6/1/2021 2:07 PM	43	0
1263148464	6/1/2021 2:08 PM	42	0
1263148464	6/1/2021 2:09 PM	43	0
1263148464	6/1/2021 2:10 PM	43	0
1263148464	6/1/2021 2:11 PM	40	0
1263148464	6/1/2021 2:12 PM	40	0
1263148464	6/1/2021 2:13 PM	30	0
1263148464	6/1/2021 2:14 PM	18	0
1263148464	6/1/2021 2:15 PM	17	0
1263148464	6/1/2021 2:16 PM	17	0
1263148464	6/1/2021 2:17 PM	14	0
1263148464	6/1/2021 2:18 PM	11	0
1263148464	6/1/2021 2:19 PM	9	0
1263148464	6/1/2021 2:20 PM	9	0
1263148464	6/1/2021 2:21 PM	11	0
1263148464	6/1/2021 2:22 PM	10	0
1263148464	6/1/2021 2:23 PM	9	0
1263148464	6/1/2021 2:24 PM	9	0
1263148464	6/1/2021 2:25 PM	8	0
1263148464	6/1/2021 2:26 PM	9	0
1263148464	6/1/2021 2:27 PM	9	0
1263148464	6/1/2021 2:28 PM	10	0
1263148464	6/1/2021 2:29 PM	11	0

To eliminate this problem of negative speed threshold values, the percentiles of the observed speeds were used to set the threshold values, instead of the ones based on the normal distributions. The empirical distributions of the observed speeds that were used were the ones generated after the two-step smoothing described in 5.2.3. Thresholds between the 1st and 1.5th percentiles of the observed speeds were tested. For example, the 1st, 1.25th, and 1.5th percentiles of the observed speeds for the same period and segment as above (2:00 p.m. to 3:00 p.m., weekdays, XD segment 1263148464) are shown in Table 6.3. These percentiles clearly can avoid the extremely small or even negative threshold values.

Table 6.3: Percentiles of observed speeds on XD 1263148464

XDID	MONTH1	MONTH2	WEEKDAY	TIME	1%	1.25%	1.50%
1263148464	5	6	1	2:00 PM	6.00	6.00	6.00
1263148464	5	6	1	2:05 PM	5.29	5.61	5.94
1263148464	5	6	1	2:10 PM	5.29	5.61	5.94
1263148464	5	6	1	2:15 PM	5.29	5.61	5.94
1263148464	5	6	1	2:20 PM	6.00	6.00	6.00
1263148464	5	6	1	2:25 PM	6.00	6.00	6.00
1263148464	5	6	1	2:30 PM	5.29	5.61	5.94
1263148464	5	6	1	2:35 PM	5.00	5.00	5.00
1263148464	5	6	1	2:40 PM	5.29	5.61	5.94
1263148464	5	6	1	2:45 PM	5.29	5.61	5.94
1263148464	5	6	1	2:50 PM	4.58	5.23	5.87
1263148464	5	6	1	2:55 PM	4.29	4.61	4.94

The results for the 30-day test are shown in Appendix 8.2, except for the days of June 5th and June 16th, for which the data available on the RITIS platform were corrupt. During the month of June 2021 there were 24 Level 2 events recorded by the MassDOT HOC, with eight of them being DMV and the rest being traffic crashes. These events are listed in Table 8.1 in Appendix 8.1. Most of the events recorded by the HOC were detected by the strategy described above. For most of these events the detection time was well before the "SENT-ON" time recorded in the HOC database. For the few events that were not detected, the speed disturbance was not significant, compared to the historical speed pattern at that time and location. Beyond these 24 events recorded by HOC and considering the events indicated by Waze reports included in the congestion scans generated by RITIS, the strategy used could detect several of them.

On the other hand, alarms were issued during probable periods of recurring congestion. An explanation of this is that the start and end of recurring congestion varies from day to day by several minutes, so during transient states when the observed speeds are low, alarms are issued.

Overall, the strategy that was developed using the empirical rules described above can detect incidents that result in perturbations in the one-minute average speeds observed for at least three consecutive minutes. Minor events that do not cause such perturbations cannot be detected.

This page left blank intentionally.

7 Conclusions

**In this study data sets available to MassDOT that can be used for real-time incident detection were identified. Such data included speed and travel time data through the GoTime and the RITIS platforms and Waze reports. From these data sets, the one available through the RITIS platform was the most suitable for developing and testing incident detection strategies. Speed data obtained through the RITIS platform was aggregated over one-minute time intervals and over short distinct roadway segments (i.e., XD segments).

For detection of traffic incidents, two models were developed and tested in this study. The first model is based on AI and the second is an empirical rule-based model. The two models were applied for detection of traffic incidents on the selected section of Interstate 93 between Quincy and Boston in MassDOT District 6.

- **AI Model**: Traffic incident detection essentially can be modeled as a classification problem. The traffic state at a specific moment is characterized by a feature vector representing speeds on the current XD segment as well as its neighbors, and corresponding confidence parameters. This feature vector is then fed into a pretrained AI classifier and classified as either incident or non-incident. Several classifiers, using *supervised* and *unsupervised learning*, have been tested. A supervised learning method integrating LSTM and Variational Autoencoders (VAE) is adopted. This requires (for the training phase and testing of the model) each record to be clearly labeled as incident or non-incident. This labeling process is too time consuming, so testing was limited to only a few 24-hour periods. Various VAE model configurations have been evaluated. The results of the best performing VAE model are FAR = 0.0069%, DR = 91.70%.
- **Empirical Rule-Based Methods:** This method uses threshold values on the observed speeds, available through the RITIS platform. For this purpose, first the distributions of speeds at different time periods and locations are developed. Various percentile values of speed, to be set as thresholds, are tested for their effectiveness in detecting incidents. If the speed observed in an XD segment falls below the threshold value, an alarm will be issued requiring the operator's attention to verify that there is an incident or cancel the alarm. For the calculation of the percentiles, different distributions are developed and tested, including the normal, the Beta and the empirical distributions of historical speeds over the last three years. An off-line test was completed for a continuous 30-day period, during which most of the event recorded by the MassDOT HOC were detected, and for most of them the detection time was well before the SENT-ON time recorded in the HOC database. In addition, the developed strategy can detect events indicated by Waze reports included in the congestion scans generated by RITIS, although these events are not recorded in the HOC database. Some false alarms were issued during periods of recurring congestion, probably because the start and end of recurring congestion varies from day to day by several minutes. Therefore, during transition periods when the observed speeds are low, alarms are issued.

Future research on both models is very likely to further improve their performance. For the AI model the performance of unsupervised learning methods should be explored, while for the empirical rule-based method, procedures for updating the speed distributions to include the most

recent observations should be investigated. The application of different empirical procedures at different locations and time periods, tailored to the historic traffic conditions, will most likely improve the performance of the model. Furthermore, combining the two models, the AI model with the empirical rules (e.g., those in Eq. (5-4)), is expected to improve the performance even more.

8 Appendixes

8.1 Events Reported by MassDOT HOC on South I-93, June 1 to June 30, 2021

Table 8.1: Events reported by MassDOT HOC on SB and NB of South I-93 (test corridor) during June 2021

Sent On	Rt. No.	Direction	City	DMV/Crash	XD Segment
Jun 01, 2021, 14:27:07 EDT	I-93	NB	MILTON	Crash	1262986967
Jun 02, 2021, 13:36:56 EDT	I-93	NB	BOSTON	DMV	1263231759
Jun 02, 2021, 15:29:01 EDT	I-93	NB	MILTON	DMV	1262993322
Jun 03, 2021, 16:24:42 EDT	I-93	SB	BOSTON	Crash	1263156327
Jun 04, 2021, 06:51:24 EDT	I-93	NB	BOSTON	Crash	1263111350
Jun 05, 2021, 18:41:42 EDT	I-93	SB	BOSTON	DMV	386964859
Jun 07, 2021, 10:10:47 EDT	I-93	NB	BOSTON	Crash	1262997395
Jun 07, 2021, 15:50:58 EDT	I-93	NB	MILTON	Crash	1262993272
Jun 08, 2021, 10:32:52 EDT	I-93	SB	BOSTON	DMV	1263217624
Jun 08, 2021, 17:55:10 EDT	I-93	NB	BOSTON	Crash	1262974043
Jun 09, 2021, 16:14:52 EDT	I-93	NB	BOSTON	Crash	1263162675
Jun 11, 2021, 08:36:10 EDT	I-93	NB	BOSTON	DMV	1263047749
Jun 11, 2021, 18:05:30 EDT	I-93	SB	BOSTON	Crash	1263156327
Jun 13, 2021, 21:01:05 EDT	I-93	NB	BOSTON	Crash	1262968954
Jun 14, 2021, 16:02:36 EDT	I-93	SB	BOSTON	Crash	386964859
Jun 16, 2021, 07:52:43 EDT	I-93	SB	BOSTON	Crash	1263184372
Jun 19, 2021, 12:57:17 EDT	I-93	NB	BOSTON	Crash	1263217624
Jun 23, 2021, 01:35:24 EDT	I-93	SB	QUINCY	DMV	1263156342
Jun 24, 2021, 01:37:39 EDT	I-93	NB	BRAINTREE	Crash	1263096881
Jun 24, 2021, 16:53:14 EDT	I-93	SB	BOSTON	Crash	1263046143
Jun 25, 2021, 02:17:04 EDT	I-93	NB	MILTON	Crash	1262974027
Jun 26, 2021, 05:09:49 EDT	I-93	NB	BOSTON	DMV	386896207
Jun 26, 2021, 05:09:49 EDT	I-93	NB	BOSTON	DMV	1263231759
Jun 26, 2021, 18:24:32 EDT	I-93	NB	BOSTON	Crash	1262974027

8.2 Results of Incident Detection Strategy Test, June 1 to June 30, 2021

In Figures 8.1 through 8.28, (a) shows the congestion scan and (b) shows the alarms issued by incident detection strategy, for southbound and northbound of south I-93 on successive days in June 2021.

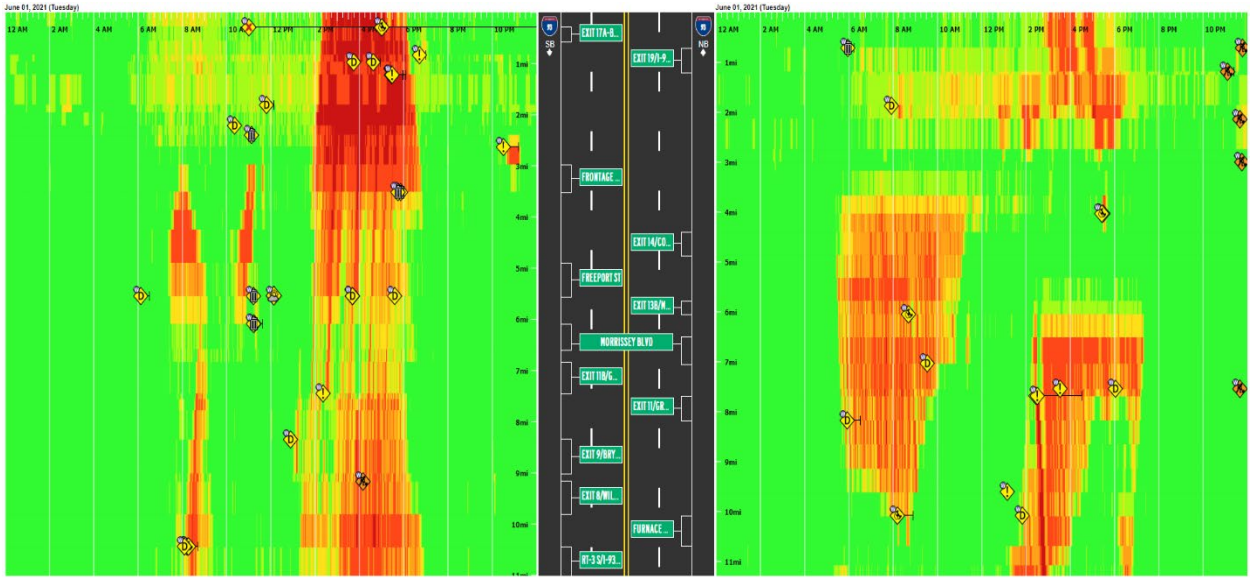

(a)

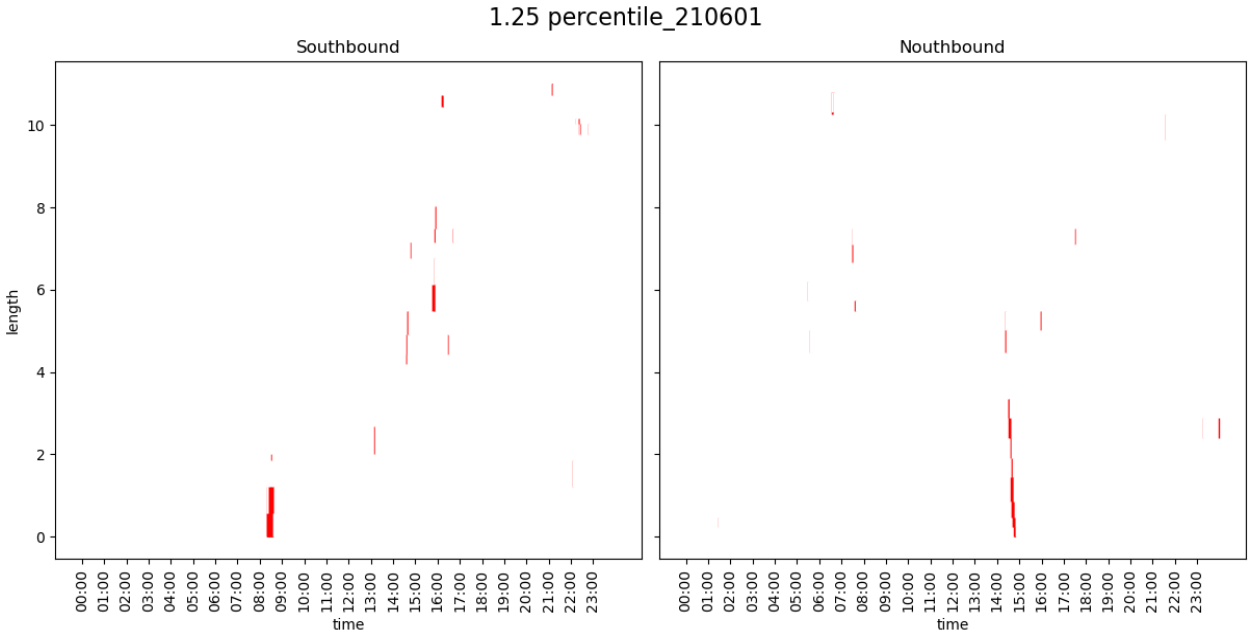

(b)

Figure 8.1: June 1, 2021

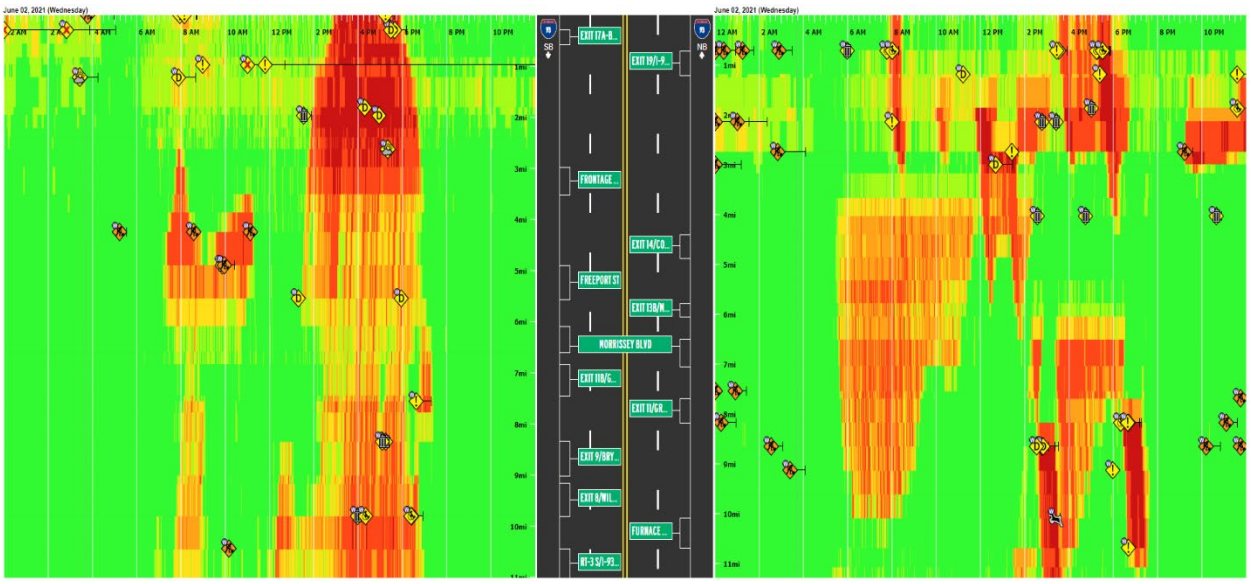

(a)

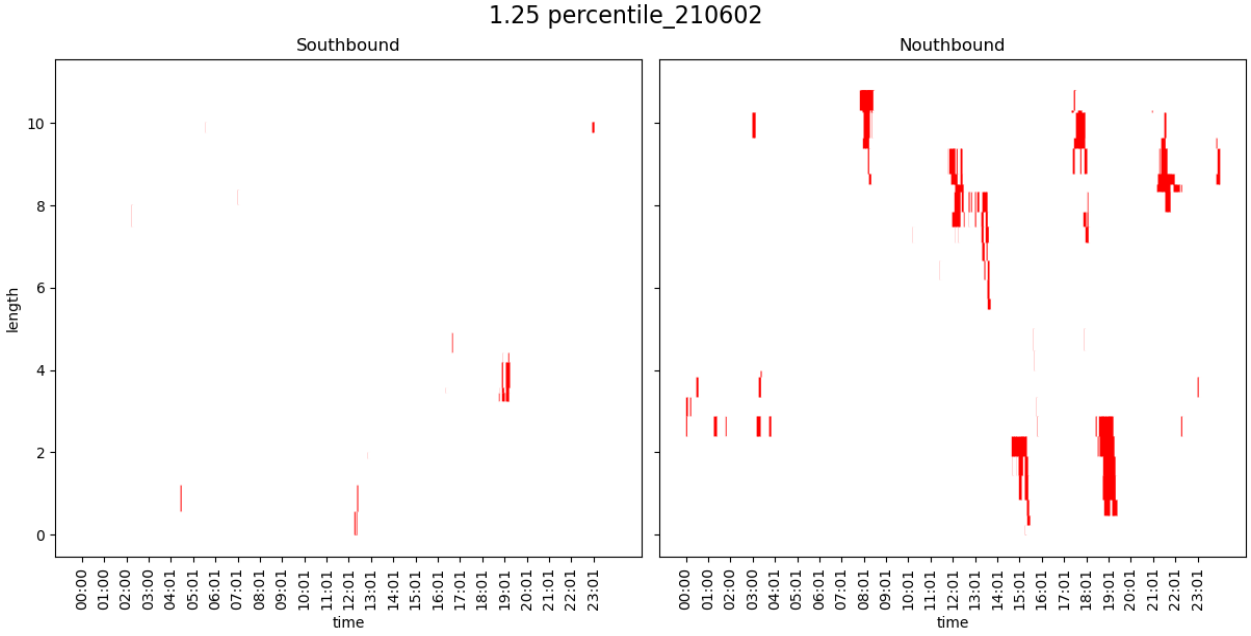

(b)

Figure 8.2: June 2, 2021

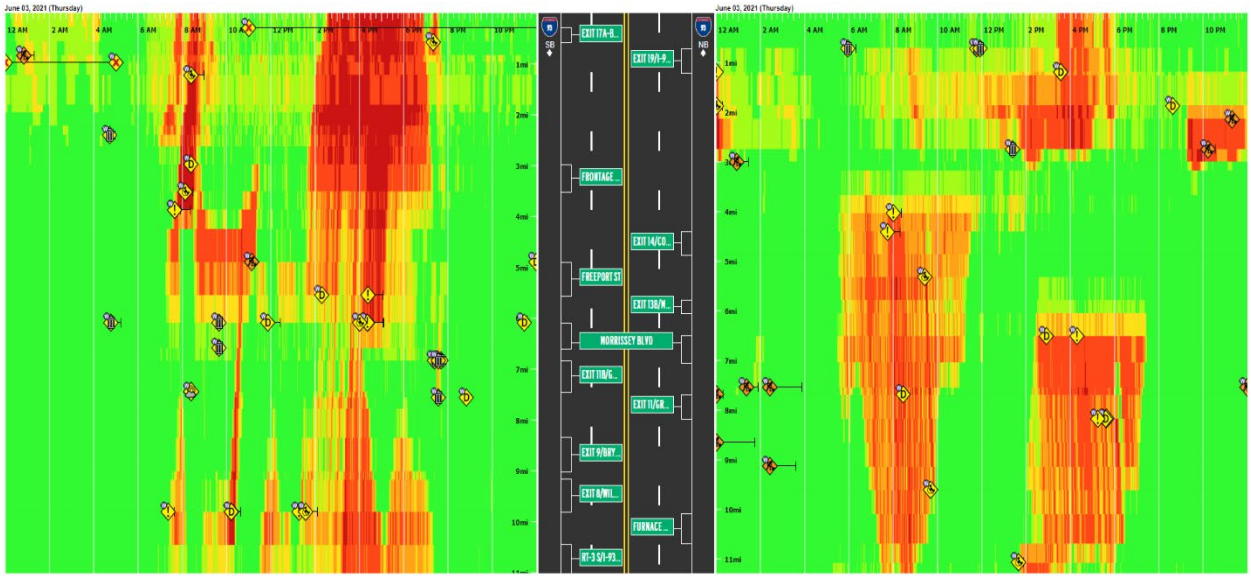

(a)

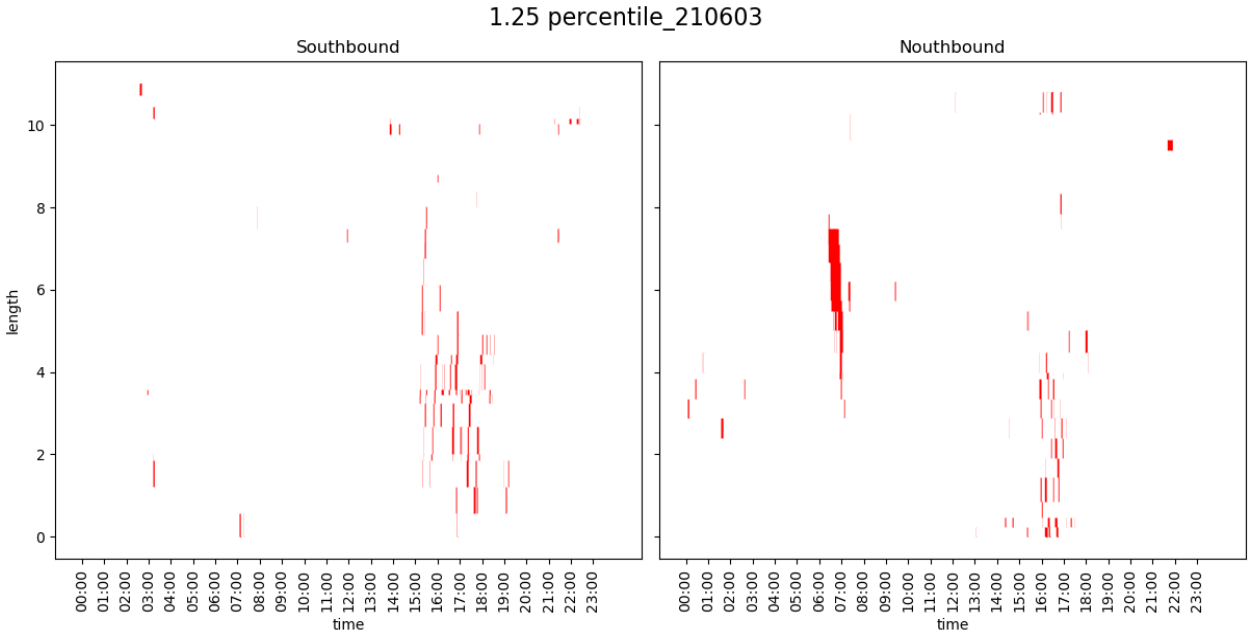

(b)

Figure 8.3: June 3, 2021

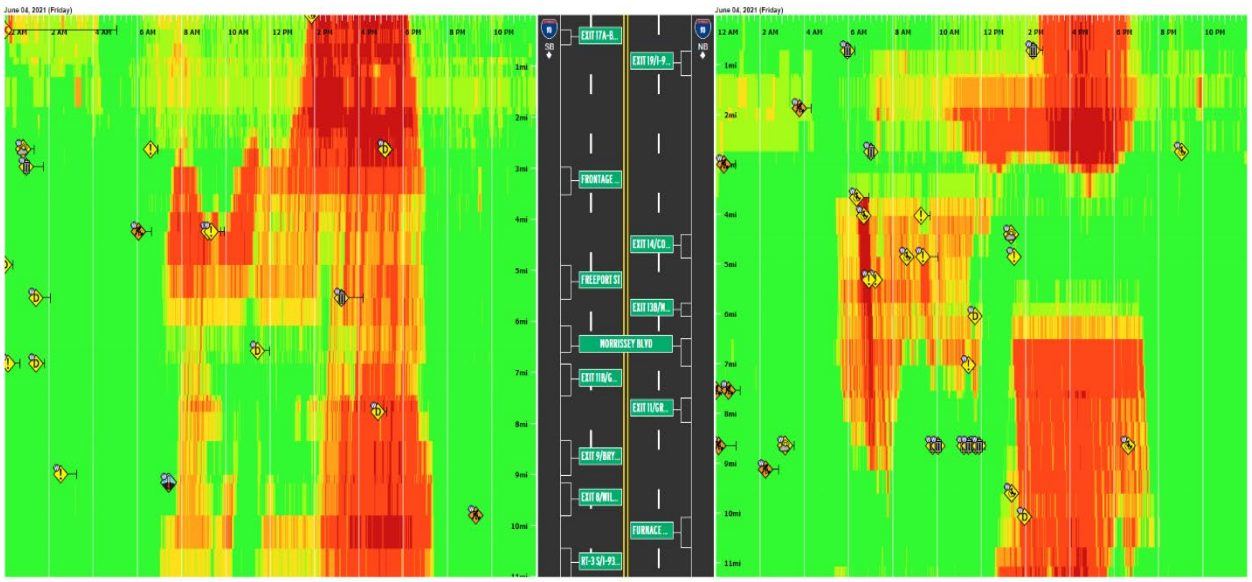

(a)

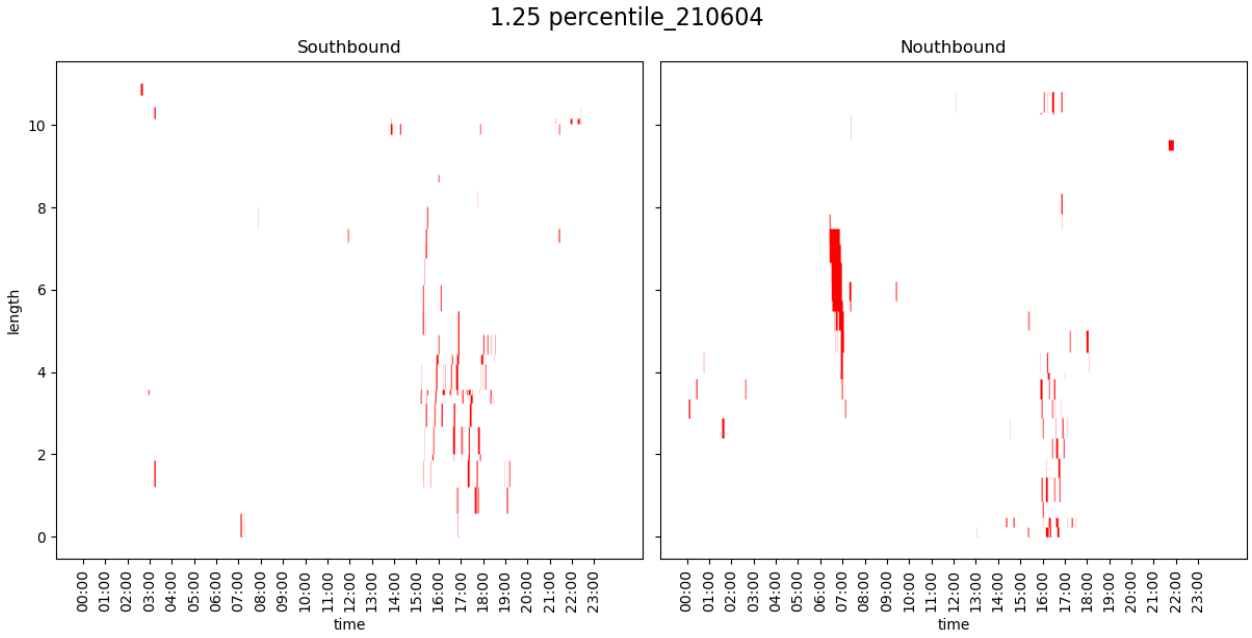

(b)

Figure 8.4: June 4, 2021

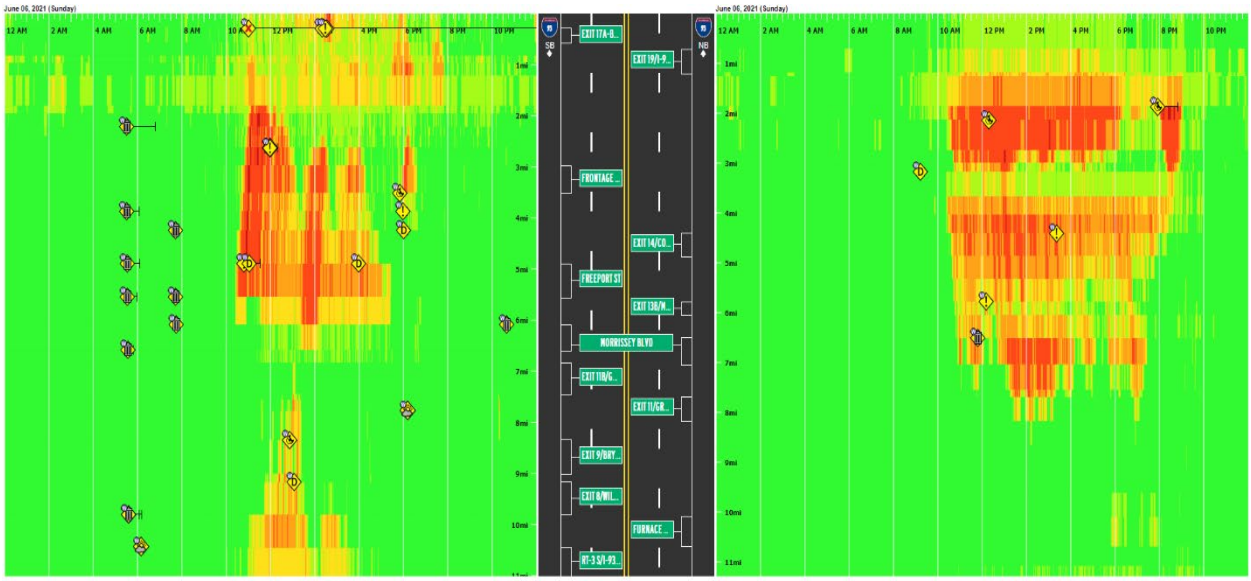

(a)

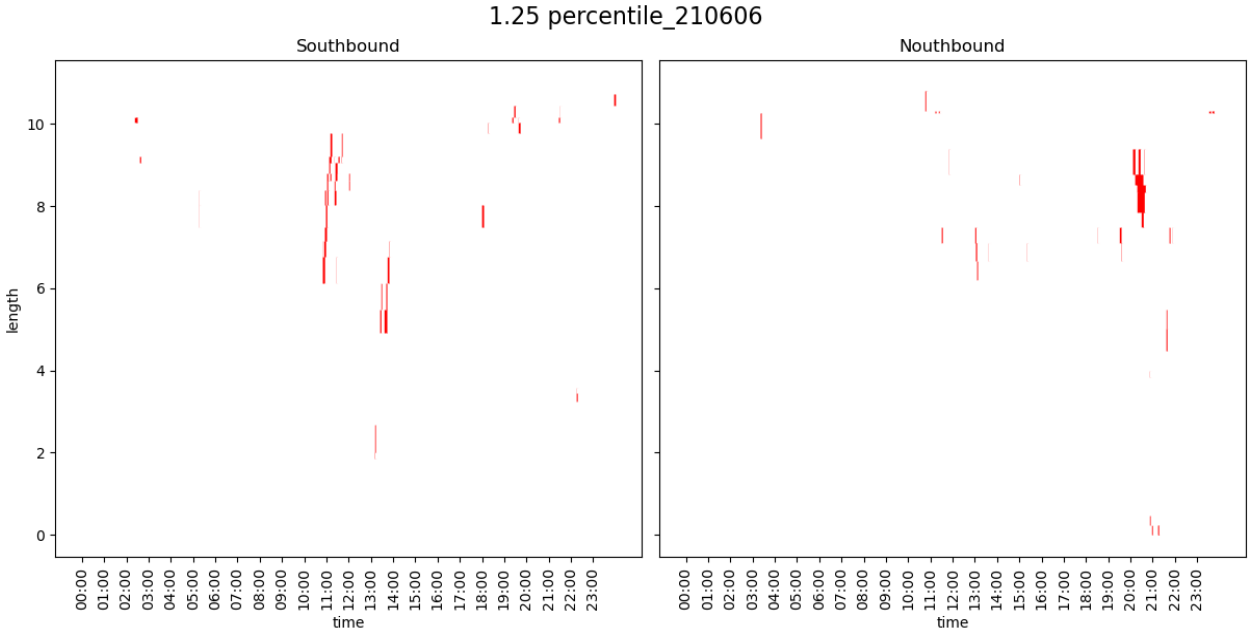

(b)

Figure 8.5: June 6, 2021

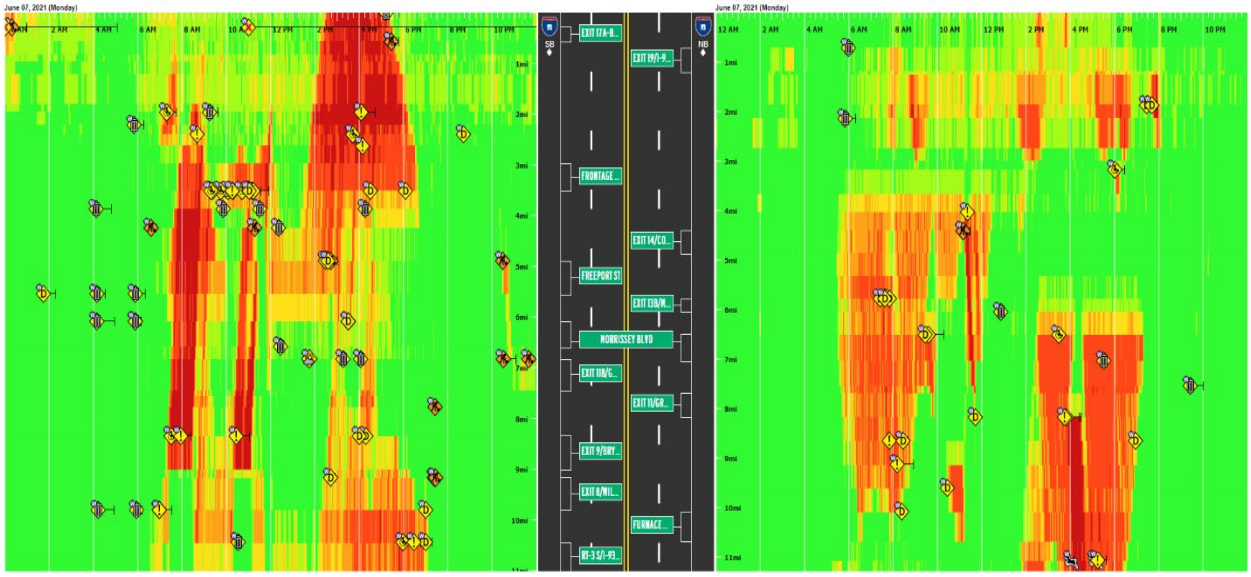

(a)

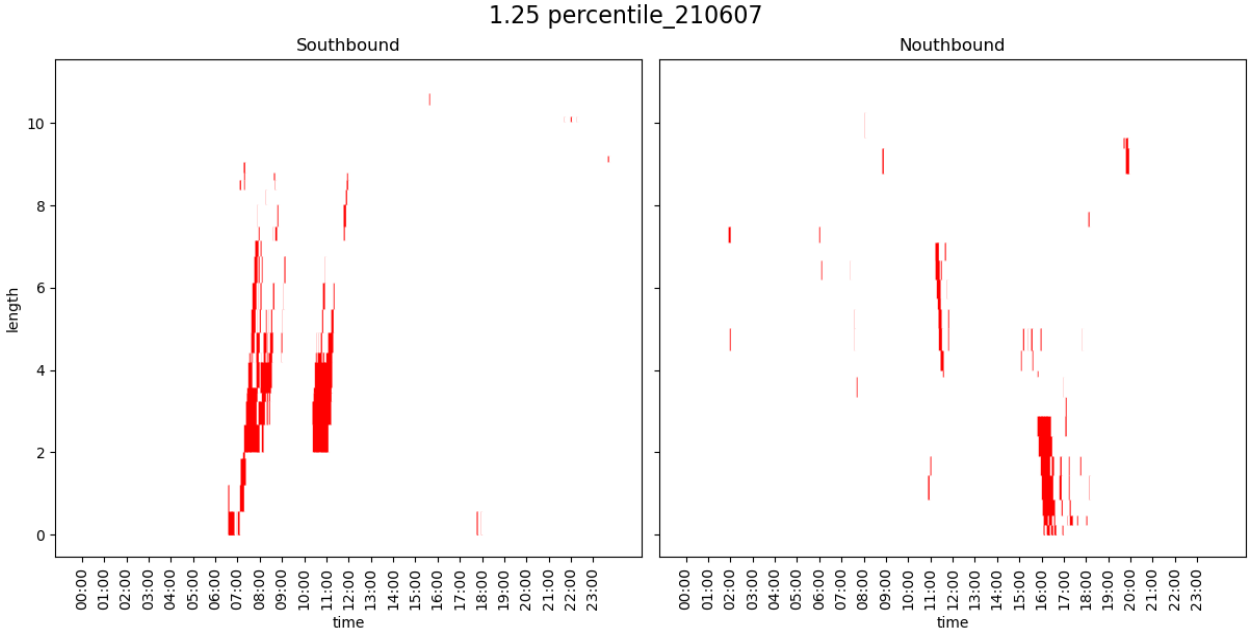

(b)

Figure 8.6: June 7, 2021

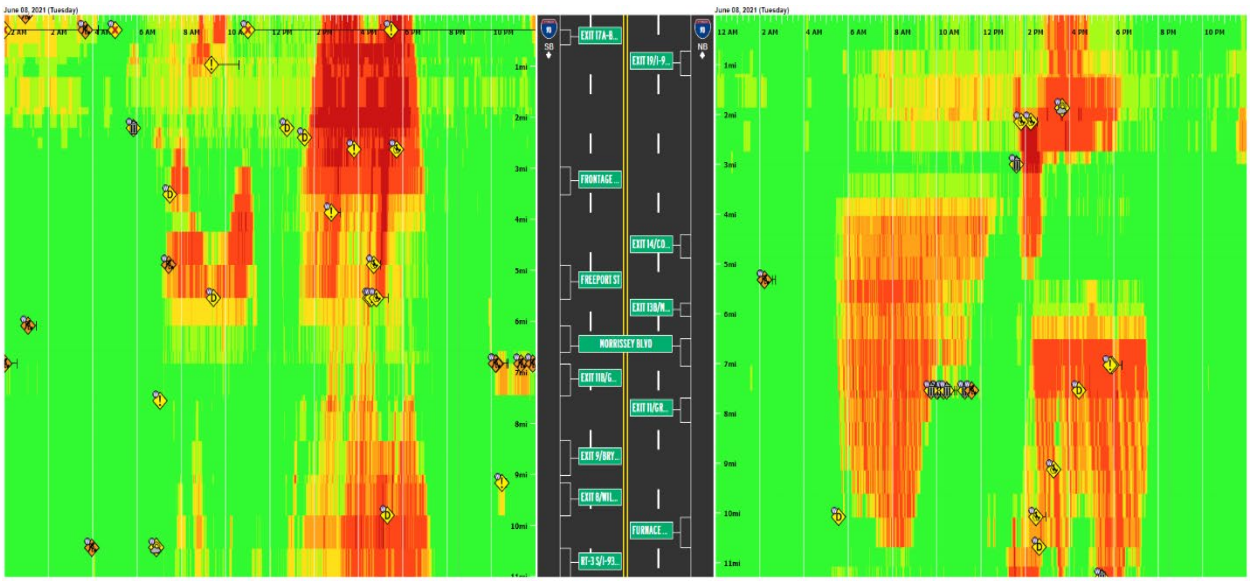

(a)

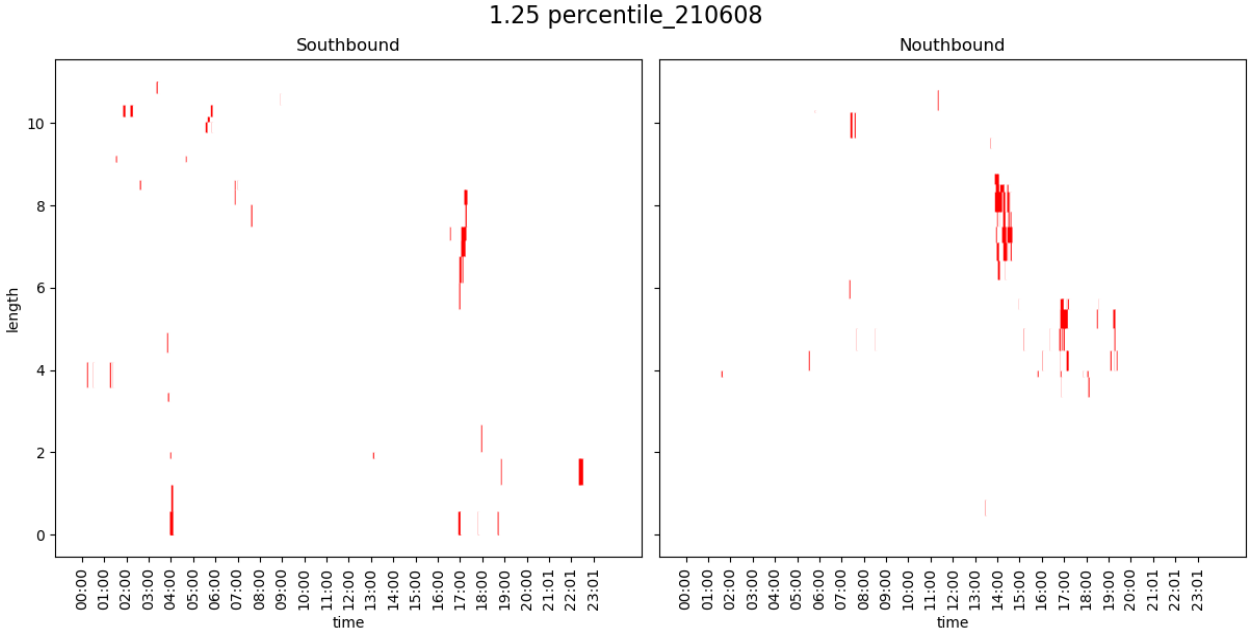

(b)

Figure 8.7: June 8, 2021

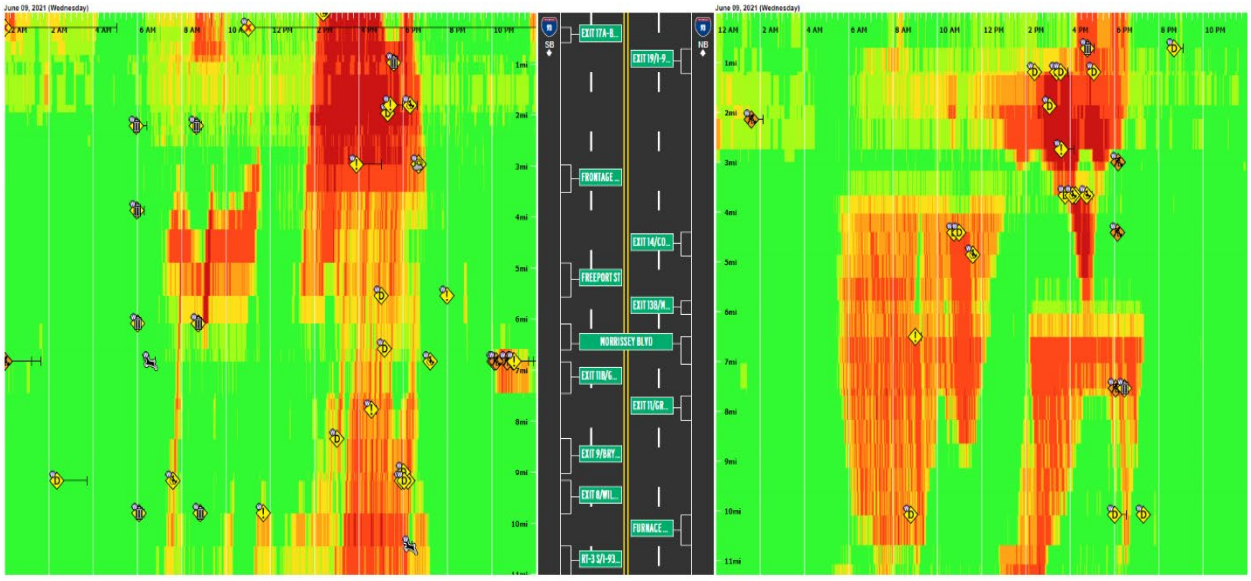

(a)

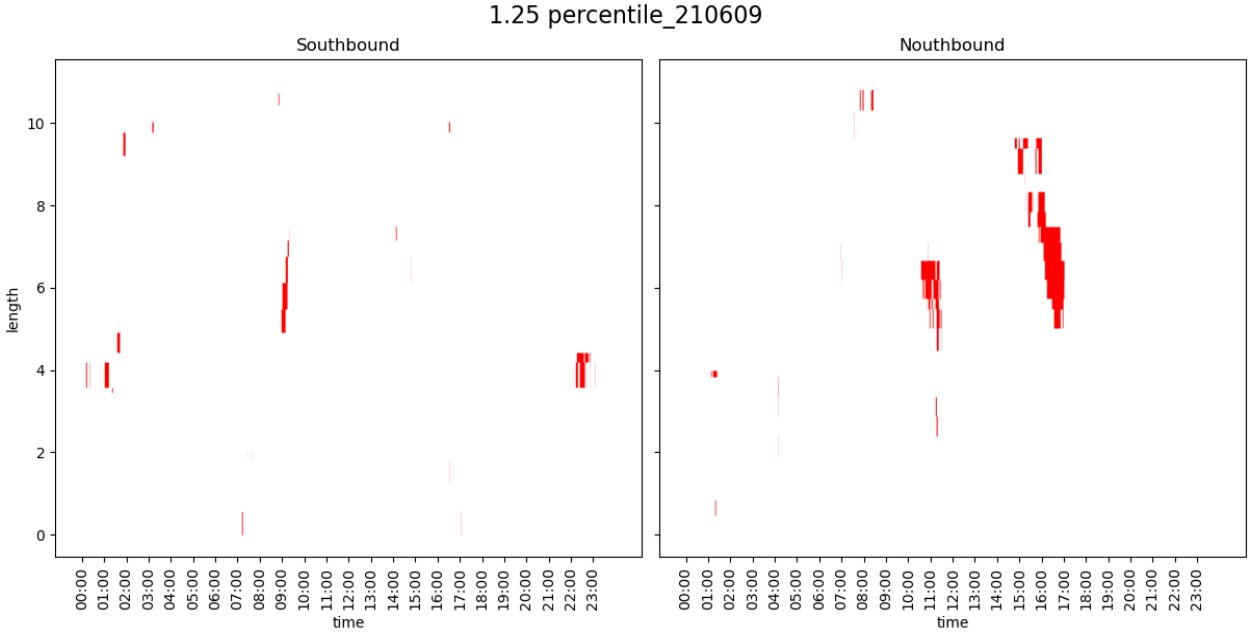

(b)

Figure 8.8: June 9, 2021

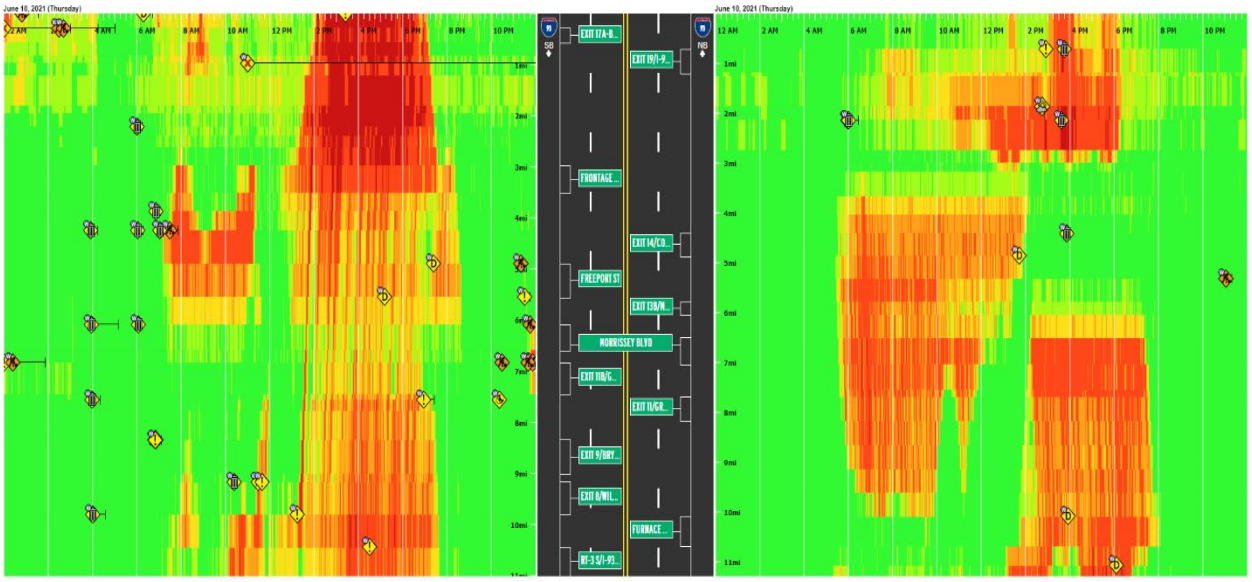

(a)

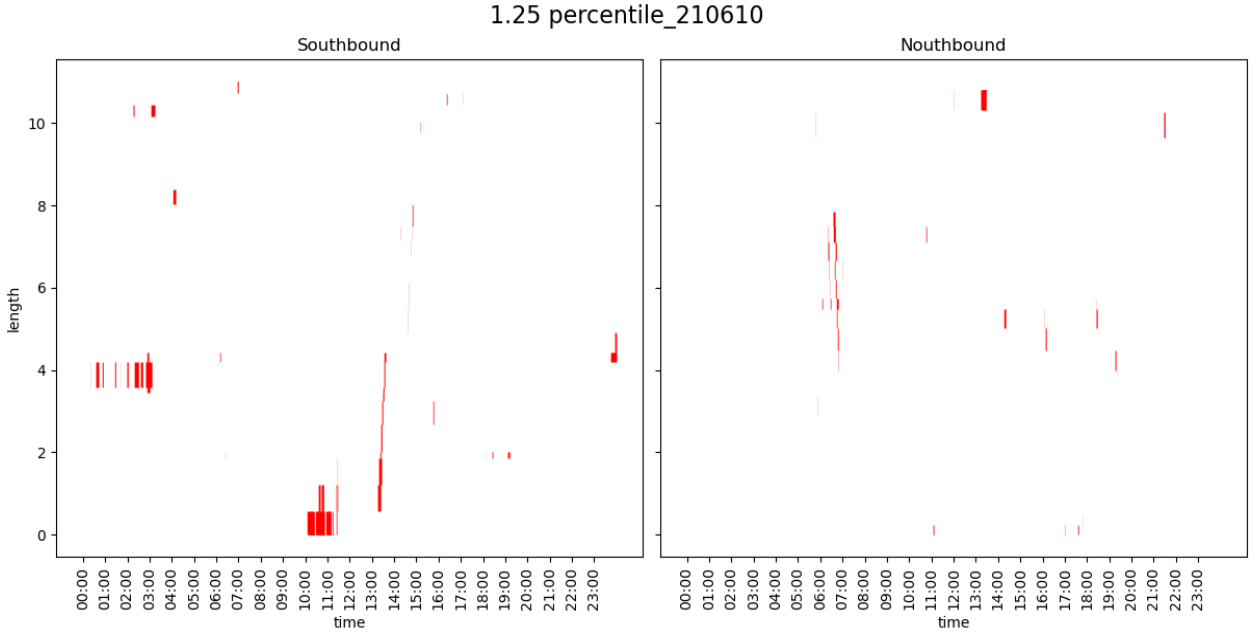

(b)

Figure 8.9: June 10, 2021

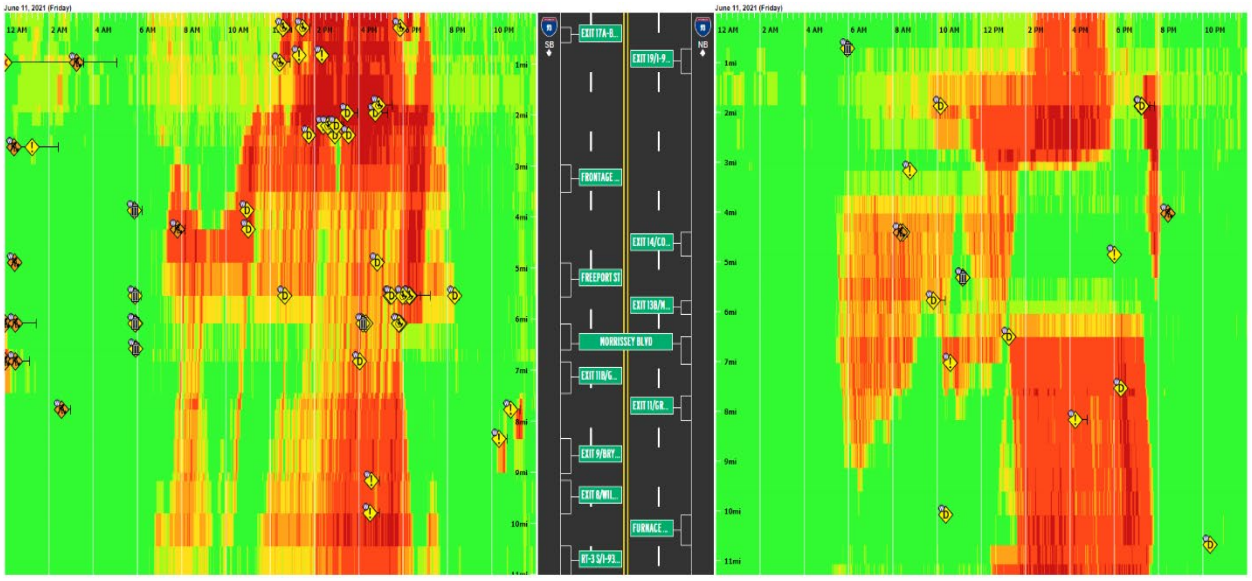

(a)

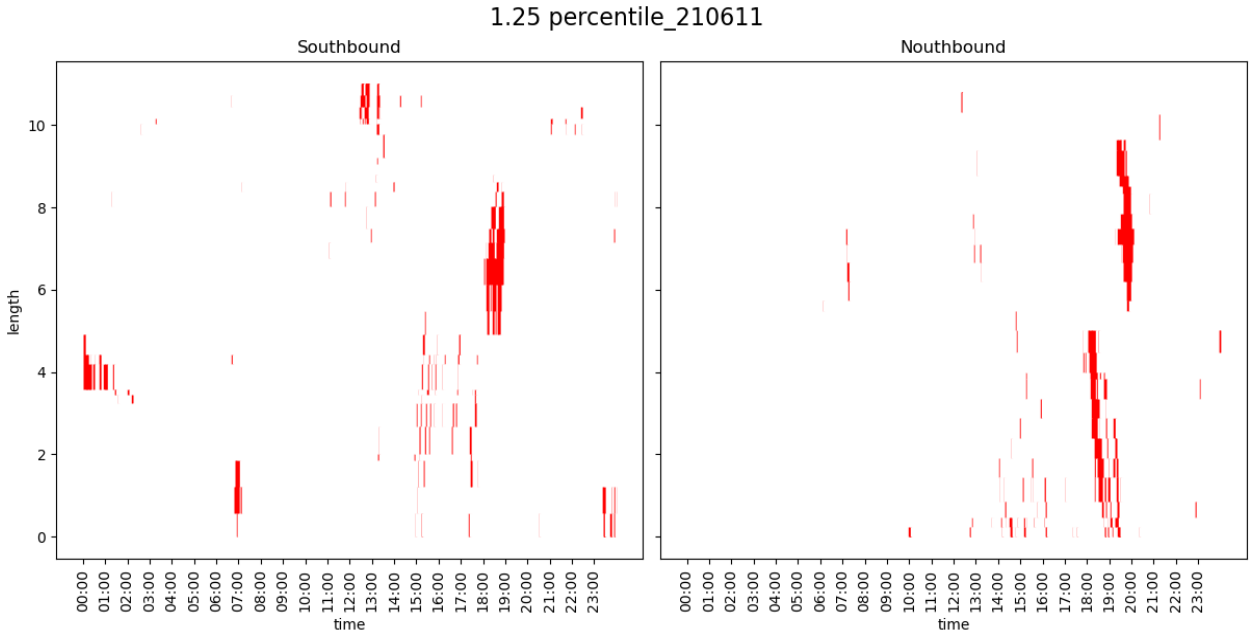

(b)

Figure 8.10: June 11, 2021

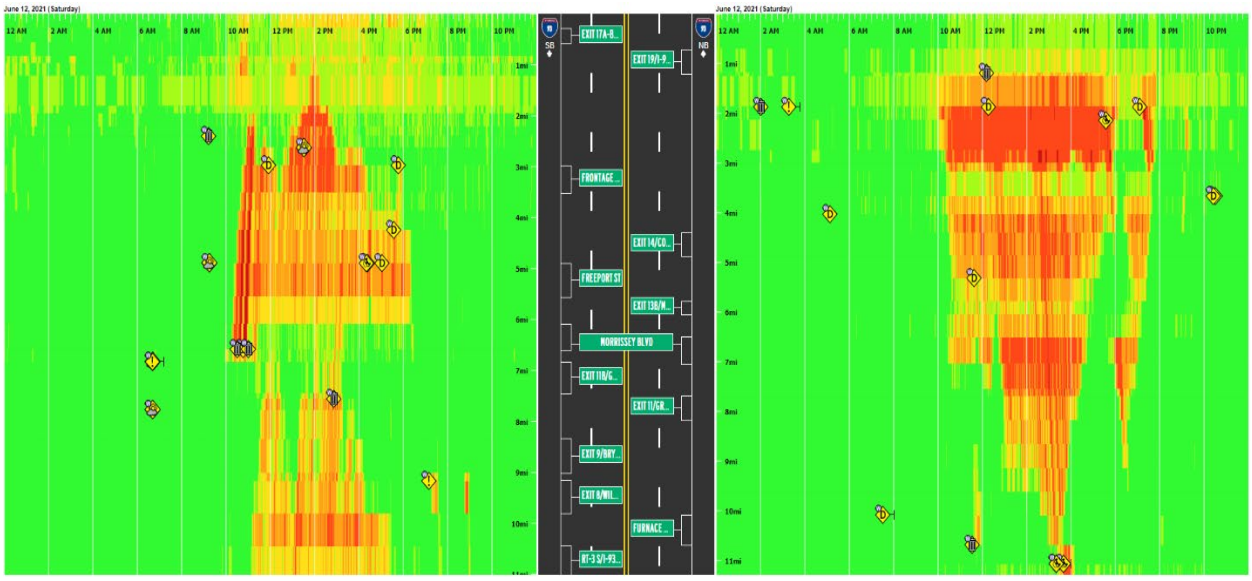

(a)

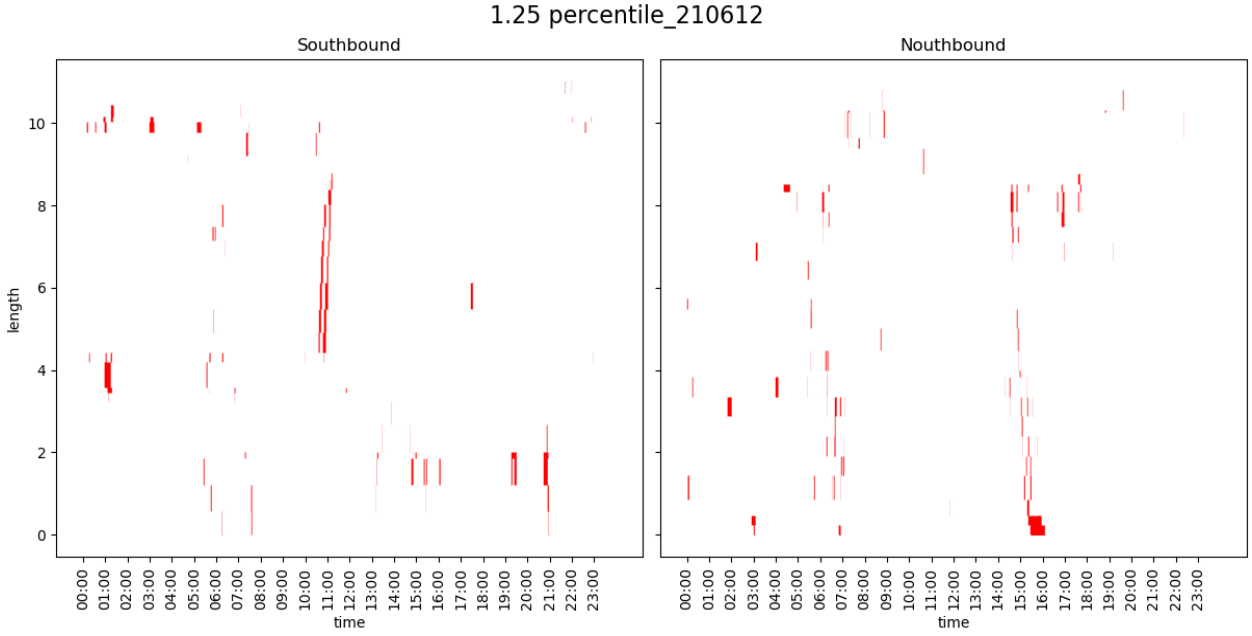

(b)

Figure 8.11: June 12, 2021

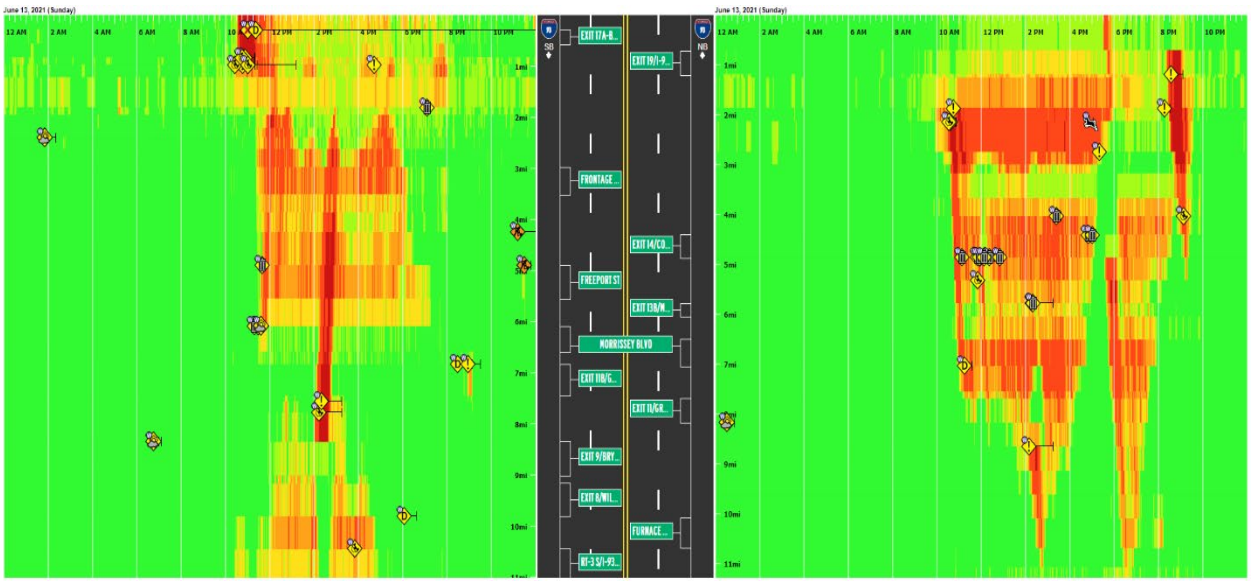

(a)

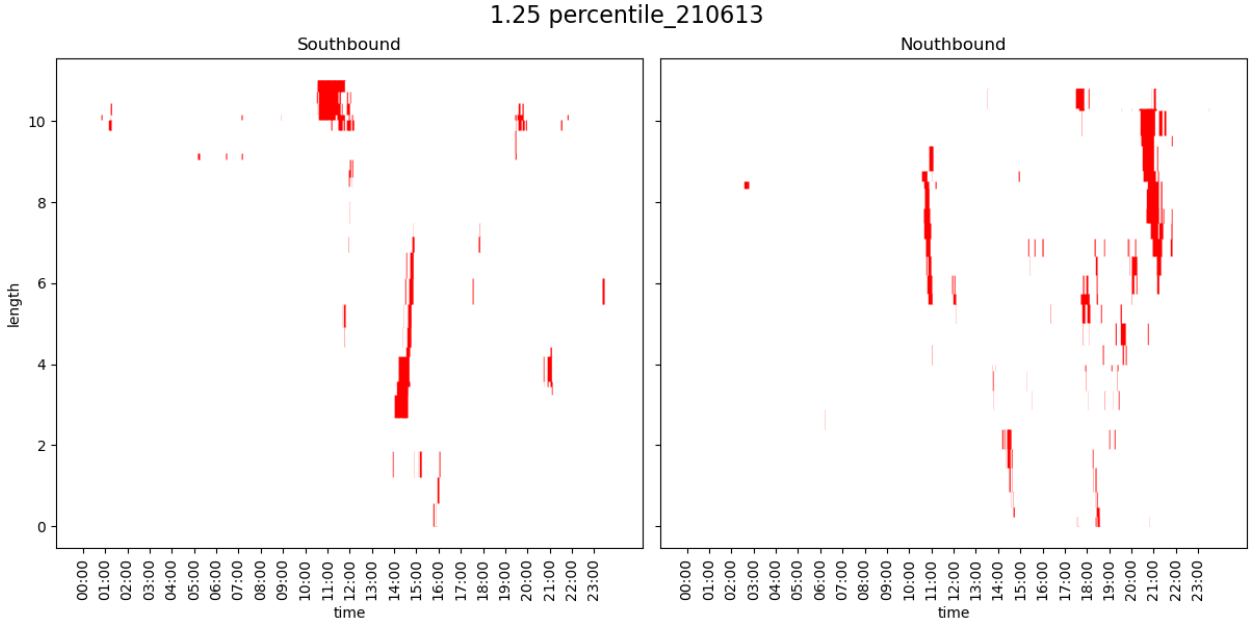

(b)

Figure 8.12: June 13, 2021

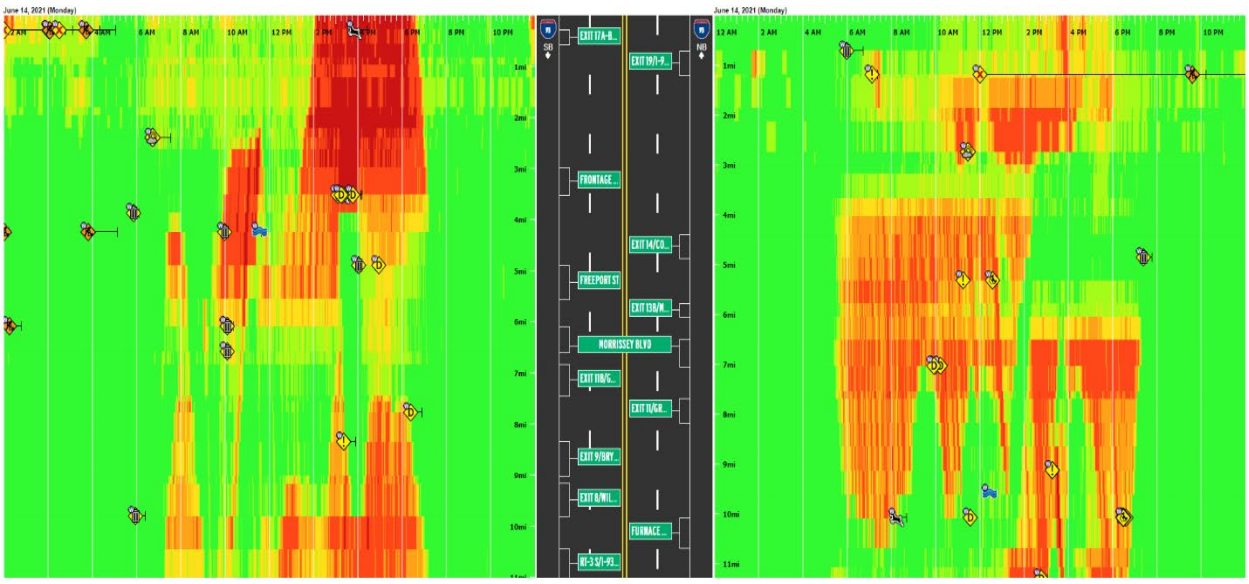

(a)

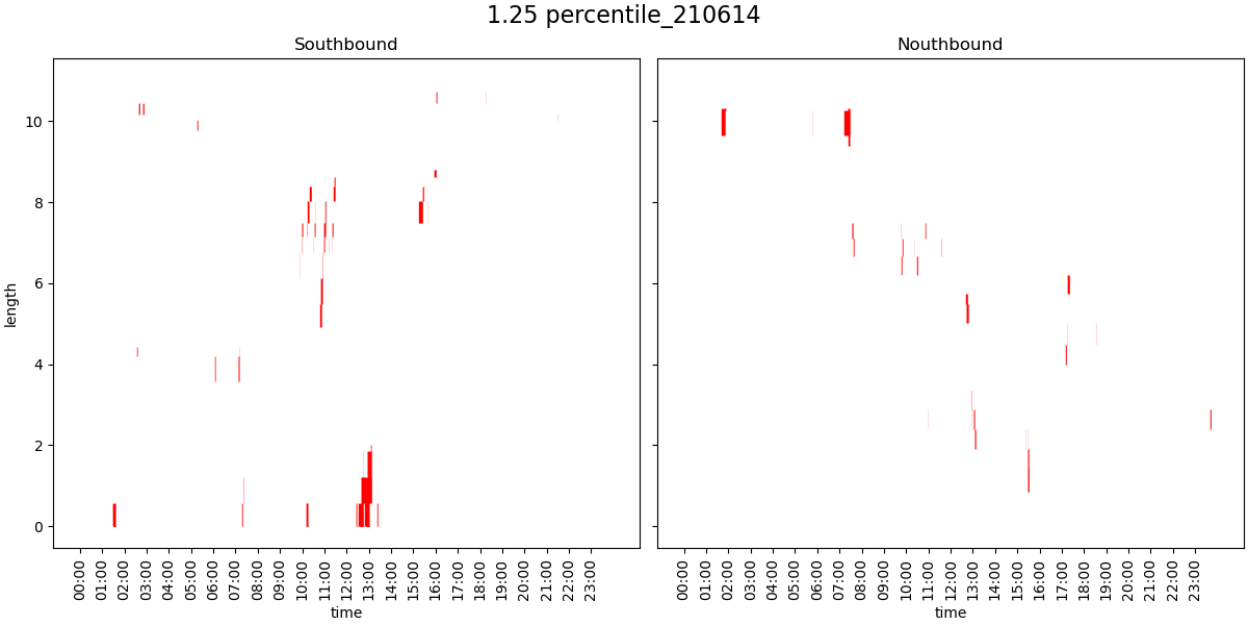

(b)

Figure 8.13: June 14, 2021

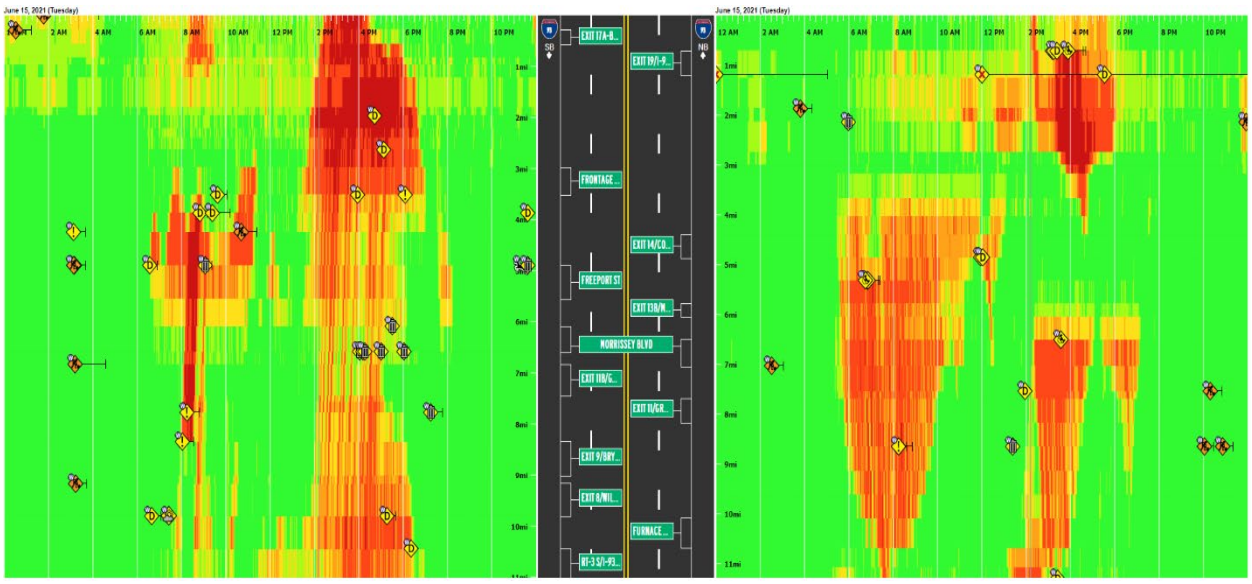

(a)

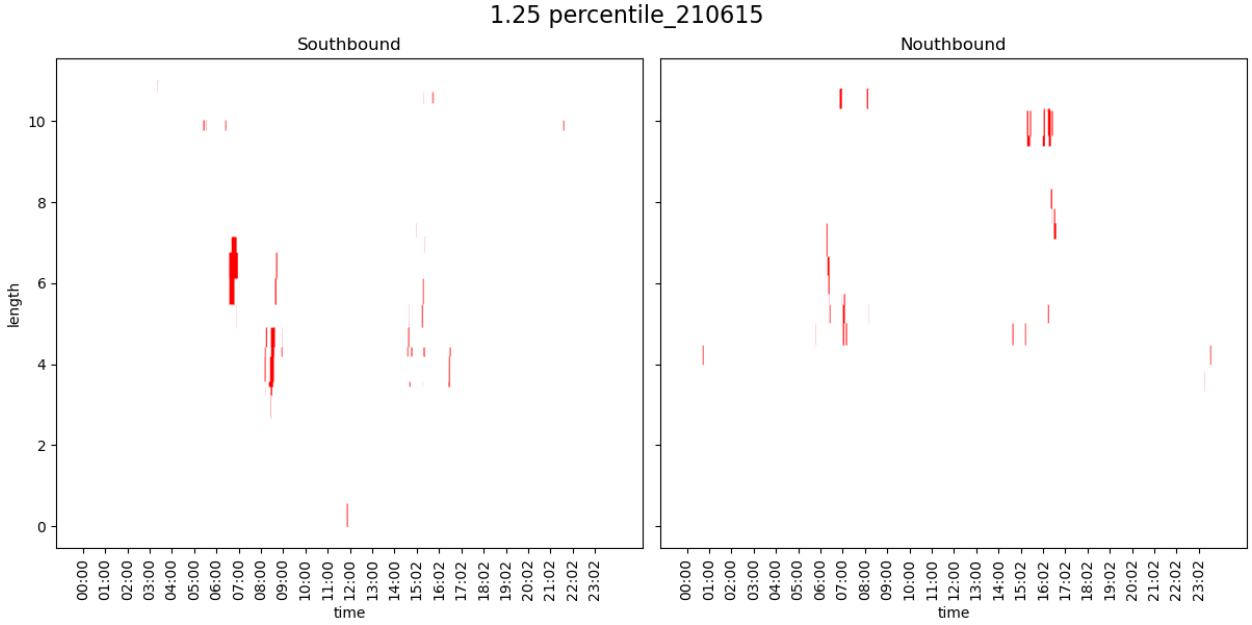

(b)

Figure 8.14: June 15, 2021

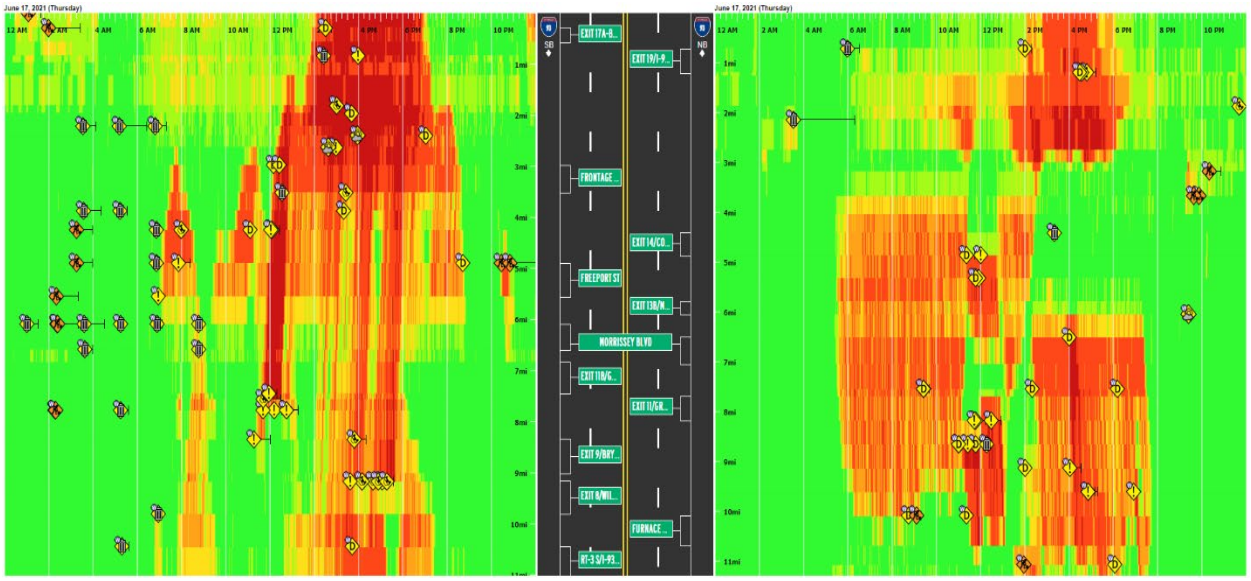

(a)

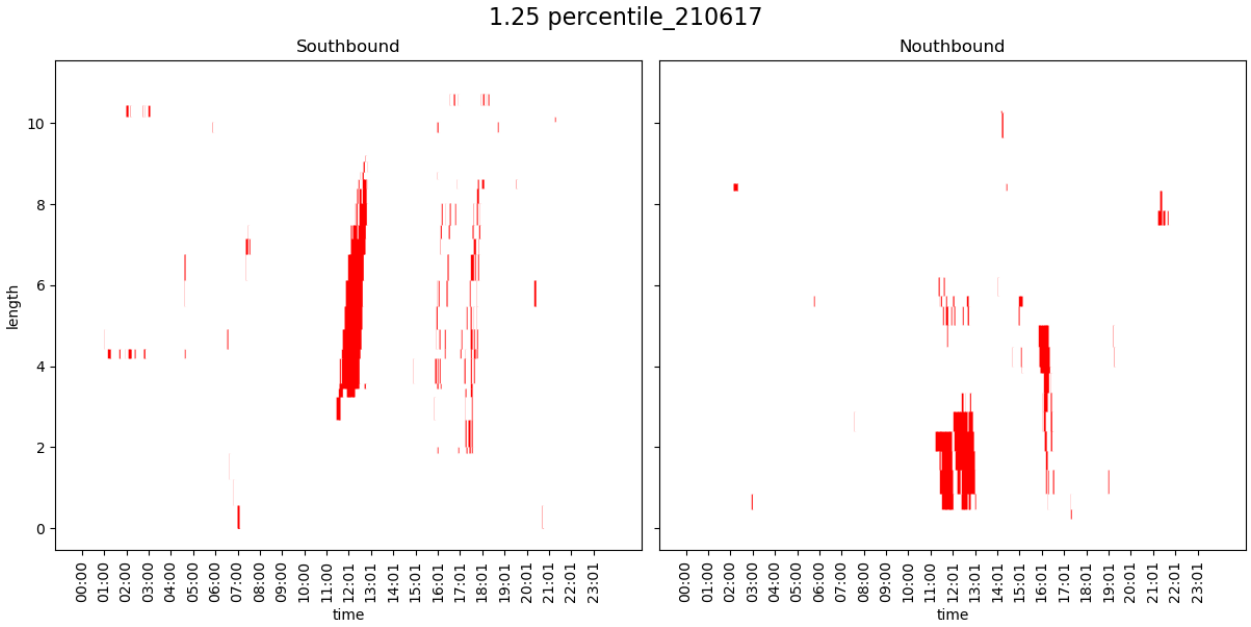

(b)

Figure 8.15: June 17, 2021

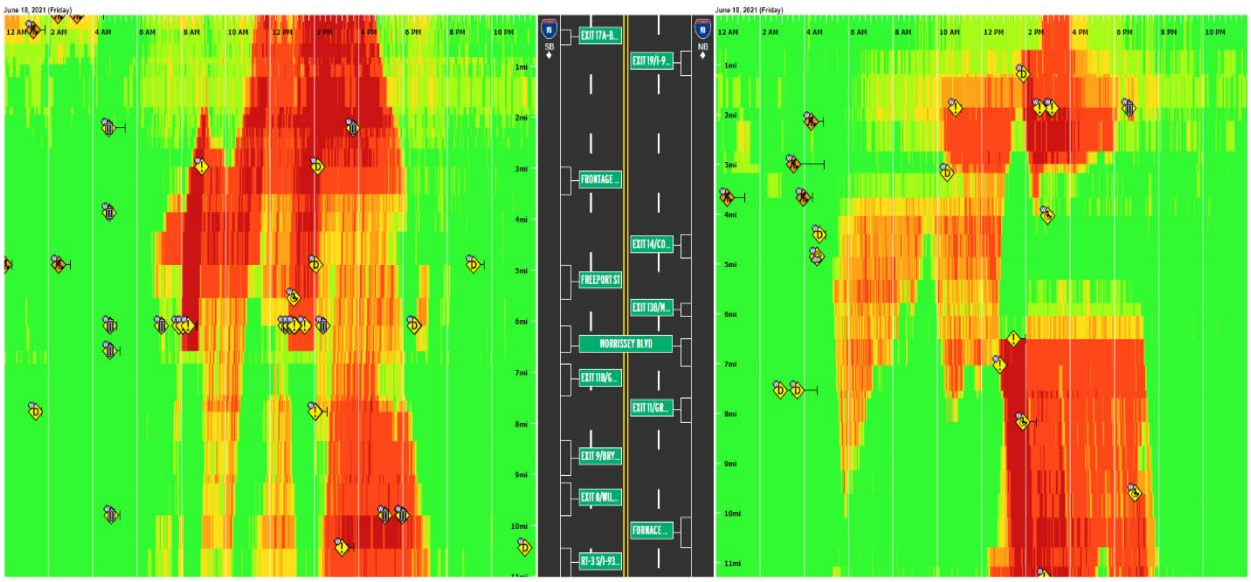

(a)

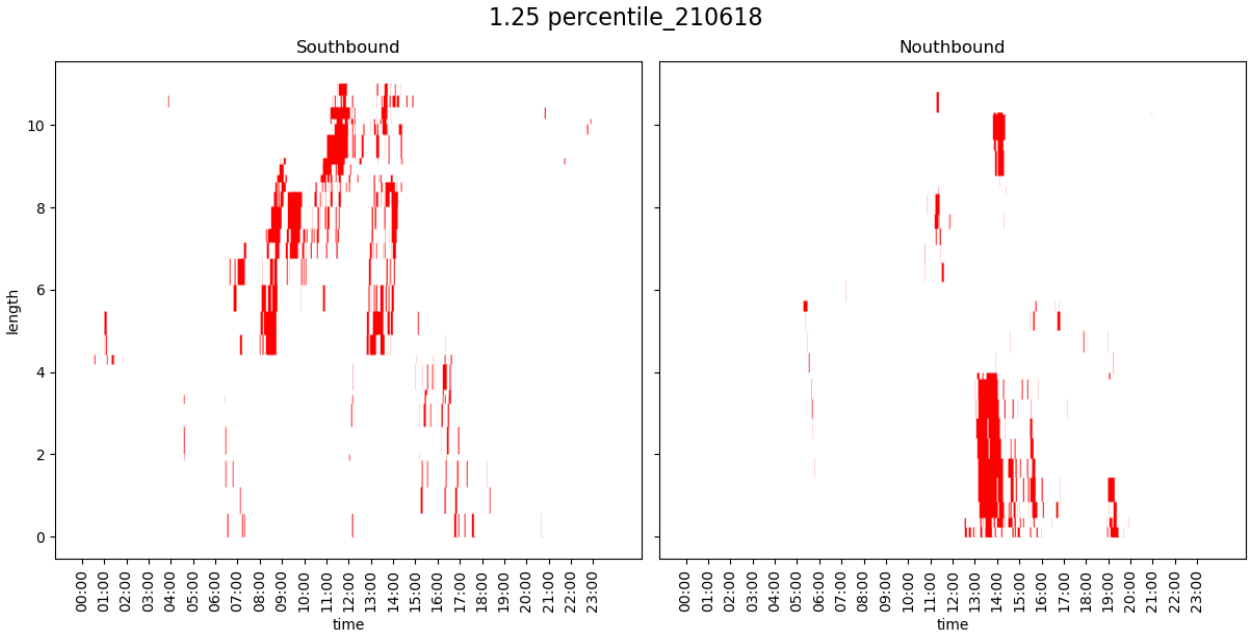

(b)

Figure 8.16: June 18, 2021

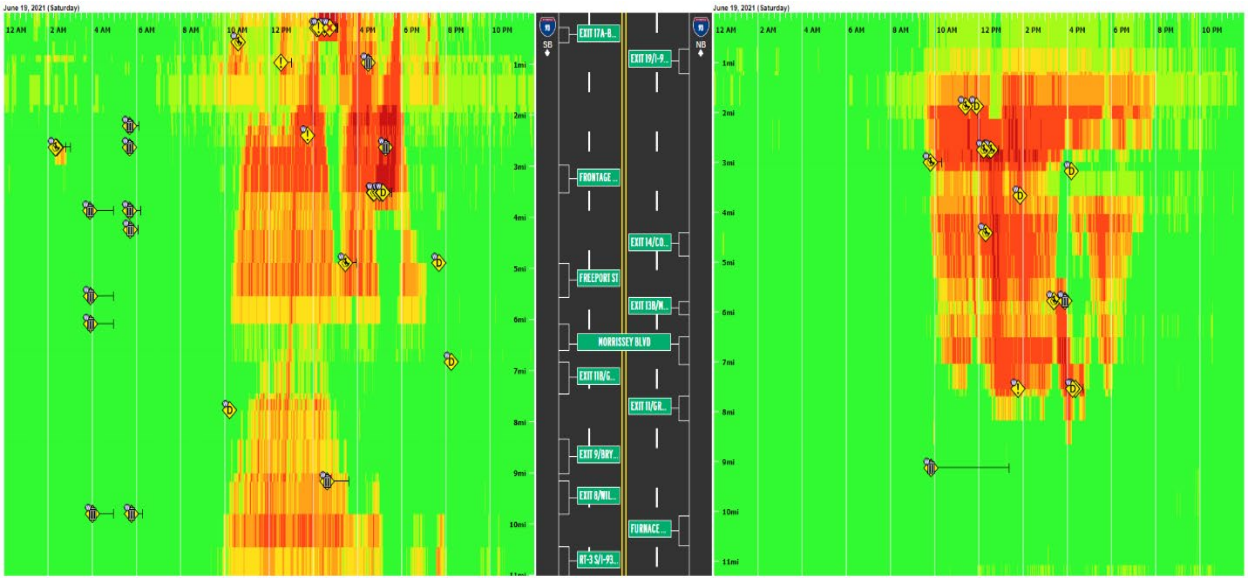

(a)

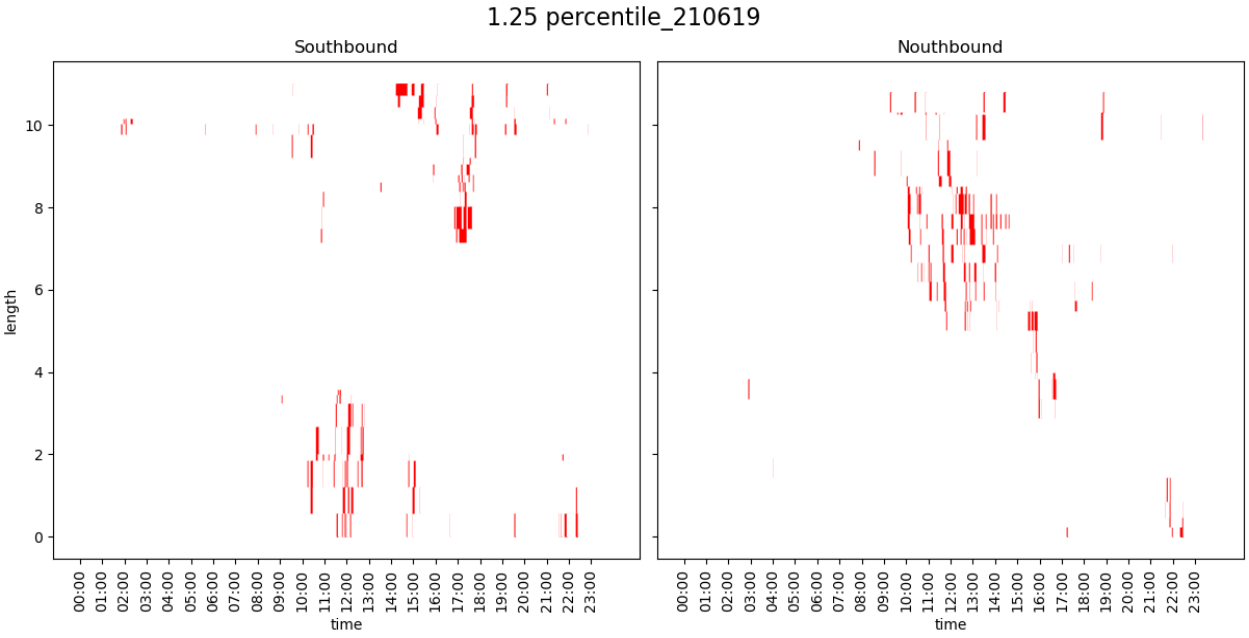

(b)

Figure 8.17: June 19, 2021

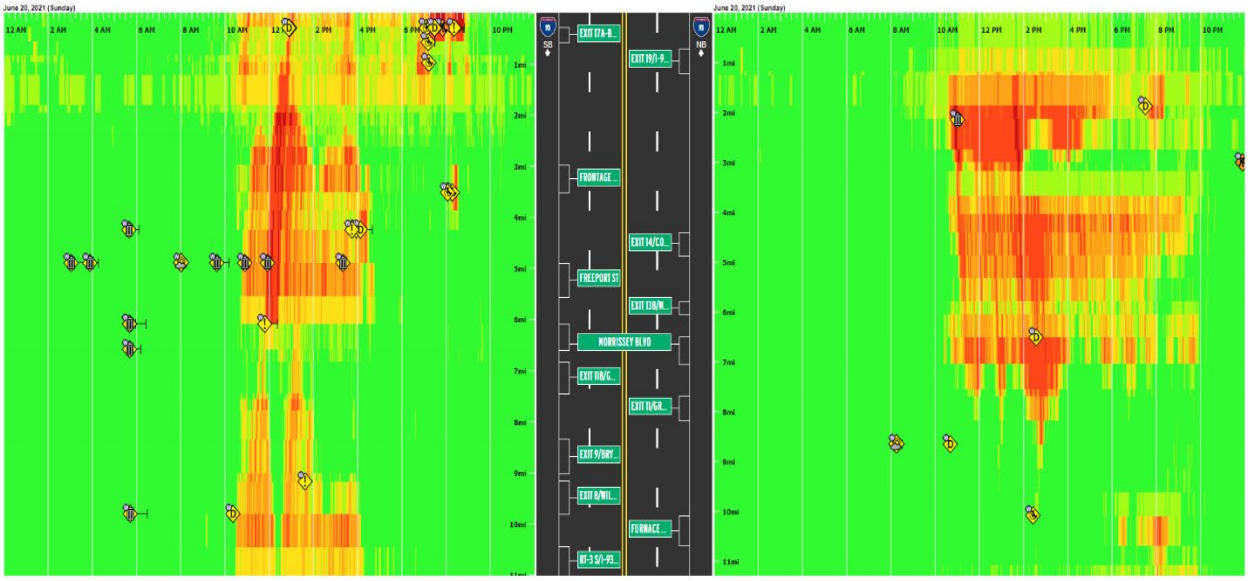

(a)

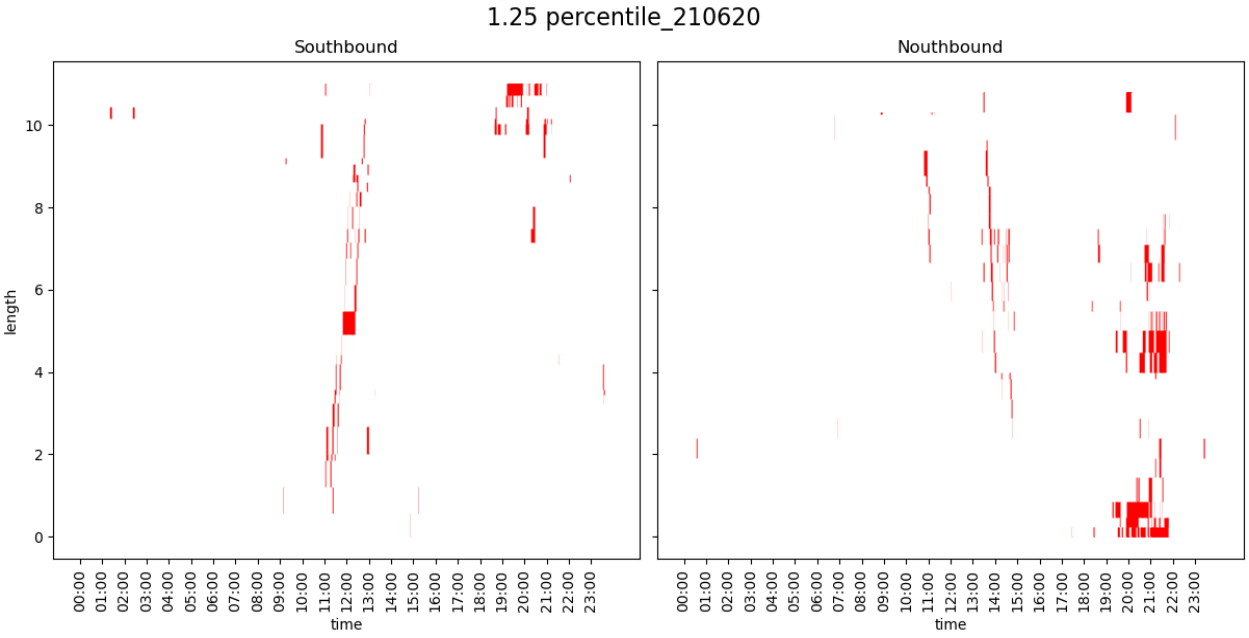

(b)

Figure 8.18: June 20, 2021

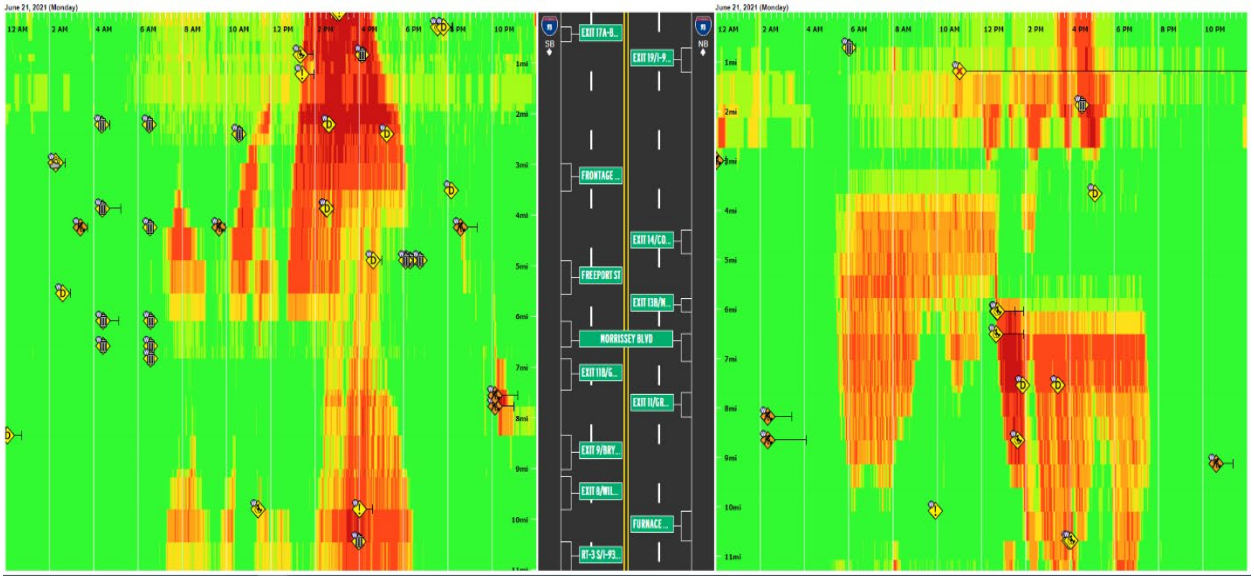

(a)

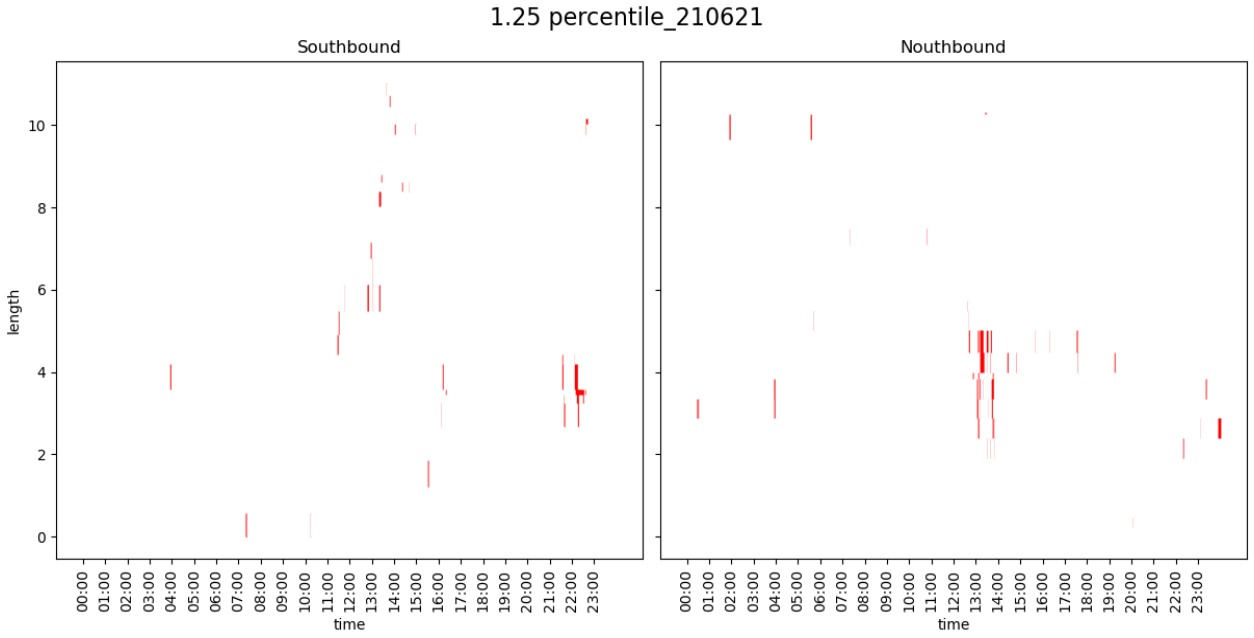

(b)

Figure 8.19: June 21, 2021

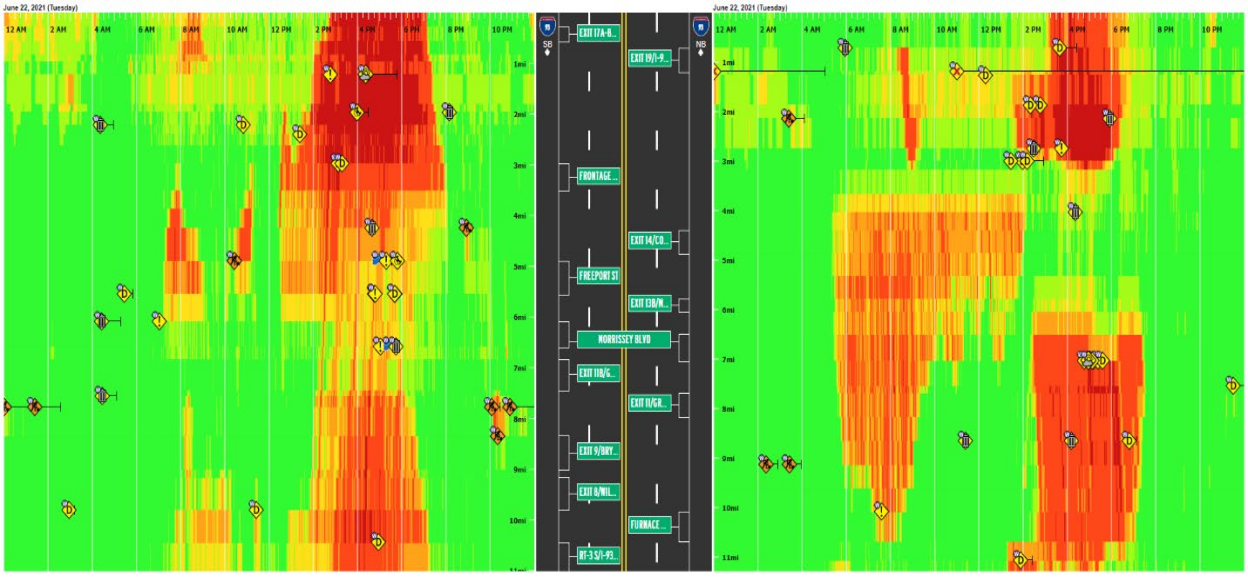

(a)

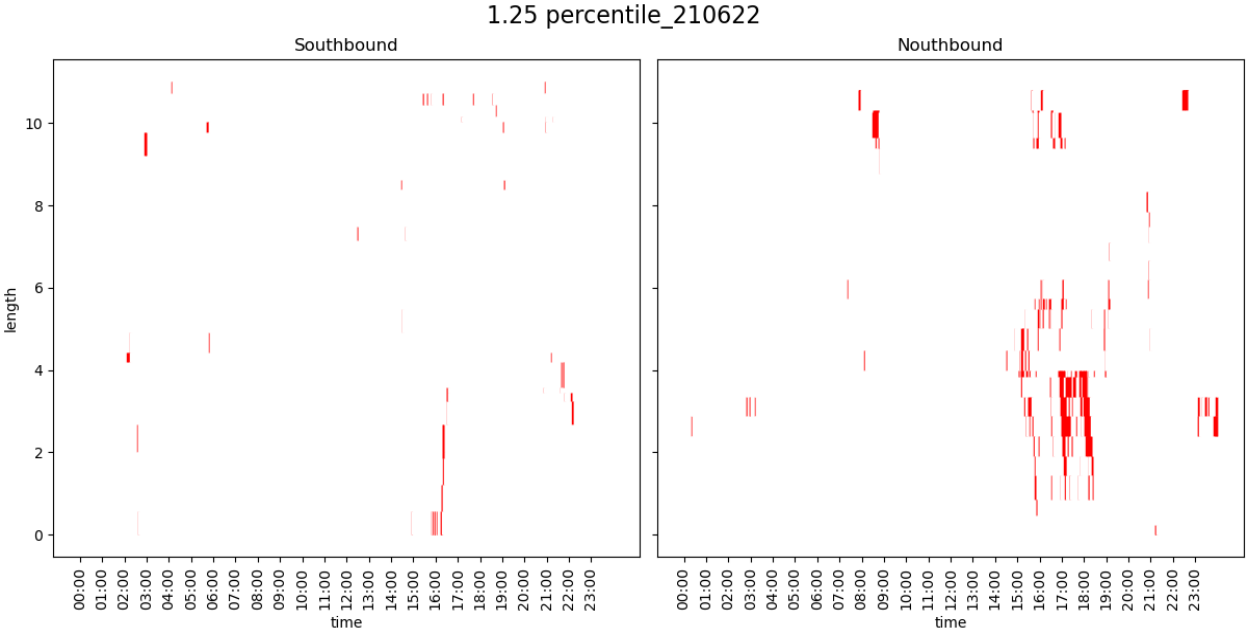

(b)

Figure 8.20: June 22, 2021

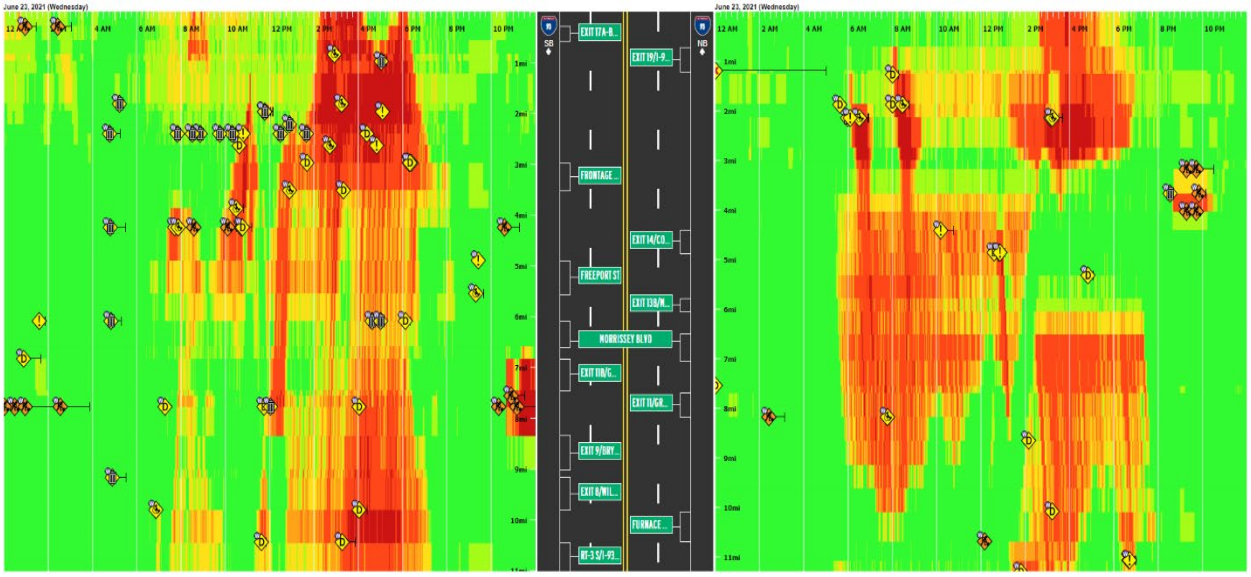

(a)

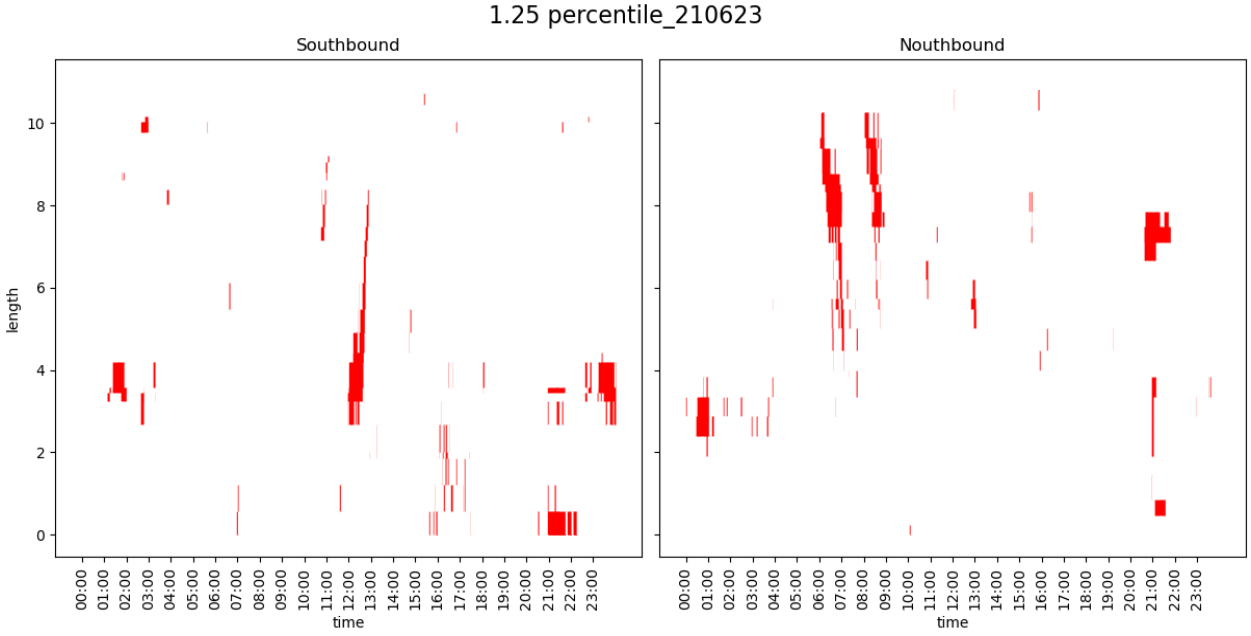

(b)

Figure 8.21: June 23, 2021

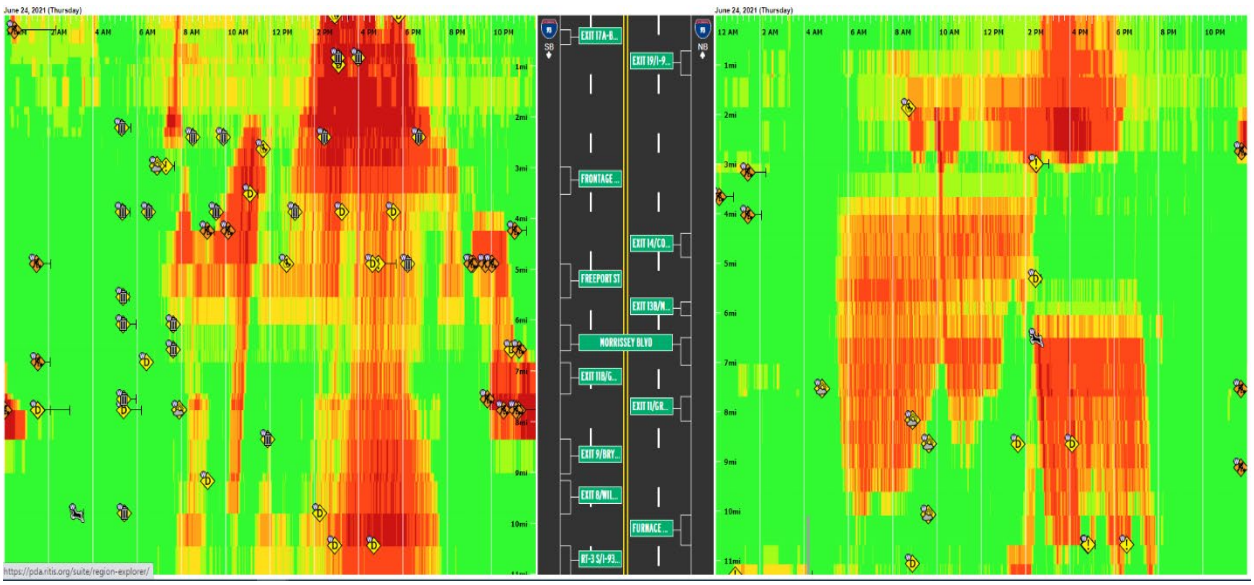

(a)

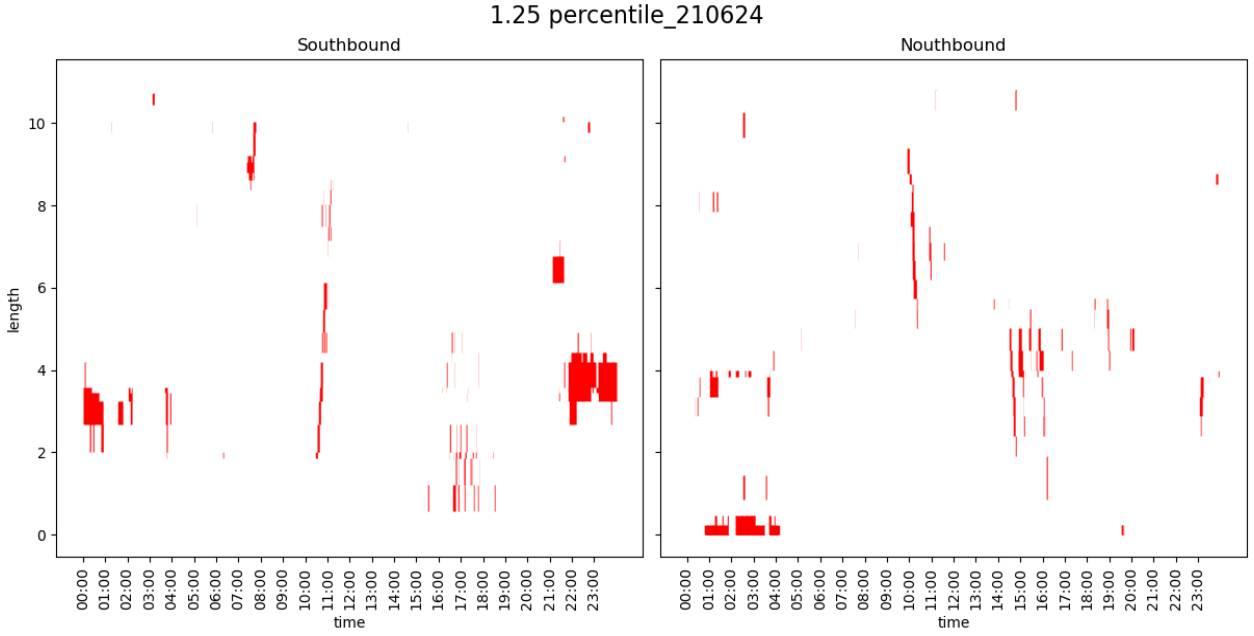

(b)

Figure 8.22: June 24, 2021

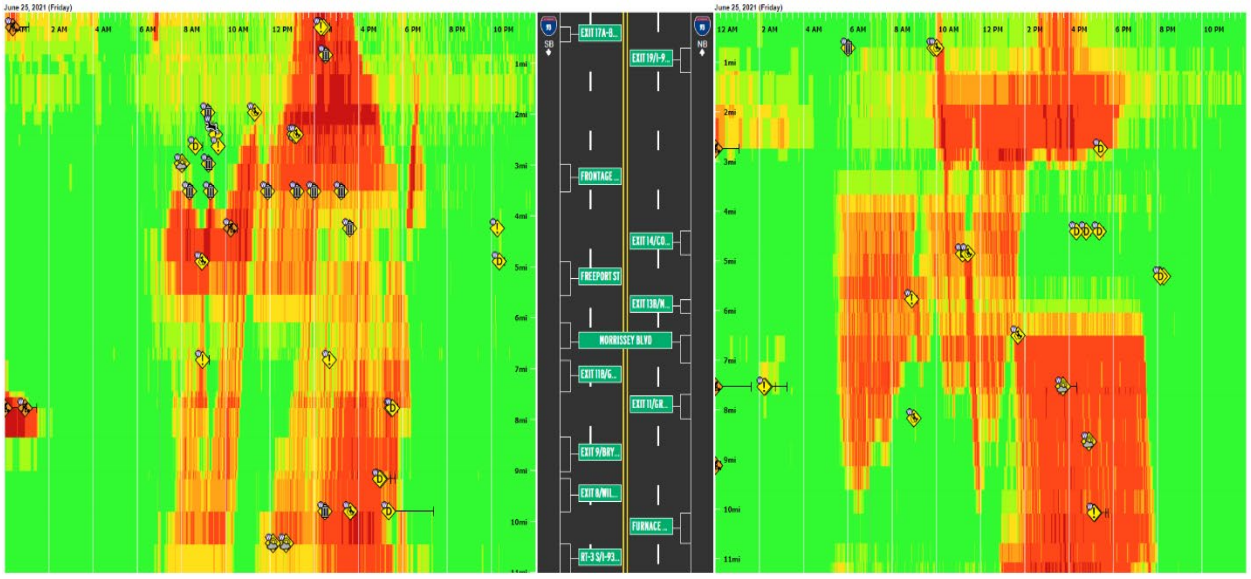

(a)

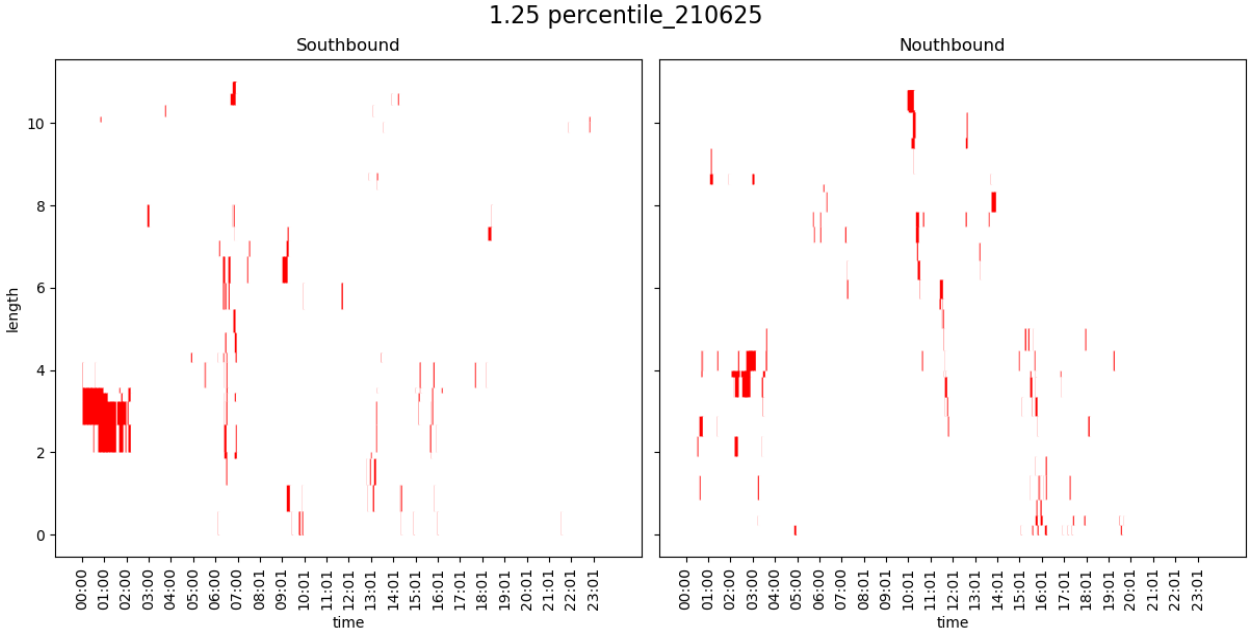

(b)

Figure 8.23: June 25, 2021

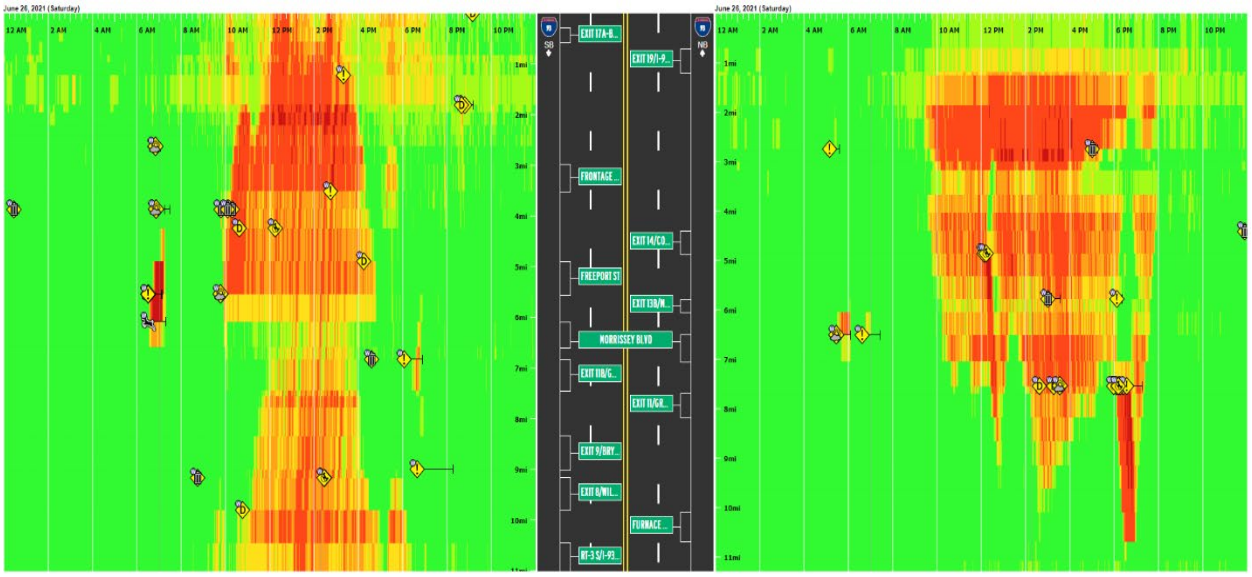

(a)

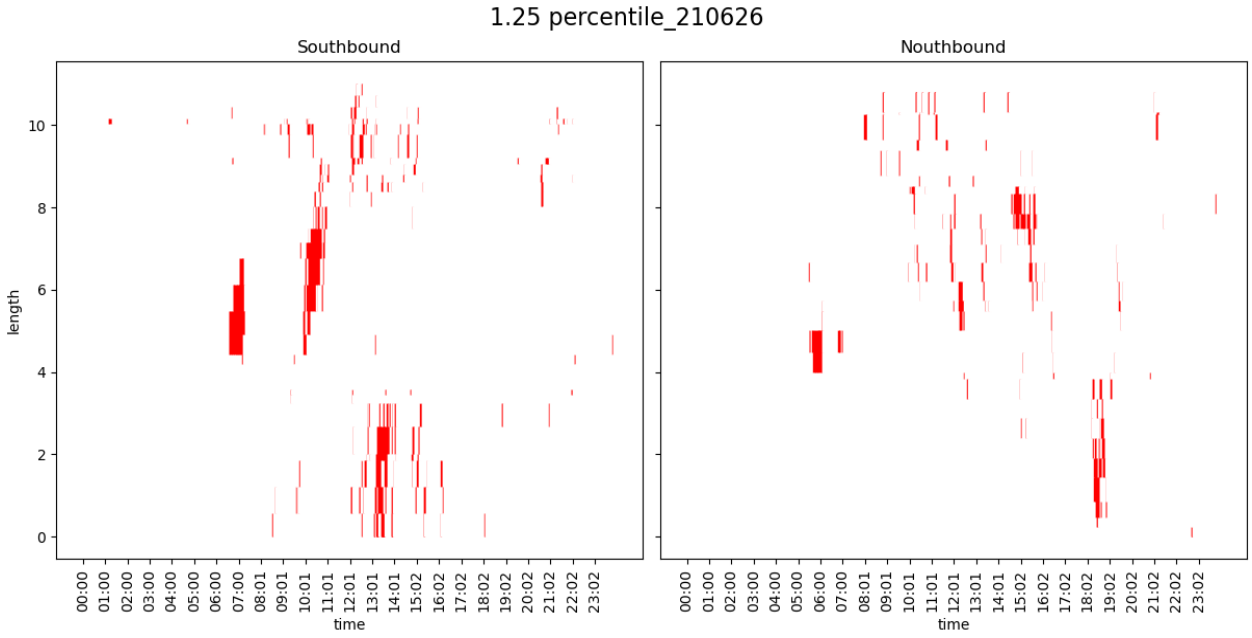

(b)

Figure 8.24: June 26, 2021

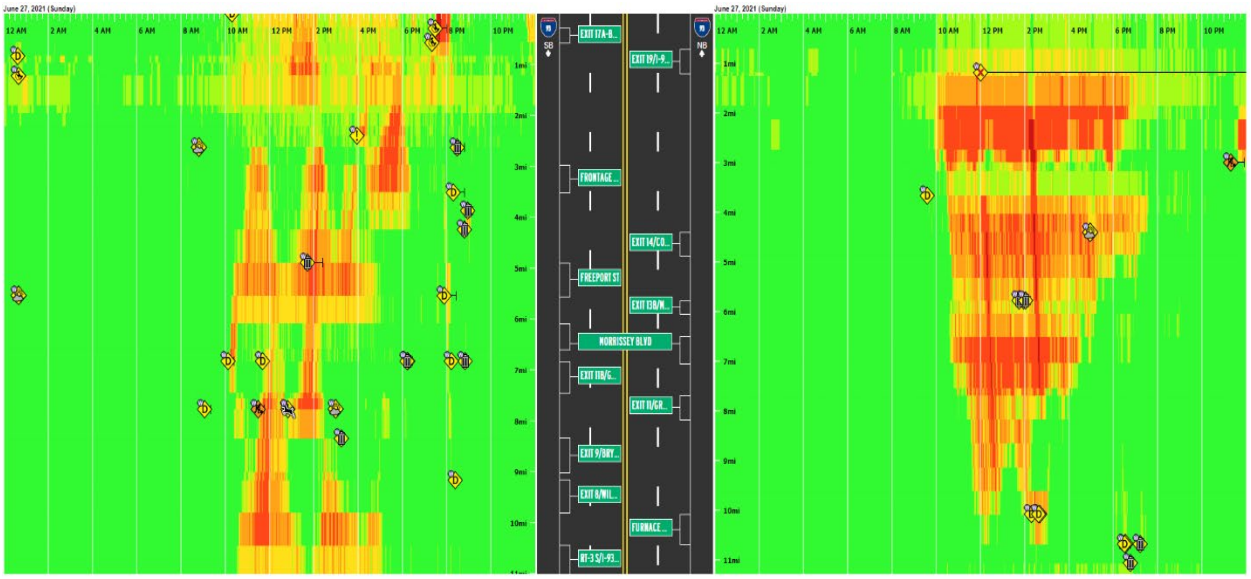

(a)

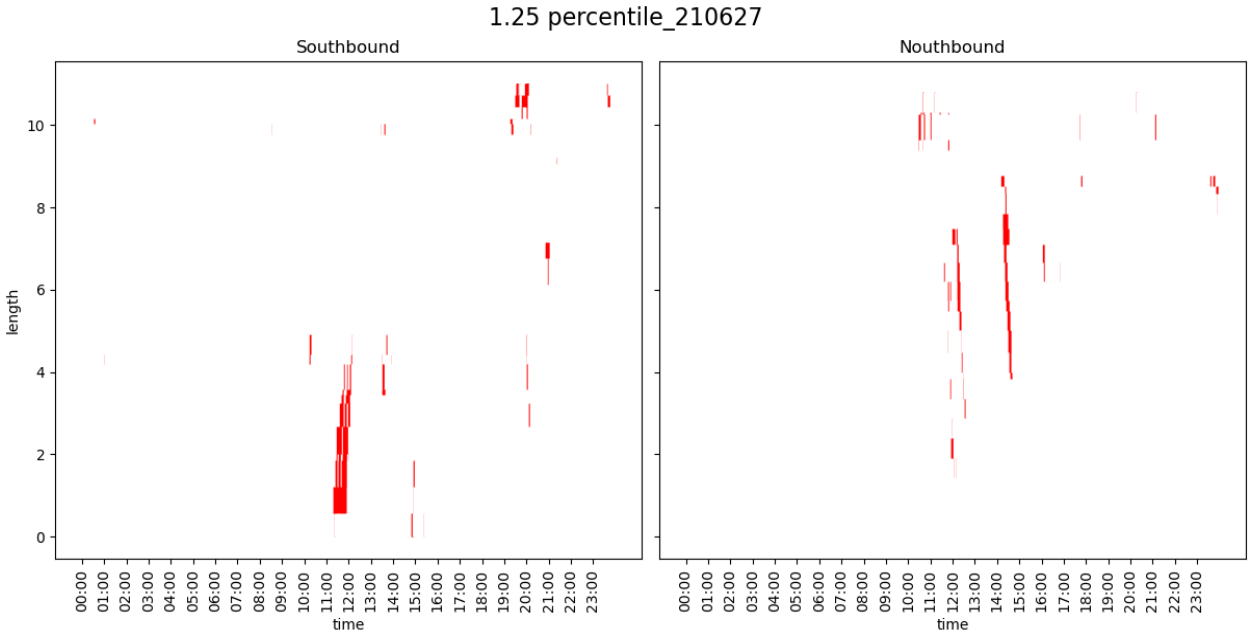

(b)

Figure 8.25: June 27, 2021

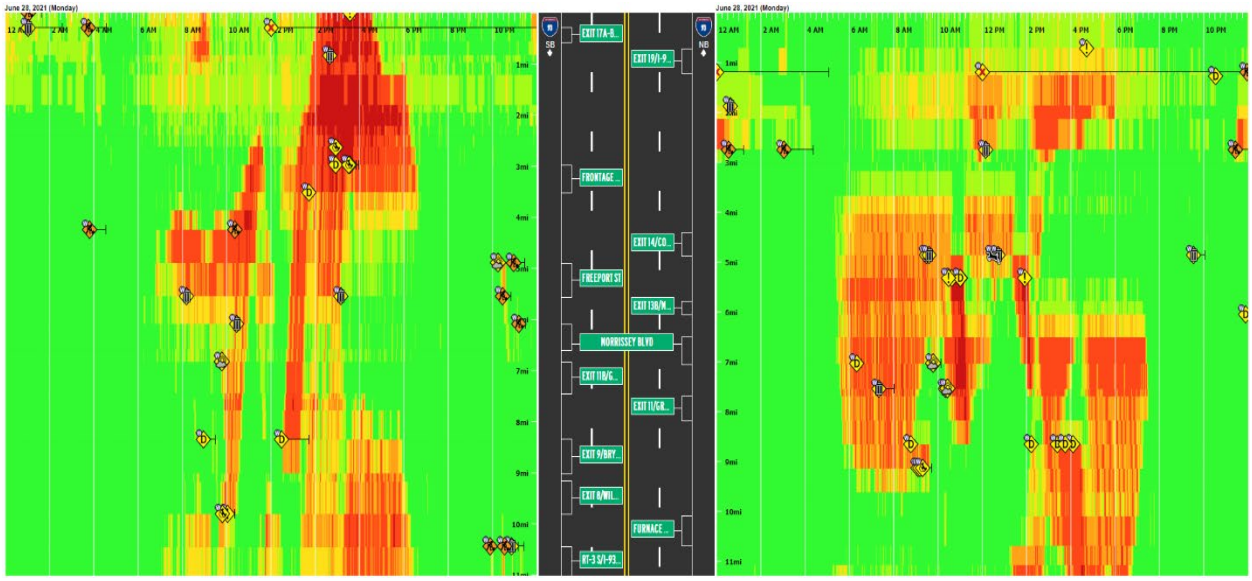

(a)

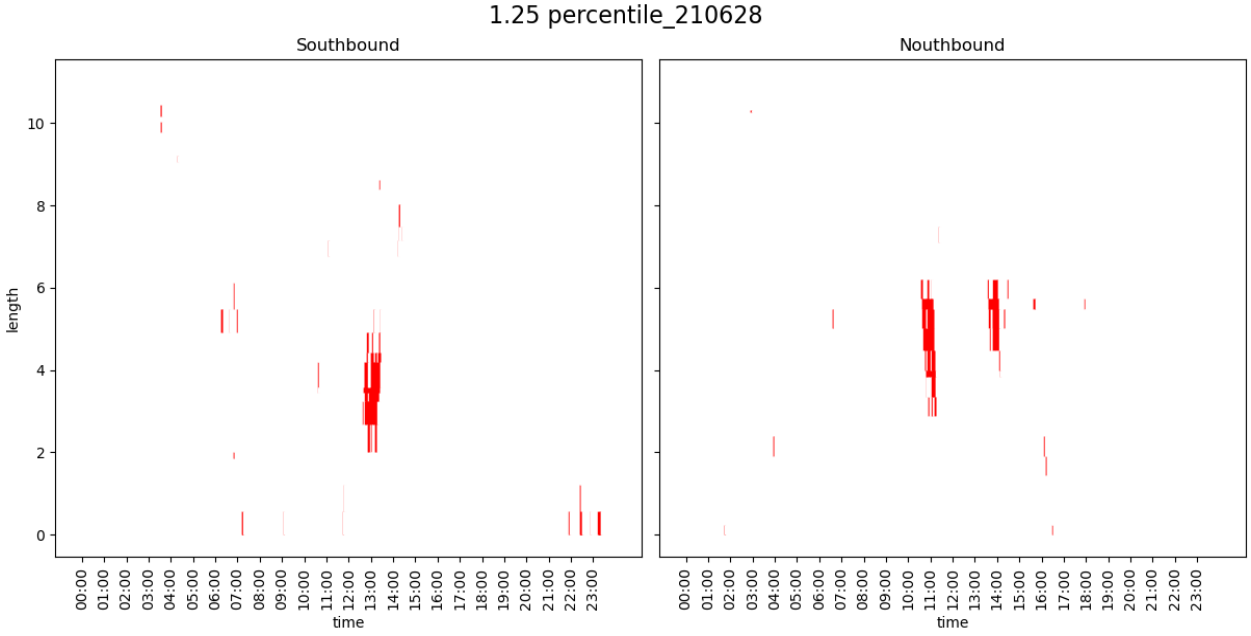

(b)

Figure 8.26: June 28, 2021

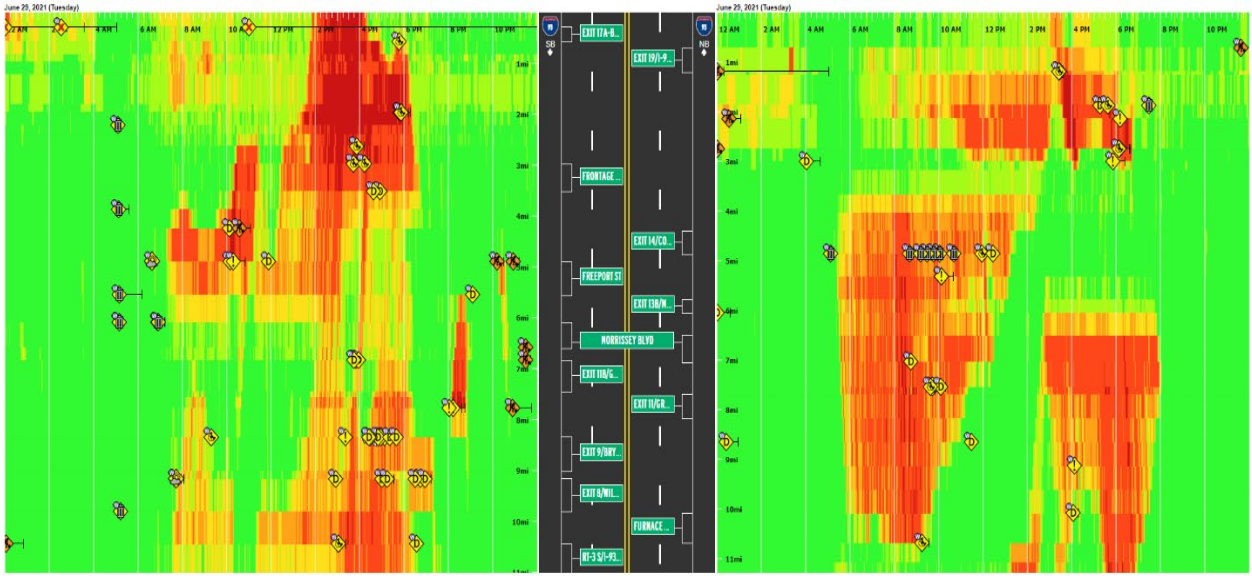

(a)

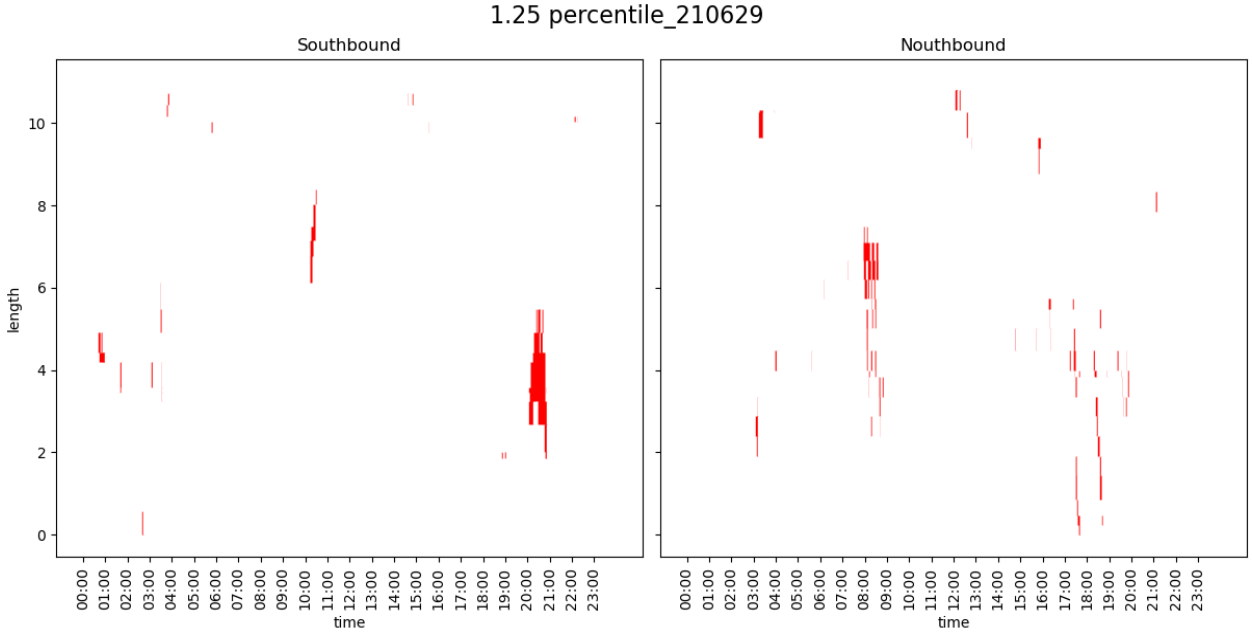

(b)

Figure 8.27: June 29, 2021

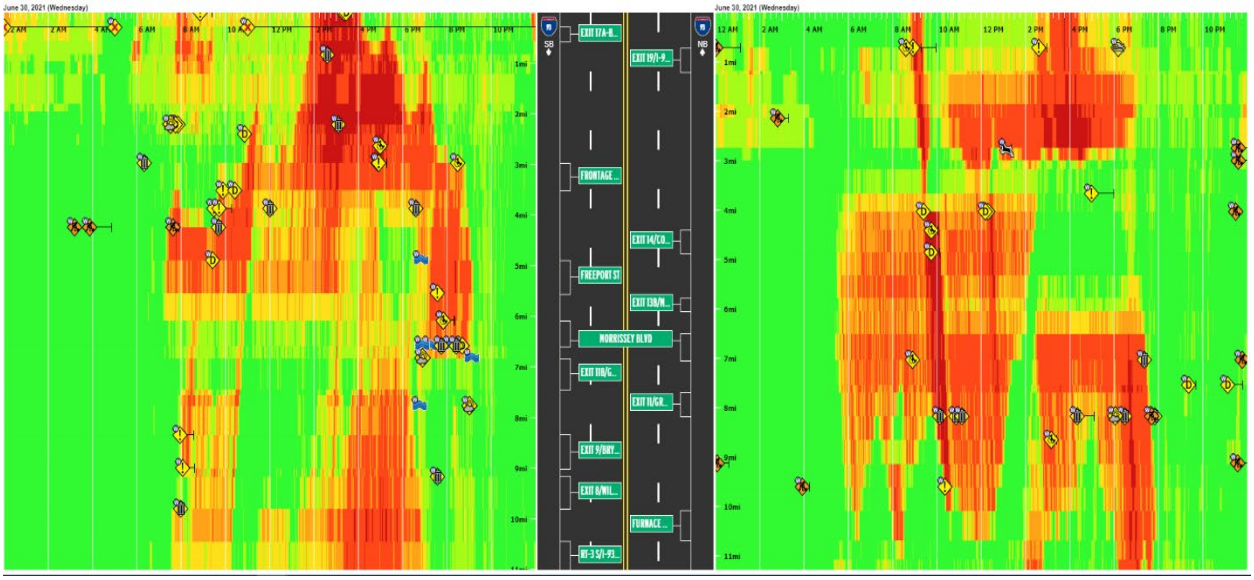

(a)

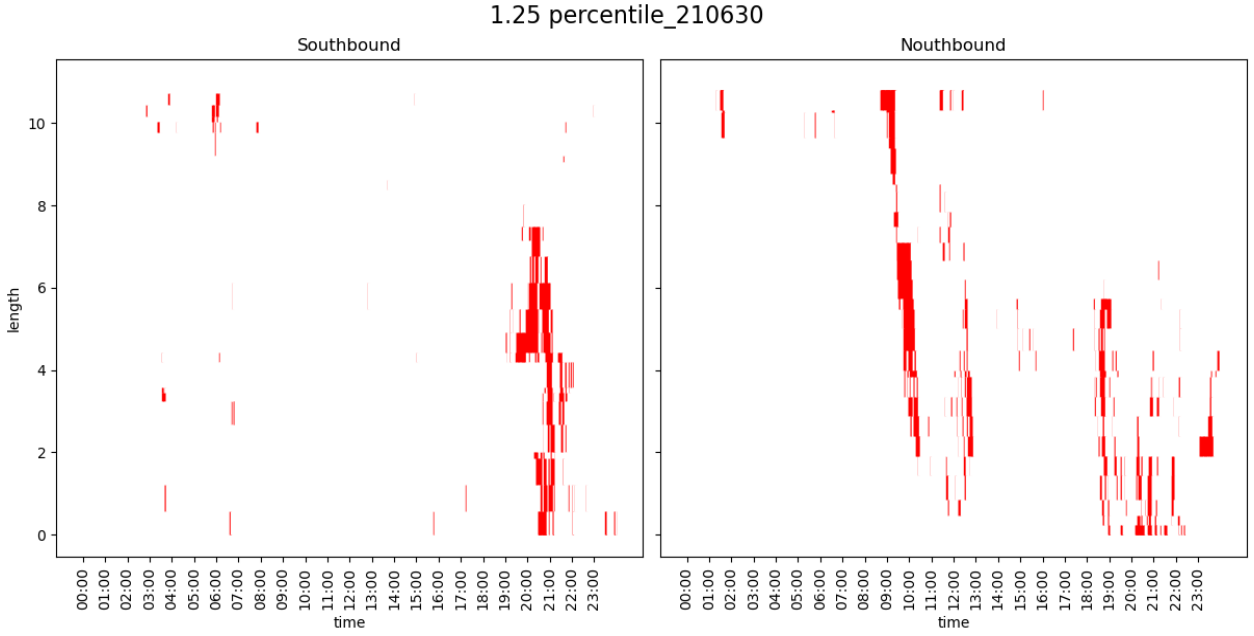

(b)

Figure 8.28: June 30, 2021

This page left blank intentionally.

9 References

1 FHWA, 2021. Process for Establishing, Implementing, and Institutionalizing a Traffic Incident Management Performance Measurement Program, https://ops.fhwa.dot.gov/publications/fhwahop15028/step1.htm.

2 Parkany, E. and Xie, C., 2005. A Complete Review of Incident Detection Algorithms & Their Deployment: What Works and What Doesn't. Report NETCR37, The New England Transportation Consortium.

3 Goodall, N. and Lee, E., 2019. Comparison of Waze crash and disabled vehicle records with video ground truth, Transportation Research Interdisciplinary Perspectives, Volume 1, 100019, https://doi.org/10.1016/j.trip.2019.100019.

4 Hadi, M. et al, 2017. Utilization of Connected Vehicle Data to Support Traffic Management Decisions. Final Report prepared for Florida Dept. of Transportation.

5 Wolfgram, J. et al, 2018. A Quick and Reliable Traffic Incident Detection Methodology Using Connected Vehicle Data. Paper sponsored by TRB committee ABJ35 Standing Committee on Highway Traffic Monitoring.

6 Stone, Tom, 2021. Wejo connected vehicle data integrated into Waycare traffic management platform. Traffic Technology International, June 2021.

7 Outay F, Mengash A., and Adnan M, 2020. Applications of unmanned aerial vehicle (UAV) in road safety, traffic and highway infrastructure management: Recent advances and challenges. Transp Res Part A, 141: 116–129.

8 Rindt, C., 2018. Situational Awareness for Transportation Management: Automated Video Incident Detection and Other Machine Learning Technologies for the Traffic Management Center. Report No. CA18-2531. Institute of Transportation Studies, University of California - Irvine.

9 Brydia, R., Johnson, J, and Balke, K., 2005. An Investigation into the Evaluation and Optimization of the Automatic Incident Detection Algorithm used in TXDOT Traffic Management Systems. Texas Transportation Institute Report 0-4770-1. URL: http://tti.tamu.edu/documents/0-4770-1.pdf.

10 Chung, E and Rosalion, N., 1999. Effective incident detection and management on freeways, Research Report ARR 327, ARRB Transport Research, Vermont South, Victoria.

11 Luk, J., Han, C. and Chin, D., 2010. Automatic Freeway Incident Detection: Review of Practices and Guidance. 24th ARRB Conference – Building on 50 years of road and transport research, Melbourne, Australia 2010.

12 Petty, K.F., Skabardonis, A. and Varaiya, P.P., 1997. Incident detection with probe vehicles: performance infrastructure requirement and feasibility. In: Transportation

Systems 1997. Proceedings Volume from the 8th IFAC/IFIP/IFORS Symposium, Chania, Greece, 16–18 June 1997.

13 Cheu, R.L., Qi, H. and Lee, D.H., 2002. Mobile sensor and sample-based algorithm for freeway incident detection. Transport. Res. Rec.: J. Transport. Res. Board 1811, 12–20.

14 Li, Y., McDonald, M., 2005. Motorway incident detection using probe vehicles. Proc. Inst. Civil Eng.-Transport 158, 11–15.

15 Kinoshita, A., Takasu, A. and Adachi, J., 2014. Traffic Incident detection using probabilistic topic model. In: Proceedings of the Workshops of the Joint Conference EDBT/ICDT 2014, Athens, Greece, 28 March 2014.

16 Eleonora D'Andrea and Francesco Marcelloni, 2016: Detection of traffic congestion and incidents from GPS trace analysis, Dipartimento di Ingegneria dell'Informazione, University of Pisa, Largo Lucio Lazzarino 1, 56122 Pisa, Italy.

17 Nanthawichit, C., Nakatsuji, T., Suzuki, H., 2003. Application of probe-vehicle data for real-time traffic state estimation and short term travel time prediction on a freeway. Transport. Res. Rec. 1855, 49–59.

18 El Faouzi, N.-E., Leung, H. and Kurian, A., 2011. Data fusion in intelligent transportation systems: progress and challenges-A survey. Inform. Fusion 12 (1), 4–10.

19 Hall, F.L, Shi, Y. and Atala, G., 2018. On-line testing of the McMaster algorithm under recurrent congestion. Transportation Research Record, no. 1394, pp.1-7.

20 Chassiakos, A.P. and Stephanedes, Y.J., 1993. Smoothing algorithms for incident detection. Transportation Research Record, no. 1394, pp.8-16.

21 Ritchie, S.G. and Cheu, R.L., 1993. Simulation of freeway incident detection using artificial neural networks, Transportation Research, vol. 1C, no. 3, pp.203-17.

22 Dia, H. and Rose, G., 1997. Development and evaluation of neural network freeway incident detection models using field data, Transportation Research, vol. 5c, no. 5, pp.313-31.

23 Abdulhai, B., and Ritchie, S.G., 1999. Enhancing the universality and transferability of freeway incident detection using a Bayesian-based neural network, Transportation Research, vol. 7C, no. 5, pp.261-80.

24 Zhang, K., and Taylor, M.A.P., 2006. Towards universal freeway incident detection algorithms, Transportation Research, vol. 14C, no. 2, pp.68-80.

25 Lin, Y., Li, L., Jing, H., Ran, B. and Sun, D., 2020. Automated traffic incident detection with a smaller dataset based on generative adversarial networks. Accident Analysis & Prevention, 144, p.105628.

26 Rizvi, S.M.A., Ahmed, A. and Shen, Y., 2020. Real-Time Incident Detection and Capacity Estimation Using Loop Detector Data. Journal of Advanced Transportation.

27 Jalali, A. and Nejad, H.T., 2020. Incident Detection in Freeway Based on Autocorrelation Factor of GPS Probe Data. International Journal of Intelligent Transportation Systems Research, 18(1), pp.174-182.

28 Iqbal, M.S., Khazraeian, S. and Hadi, M., 2018. A Methodology to Assess the Quality of Travel Time Estimation and Incident Detection Based on Connected Vehicle Data. Transportation Research Record, 2672(42), pp.203-212.

29 Singh, D. and Mohan, C.K., 2018. Deep spatio-temporal representation for detection of road accidents using stacked autoencoder. IEEE Transactions on Intelligent Transportation Systems, 20(3), pp.879-887.

30 Qian, Z.S., 2016. Real-time incident detection using social media data (No. FHWA-PA-2016-004-CMU WO 03). Pennsylvania. Dept. of Transportation.

31 Parsa, A.B., Taghipour, H., Derrible, S. and Mohammadian, A.K., 2019. Real-time accident detection: coping with imbalanced data. Accident Analysis & Prevention, 129, pp.202-210.

32 Karatsoli, M., Margreiter, M. and Spangler, M., 2017. Bluetooth-based travel times for automatic incident detection–A systematic description of the characteristics for traffic management purposes. Transportation research procedia, 24, pp.204-211.

33 Mercader, P. and Haddad, J., 2020. Automatic incident detection on freeways based on Bluetooth traffic monitoring. Accident Analysis & Prevention, 146, p.105703..

34 Evans, J., Waterson, B. and Hamilton, A., 2020. A random forest incident detection algorithm that incorporates contexts. International Journal of Intelligent Transportation Systems Research, 18(2), pp.230-242.

35 Chakraborty, P., Hegde, C. and Sharma, A., 2019. Data-driven parallelizable traffic incident detection using spatio-temporally denoised robust thresholds. Transportation research part C: emerging technologies, 105, pp.81-99.

36 Bartlett, A. and Sadek, A.W., 2017. Buffalo-Niagara Transportation Data-warehouse Prototype and Real-time Incident Detection.

37 Chien, S., Chen, Y., Yi, Q. and Ding, Z., 2019. Development of Automated Incident Detection System Using Existing ATMS CCTV.

38 Liu, C., Zhao, M., Sharma, A. and Sarkar, S., 2019. Traffic dynamics exploration and incident detection using spatiotemporal graphical modeling. Journal of Big Data Analytics in Transportation, 1(1), pp.37-55.

39 Nguyen, H., Cai, C. and Chen, F., 2017. Automatic classification of traffic incident's severity using machine learning approaches. IET Intelligent Transport Systems, 11(10), pp.615-623.

40 Zhang, A., Lipton, Z. C., Li, M., & Smola, A. J. (2021). Dive into deep learning. arXiv preprint arXiv:2106.11342.

41 Kingma, D. P., & Welling, M. (2019). An introduction to variational autoencoders. Foundations and Trends® in Machine Learning, 12(4), 307-392.

42 Bank, D., Koenigstein, N., & Giryes, R. (2020). Autoencoders. arXiv preprint arXiv:2003.05991.

43 Rocca, J. (2019). Understanding Variational Autoencoders (VAEs). Available online at https://towardsdatascience.com/understanding-variational-autoencoders-vaes-f70510919f73, Accessed on December 31, 2022.

44 Kingma, D. P., & Welling, M. (2013). Auto-encoding variational bayes. arXiv preprint arXiv:1312.6114.

45 Alto, V. (2021). Variational Autoencoders in Computer Vision. Available online at https://valentinaalto.medium.com/variational-autoencoders-in-computer-vision-f198cefe12ca, Accessed on December 31, 2022.

46 Martin, P. T., Perrin, J., Hansen, B., Kump, R., & Moore, D. (2001). Incident detection algorithm evaluation (No. MPC-01-122). Upper Great Plains Transportation Institute.

47 Chawla, N. V., Bowyer, K. W., Hall, L. O., & Kegelmeyer, W. P. (2002). SMOTE: synthetic minority over-sampling technique. Journal of artificial intelligence research, 16, 321-357.

48 He, H., Bai, Y., Garcia, E. A., & Li, S. (2008, June). ADASYN: Adaptive synthetic sampling approach for imbalanced learning. In 2008 IEEE international joint conference on neural networks (IEEE world congress on computational intelligence) (pp. 1322-1328). IEEE.

49 D. R. Drew, “Traffic Flow Theory and Control”, McGraw Hill Book Co., 1968.

50 SciPy. Available online at https://scipy.org/, Accessed on December 31, 2022.

51 Wikipedia - Beta distribution. Available online at https://en.wikipedia.org/wiki/Beta_distribution#Two_unknown_parameters, Accessed on December 31, 2022.

52 PyCaret. Available online at https://github.com/pycaret/pycaret, Accessed on December 31, 2022.

53 Ruff, L., Vandermeulen, R. A., Görnitz, N., Binder, A., Müller, E., Müller, K. R., & Kloft, M. (2019). Deep semi-supervised anomaly detection. arXiv preprint arXiv:1906.02694.

54 Xie, Q., Dai, Z., Hovy, E., Luong, T., & Le, Q. (2020). Unsupervised data augmentation for consistency training. Advances in Neural Information Processing Systems, 33, 6256–6268.